Funktion von Abp1, einem Signal-responsiven Verbindungsglied zwischen Aktinzytoskelett und Membrantransport, in neuronaler Morphologie

Function of Abp1, a signal-responsive linker between actin cytoskeleton and membrane transport, in neuronal morphology

Dissertation
zur Erlangung des akademischen Grades doctor rerum naturalium (Dr. rer. nat.)

vorgelegt dem Rat der Biologisch-Pharmazeutischen Fakultät der Friedrich-Schiller-Universität Jena

von M. Sc. Biol. (Master of Sciences in Biology) Akvile Häckel

geboren am 13.10.1977 in Vilnius (Litauen)

Gutachter:

1. Prof. Dr. Tobias M. Böckers

Universität Ulm
Institut für Anatomie und Zellbiologie
Albert Einstein Allee 11
89081 Ulm

2. Prof. Dr. Siegrid Löwel

Friedrich-Schiller-Universität Jena
Institut für Allgemeine Zoologie und Tierphysiologie
Erbertstr. 1
07743 Jena

3. Prof. Dr. Britta Qualmann

Friedrich-Schiller-Universität Jena
Institut für Biochemie I
Nonnenplan 2
07743 Jena

Datum der Verteidigung: 12.04.2010

Ehrenwörtliche Erklärung

Hiermit erkläre ich, dass die vorliegende Dissertation von mir selbst und ohne unzulässige Hilfe geschrieben ist. Die benutzte Literatur sowie Hilfsmittel sind vollständig im Text und Literaturverzeichnis erwähnt. Diese Dissertation stellt keine Kopie anderer Arbeiten dar.

Akvile Häckel

Die vorliegende Dissertation wäre nicht geschafft geworden, wenn ich nicht umfangreiche Unterstützung und Hilfe gehabt hätte.

An erster Stelle bedanke ich mich bei Dr. Michael Kessels und Prof. Britta Qualmann für die großzügige Betreuung meiner Arbeit. Sie haben mir immer nicht nur in fachspezifischen, sondern auch in privaten Gesprächen Rückhalt gegeben.

Bedanken möchte ich mich auch bei Dr. Christina Spilker, Dr. Thomas Dresbach, Dr. Anna Fejtova und Dr. Renato Frischknecht, die mir mit ihren Erfahrungen immer tatkräftig zur Seite standen.
Für die kreativen Diskussionen und fachlichen Hinweise bedanke ich mich bei Prof. Eckart Gundelfinger, Dr. Michael Kreutz, Dr. Karl-Heinz Smalla, Dr. Ulrich Thomas.

Des Weiteren gilt mein großer Dank zu Katholischem Akademischem Ausländer-Dienst (KAAD). Durch das Stipendium von KAAD konnte ich ein Forschungsprojekt am Leibniz Institut für Neurobiologie in Magdeburg anfangen und es weiter zur Promotion bringen.

Mein herzlicher Dank richtet sich auch an Nicole K., Dennis, Roser, Ela, Rashmi, Anne, Anke, Wilko, Bettina, Nora, Diana, Dirk, Lukas, Heidi, Kathi, Moni für ihre Hilfsbereitschaft, Freundschaft und Unterstützung.

Noch ein besonderer Dank gilt für Irina und Nicole R. für ihre Freundschaft und Aufmunterung.

Auch geht mein besonderer Dank an meine Eltern, meinen Bruder und an meinen Mann Christian, die mich stets bestärkt haben, wenn ich an mir gezweifelt habe. Christian stand die ganze Zeit hinter mir und daher widme ich ihm diese Arbeit.

Ebenso sei allen denen ein Dankeschön ausgesprochen, die nicht namentlich Erwähnung fanden, aber zum Gelingen dieser Arbeit beigetragen haben.

Vielen Dank.

INDEX

Summary

Polymerization and organization of actin into complex superstructures, including those found in neuronal growth cones and dendritic spines, is indispensable for structure and function of neuronal networks. This work shows that the F-actin-binding protein 1 (Abp1), which is important for endocytosis, controls Arp2/3 complex-mediated actin nucleation via the neural Wiskott-Aldrich syndrome protein (N-WASP) and binds to postsynaptic scaffold proteins of the ProSAP/Shank family, has a profound impact on synaptic organization. In early neuronal development, RNAi mediated knock-down of Abp1 expression results in changes in axon development virtually identical to Arp2/3 complex inhibition, i.e. a selective increase of axon length. This work reveals an essential role of Abp1 and its cooperation with Cdc42 in N-WASP-induced rearrangements of the neuronal cytoskeleton. Furthermore, it shows that introduction of N-WASP mutants lacking the ability to bind Abp1 or Cdc42, Arp2/3 complex inhibition, Abp1 knock-down, N-WASP knock-down and Arp3 knock-down all cause identical neuromorphological phenotypes.

Secondly, Abp1 controls the formation and morphology of dendritic spines harboring the postsynaptic signal reception and transduction apparatus. Overexpression of the two Abp1 F-actin-binding domains increases the length of thin, filopodia-like and mushroom-type spines but dramatically reduces mushroom spine density, due to lack of the Abp1 SH3 domain. In contrast, overexpression of full-length Abp1 increases mushroom spine and synapse density. The SH3 domain alone has a dominant-negative effect on mushroom spine density, whereas the density of filopodia and thin, immature spines remains unchanged. This suggests that both actin-binding and SH3 domain interactions are crucial for Abp1's role in spine maturation. Indeed, Abp1 knock-down significantly reduces mushroom spine and synapse density. Abp1 hereby works in close conjunction with ProSAP1/Shank2 and ProSAP2/Shank3, because ProSAP2 RNAi suppressed Abp1 effects, and the ProSAP/Shank-induced increase of spine head width is further promoted by Abp1 cooverexpression and reduced upon Abp1 knock-down. Also, interfering with the formation of functional Abp1-ProSAP protein complexes prevents ProSAP-mediated spine head extension. Spine head extension furthermore depends on local Arp2/3 complex-mediated actin polymerization, which is controlled by Abp1 via the Arp2/3 complex activator N-WASP.

Abp1 thus plays an important role in the formation and morphology control of synapses by making a required functional connection between PSD components and postsynaptic actin dynamics as well as in the in cytoskeletal processes underlying neuronal network formation.

Zusammenfassung

Polymerisation und Organisation von Aktin in komplexe Superstrukturen, wie sie auch in neuronalen Wachstumskegeln und dendritischen Dornen auftreten, sind für die Struktur und Funktion von neuronalen Netzen unentbehrlich. Diese Arbeit zeigt, dass das F-Aktin-bindende Protein 1 (Abp1), das für Endozytose wichtig ist, die Arp2/3 Komplex-vermittelte Nukleation von Aktin über das neuronale Wiskott-Aldrich Syndrom Protein (N-WASP) kontrolliert und die postsynaptischen Gerüst-Proteine der ProSAP/Shank Familie bindet, einen tiefen Einfluss auf synaptische Organisation hat. Die RNAi-vermittelte Unterdrückung von endogenem Abp1 führt in der frühen neuronalen Entwicklung zu einer selektiven Zunahme der Axon-Länge, wie sie auch bei Hemmung des Arp2/3 Komplexes beobachtet wird. Diese Arbeit offenbart damit eine wesentliche Rolle von Abp1 selbst und seiner Kooperation mit Cdc42 in N-WASP-induzierten Neuordnungen des neuronalen Zytoskeletts. Der Befund wird dadurch untermauert, dass die Expression von N-WASP-Mutanten, die nicht in der Lage sind, Abp1 oder Cdc42 zu binden, die Inhibition des Arp2/3 Komplexes und die RNAi-vermittelte Reduktion der Proteinniveaus von endogenen Abp1, N-WASP oder Arp3 alle identische neuro-morphologische Phänotypen verursachen.

Weiterhin kontrolliert Abp1 die Bildung und Morphologie der dendritischen Dornen, die den postsynaptischen Signalempfangs- und Transduktionsapparat beherbergen. Die Überexpression der zwei F-Aktin-bindenden Domänen von Abp1 verlängert sowohl die dünnen, Filopodien-ähnlichen Dornen als auch die pilzförmigen Dornen, aber reduziert drastisch die Dichte von pilzförmigen Dornen, was über den Mangel der Abp1 SH3-Domäne zu erklären ist. Im Gegensatz dazu vergrößert die Überexpression vom Abp1-Gesamtprotein die Dichte der pilzförmigen Dornen und der Synapsen. Die isolierte SH3-Domäne hat eine dominant-negative Wirkung auf die Dichte der pilzförmigen Dornen, wohingegen die Dichte der Filopodien und der dünnen, unreifen Dornen unverändert bleibt. Das weist darauf hin, dass sowohl die durch Aktin-Bindung als auch die durch die SH3-Domäne vermittelten Interaktionen für die Rolle von Abp1 in der Reifung der Dornen entscheidend sind. Tatsächlich vermindert die Reduktion der Expression von endogenem Abp1 signifikant die Dichte von pilzförmigen Dornen und Synapsen. Abp1 arbeitet hiermit eng mit ProSAP1/Shank2 und ProSAP2/Shank3 zusammen, da ProSAP2 RNAi Abp1-Effekte unterdrückt, und da die ProSAP/Shank-induzierte Zunahme der Kopfbreite von Dornen durch Abp1 Co-Überexpression weiter gefördert bzw. bei Abp1 Expressionsverringerung reduziert wird. Außerdem verhindert das Stören der Bildung von funktionellen Abp1-ProSAP-Protein-Komplexen die ProSAP-vermittelte Kopfvergrösserung von Dornen. Die Verbreitung der Köpfe der dendritischen Dornen hängt außerdem von lokaler Arp2/3 Komplex-vermittelter Aktinpolymerisation ab, die von Abp1 über den Aktivator des Arp2/3 Komplexes N-WASP kontrolliert wird.

Somit spielt Abp1 eine wichtige Rolle in der Bildung und Morphologiekontrolle von Synapsen und durch Ausbildung einer funktionellen Verbindung zwischen PSD-Bestandteilen und postsynaptischer Aktin-Dynamik sowie in zytoskeletalen Prozessen, die neuronaler Netzbildung unterliegen.

1. Introduction

1.1 Neurite initiation and outgrowth

Neurites, cylindrical extensions of the neuronal cell body that serve as precursors to axons and dendrites, are a crucial part of the neuronal architecture that underlies brain function (McAllister, 2000; Cline, 2001, see also Fig. 1). Neuritic morphogenesis requires an intrinsic differentiation program that is further instructed by extracellular cues and electrical activity. Eventually, these different forces converge to control cytoskeletal dynamics that specify dendritic and axonal growth, branching, and the formation of dendritic spines (Scott and Luo, 2001).

The original round shape of the cell must be broken to form a bud that develops into a neurite. Neurite initiation and outgrowth involves coordinated changes between the actin cytoskeleton, which provides the means for force generation within the cell, and the microtubule network, which stabilizes and maintains the neurites (da Silva and Dotti, 2002). Fig. 1 shows developmental stages 1-5 of cultured hippocampal neurons: at first a lamellipodium is formed when the cells attach to the substratum, and shortly thereafter neurites begin to sprout. The neurites are thin protrusions that contain a growth cone at their distal tip and still lack the molecular and structural characteristics of mature axonal or dendritic processes. These neurites extend and retract without net elongation. The following day, one of the neurites with an enlarged growth cone at its tip elongates rapidly without retraction to form the axon. Several days later, the remaining neurites continue to grow and branch to form the dendrites, and in a final step of maturation, the axon and dendrites develop further and dendritic protrusions, or spines, appear.

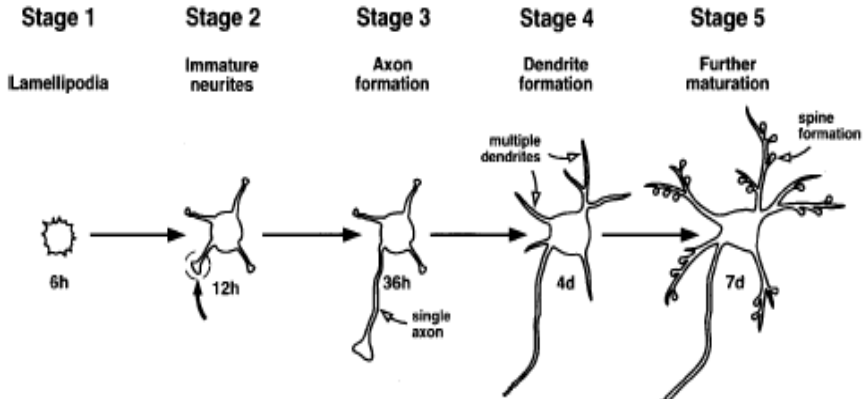

Figure 1. Stages of neuronal development in hippocampal neurons (Govek et al., 2005).

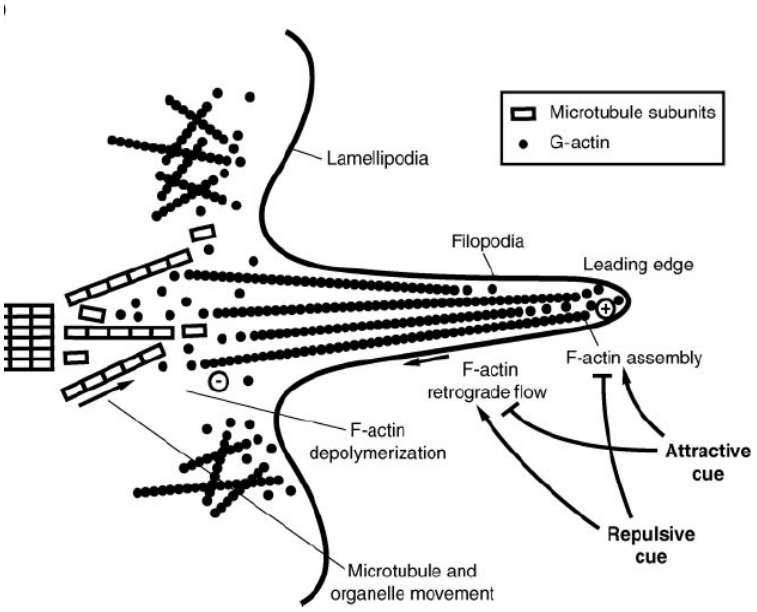

Figure 2. Growth cone structure. The growth cone detects and responds to axon guidance cues. The lamellipodia contain cross-linked F-actin filaments. The filopodia extend and retract through regulation of the rates of actin polymerization and depolymerization at the plus and minus ends of actin filaments, respectively, and of F-actin retrograde flow. Repulsive and attractive cues influence growth cone morphology by regulating these processes (Yuste and Bonhoeffer, 2001).

The task of locating a target is delegated to the growth cone, the motile tip of a growing axon or dendrite (Fig. 2). Extracellular guidance cues instruct the growth cone to advance, retract, or turn. They do this by regulating the actin cytoskeleton within the growth cone. Small GTPases (guanosine triphosphatases) of the Rho family - primarily Rac, Cdc42 and Rho - are key regulators of cytoskeletal dynamics in non-neuronal cells and neuronal growth cones (Luo et al., 2000, 2002; Dickson, 2001).

1.2 Spine morphology, ultrastructure and functions

Dendritic spines are small protrusions on the surface of dendrites of neurons, which form connections with axon terminals and represent the postsynaptic component of most excitatory synapses (Hering and Sheng, 2001). They are focal points of synaptic plasticity, and the structure of a spine is determined by its underlying actin cytoskeleton (Matus, 2000; Carlisle and Kennedy, 2005). The typical dendritic spine is mushroom-shaped, i. e. is composed of a bulbous head connected to the dendritic shaft by a narrow neck. But even within the same neuronal cell, spines come in a wide range of shapes and sizes: stubby spines without a neck and filopodial spines without a head can be found beside mushroom-type spines with a clear distinguishable head (Fig. 3). Between spine head size and the strength of synapse exist a strong correlation, most related to the higher levels of AMPA

receptors in larger spines. Preferentially small spines undergo long-term potentiation (LTP), whereas large spines are more stable and show less plasticity (Matzusaki et al., 2001, Tada and Sheng, 2006).

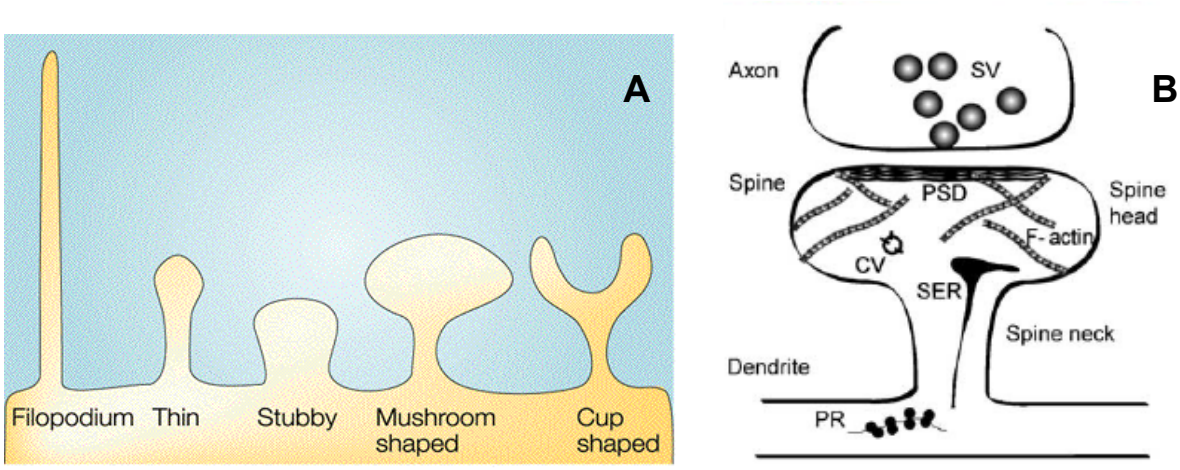

Figure 3. Dendritic spine morphology and ultrastructure. *A*, Schematic representation of the most common types of dendritic spine morphologies (Hering and Sheng, 2001). *B*, Dendritic spine ultrastructure. CV, coated vesicles; PSD, postsynaptic density; PR, polyribosome; SER, smooth endoplasmic reticulum; SV, synaptic vesicles (Ethell and Pasquale, 2005).

The spine head contains the postsynaptic density (PSD), an electron-dense structure positioned next to the active zone of the presynaptic terminal where neurotransmitters are released into synaptic cleft. The PSD consists of densely packed ion channels and cell surface receptors in complex with cytoplasmic scaffolding and signaling proteins (see also chapter 1.6). Some proteins in the PSD provide a link to actin filaments, which represent the main cytoskeletal component of spines. Microtubules and neurofilaments have been detected in dendritic spines, but the presence of these components remains poorly characterized (van Rossum and Hanisch, 1999). A couple of spines contain elements of smooth endoplasmic reticulum, which forms the so-called spine apparatus in the larger spines. This structure serves as a calcium store and as reservoir of receptors and ion channels, which traffic to the PSD during synaptic plasticity (Tarrant and Routtenberg, 1979).

The major function of spines is to provide a micro-compartment where chemical responses, for example elevated calcium, are segregated (Sabatini et al., 2001). In the segregation of the spine compartment, spine neck geometry plays a fundamental role: calcium responses in thin spines with long necks have a shorter latency and slower decay kinetics than mushroom-shaped spines with short necks. Spine neck changes, as they

occur during spine motility, also correlate with altered diffusional coupling between dendrite and spine and with rearrangements of calcium kinetics within the spine (Korkotian and Segal, 2000). But it is still not clear, which physiological significance for cognitive brain functions is represented by the dynamic changes of dendritic spines and by their different morphologies (Tada and Sheng, 2006).

1.3 Models of spinogenesis

There are two major views explaining the origin of dendritic spines. One model postulates filopodia as spine precursors, it proposes that filopodia, the highly flexible structures covering dendrites in early stages of synaptogenesis, undergo a morphological and functional transformation marked by decreased motility, extensive shortening and enlargement of the distal part to become a typical mushroom-shaped spine after an appropriate contact site on an axon was found (Ziv and Smith, 1996; Marrs et al., 2001; Trachtenberg et al., 2002). The second model suggests that axonal but not dendritic filopodia may be involved in finding an adequate region for synaptic contact on the dendrite because the majority of synapses in young pyramidal neurons are located on the dendritic shaft (Harris et al., 1992). Indeed, an emergence of mature spines from shaft synapses has been described (Dailey and Smith, 1996), and axonal filopodia in synaptic contact with dendrites have been observed in electron microscopy images (Fiala et al., 1998). Summarizing the currently available data, it seems well possible that dendritic spine development in hippocampal and cortical neurons takes place through both of the here-described mechanisms or through the combination of them (Ethell and Pasquale, 2005).

1.4 Actin dynamics is essential for the development of neurites and for dendritic spine growth and remodeling

Actin, a fundamental part of the cytoskeleton, is present as a soluble pool of monomeric G-actin and as polymerized F-actin filaments. It is an essential structural component of neurite growth cones and of dendritic spines (Matus et al., 1982; Halpain, 2000; Dickson, 2001; see also Fig. 2 and 3). Therefore various signaling pathways regulating dendritic and axonal development, spine formation and growth must eventually converge on modulations of actin dynamics. It is established that actin rearrangements drive growth cone shape and motility, the formation and loss on dendritic filopodia and spines as well as their morphological plasticity (reviewed in Ethell and Pasquale, 2005).

Rho family of small GTPases - well-known regulators of actin organization - notably RhoA, Rac, and Cdc42, together with related molecules play an important role in various aspects of neuronal development, including neurite outgrowth and differentiation, axon pathfinding, extension and branching as well as spine formation (Cline, 2001; Luo, 2002; Redmond and Ghosh, 2001).

Rac and Cdc42 activation promotes the formation of lamellipodia and filopodia and also plays a role in neurite formation, growth and attractive guidance, while Rho activity induces loss of spines, prevents neurite initiation and induces their retraction or repulsive guidance (Nakayama et al., 2000; Wong et al., 2000; Tashiro et al., 2000). Perturbation of activities of Rho GTPases by expression of dominant-negative or constitutively active versions of different Rho GTPases often leads to dramatic effects in neuronal morphogenesis (Luo, 2000; Redmond and Ghosh, 2001).

Downstream of Rho GTPases, a variety of actin-binding proteins were identified, which serve as effectors and bring about actin rearrangements by affecting the assembly, stability and disassembly of actin filaments. Spine formation and dynamics, involving actin-based protrusive activity, are modulated by changes in intracellular calcium concentration (Ethell and Pasquale, 2005; Sala et al., 2008; Fig. 4).

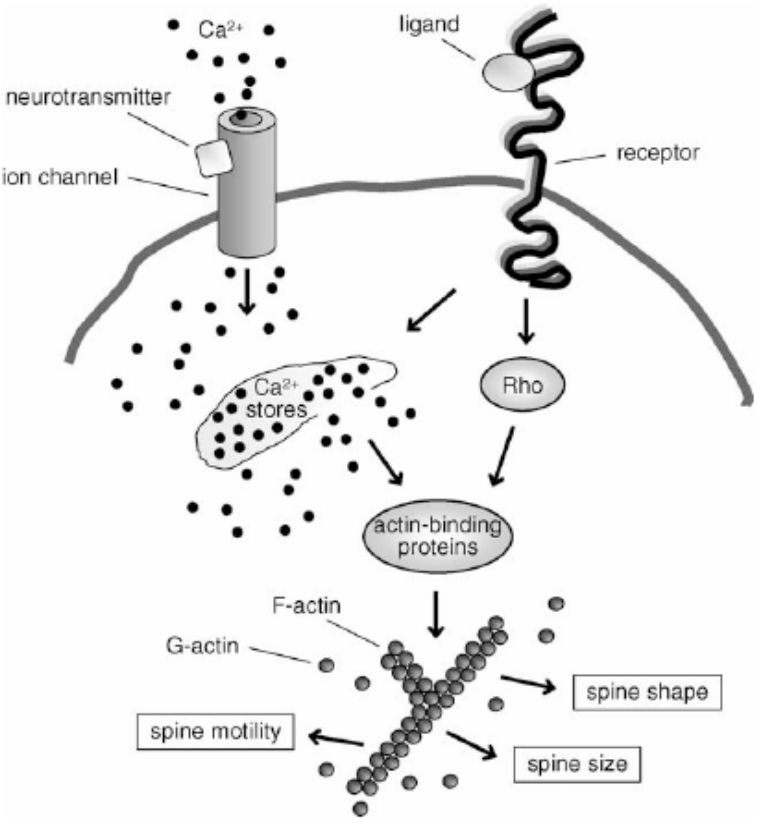

Figure 4. The major signaling cascades that regulate dendritic spine shape and motility. Involved are cell surface receptors and ion channels, which activate signaling cascades controlling the activity of Rho

GTPases and the calcium concentration within the spine. Calcium permeable ion channels include neurotransmitter-gated ion channels, as shown, and voltage-gated calcium channels. Cell surface receptors include receptor tyrosine kinases and cell adhesion and recognition molecules. These receptors can bind soluble ligands, as shown, or ligands anchored to adjacent cell surfaces or to the extracellular matrix (Ethell and Pasquale, 2005).

Actin filaments are constantly turned over. Mechanistically, actin dynamics is achieved by "treadmilling" of existing filaments, i. e. polymerization occurring at the fast growing "barbed" ends and depolymerization on the "pointed" ends. Branching, capping and severing of filaments as well as nucleation of new filaments are crucial processes in actin restructuring within neurites and spines (Pollard, 2003; Fig. 4).

1.5 Actin-binding proteins are key effectors of neuronal morphology

As already mentioned, numerous actin-binding proteins function downstream of the GTPases of the Rho family and/or are regulated by Ca^{2+} and control the organization of the actin cytoskeleton in neurons. Some of them, involved in the *de novo* formation of actin filaments, are presented below in details. The major process underlying protrusive morphology changes is the generation of new actin filaments.

An important actin nucleator is the Arp2/3 complex, composed of the actin-related proteins 2 and 3 (Arp2/3) and five other subunits, which is the final target of several signaling pathways influencing cell shape and motility (Higgs and Pollard, 2001, see also Fig. 4). When activated by upstream signals, including N-WASP/Scar (WAVE) family proteins and cortactin, the Arp2/3 complex binds to the sides of actin filaments and initiates polymerization of branched filaments (Mullins et al., 1998). Arp2/3 inhibition in neuronal growth cones minimally affects actin organization and dynamics, but significantly enhances axon elongation and causes defects in growth cone guidance (Strasser et al., 2004). In mature neurons, the Arp2/3 complex seems to play an important role in shaping the spine head (Irie and Yamaguchi, 2002; Wegner et al., 2008).

One of the key mechanisms, by which Rac and Cdc42 relay signals to the actin cytoskeleton, involves the Wiskott-Aldrich-syndrome family of proteins (Machesky and Insall, 1999; Suetsugu et al., 2002; Miki and Takenawa, 2003; Millard et al., 2004). The Wiskott-Aldrich syndrome protein (WASP) and its relative neuronal WASP (N-WASP) are regulated by Cdc42 (Rohatgi et al., 1999). WASP family proteins contain a carboxy-terminal "output" region (VCA) that binds both the Arp2/3 complex and actin monomers and an amino-terminal "control" region, which binds activated Cdc42 and PIP_2 (phosphatidylinositol 4,5-bisphosphate). The latter induces a conformational change that

releases the WASP/N-WASP VCA domain from auto-inhibition, allowing it to activate the Arp2/3 complex and to promote nucleation and branching of actin filaments *in vitro* as well as in cells, for example in neuritic processes and in the heads of dendritic spines (Machesky et al., 1999; Rohatgi et al., 2000; Dickson, 2001; Irie and Yamaguchi, 2002). PIP_2 also promotes the extension of existing filaments by inhibiting barbed end capping proteins. PIP_2 thus promote both the nucleation of new actin filaments via WASP family members and the extension of existing filaments. These pathways are likely to be critical for growth cone motility, as suggested by the fact that a dominant-negative form of N-WASP inhibits neurite extension in primary hippocampal neurons (Banzai et al., 2000; Dickson, 2001).

Three other members of the WASP superfamily family, WAVE/Scar 1–3, mediate actin-based processes triggered by Rac1 (Miki et al., 1998; Machesky et al., 1999; Yamazaki et al., 2003). Unlike N-WASP, WAVE proteins lack a known GTPase-binding domain, and so its activation by Rac is presumably indirect (Ethell and Pasquale, 2005). WAVE proteins do however contain a basic region similar to the PIP_2-binding site of N-WASP. Oikawa et al. (2004) showed that WAVE-2 binds preferentially to PIP_3 (phosphatidyl-inositol (3,4,5)-trisphosphate) than to PIP_2 *in vitro* and that PIP_3 recruitment of WAVE-2 to the cellular plasma membrane is essential for lamellipodium formation at the leading edge.

Sonderling et al. (2007) observed reduced spine density in the knock-out mouse model of WAVE-1, as well as in knock-in mice that expressed a form of WAVE-1 without the WRP (WAVE-associated Rac GTPase-activating protein, see also chapter 1.8) binding sites. WRP is proposed to function as a signal termination factor for Rac (Sonderling et al., 2002). Surprisingly, overexpressed WAVE-3 in mature hippocampal neurons decreases spine numbers in a manner dependent on its VCA domain (Pilpel and Segal, 2005).

A huge repertoire of actin-binding proteins is additionally required in fine-tuning of actin cytoskeleton dynamics in neuronal development, including Abp1.

1.6 Abp1 – an important member of the family of actin-binding proteins

Mammalian actin-binding protein 1 (mAbp1), also called SH3P7 or HIP-55, has been identified as a signal responsive protein that binds to actin filaments (Larbolette et al., 1999; Kessels et al., 2000, 2001; Han et al., 2003; Le Bras et al., 2004) and interacts directly with ProSAP/Shanks (Qualmann et al., 2004), prominent members of postsynaptic

scaffolds, which promote dendrite spine morphogenesis (Boeckers et al., 2002; Sheng and Kim, 2000). Both the N-terminal ADF-homology region and a helical region of Abp1 independently mediate F-actin binding (Kessels et al., 2000; Fig. 5).

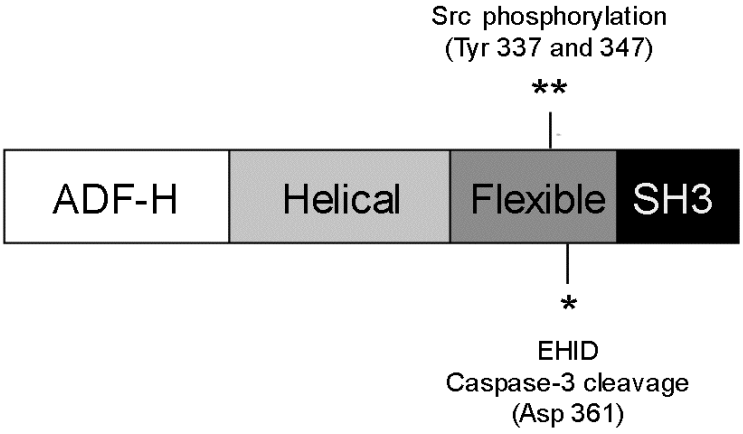

Figure 5. Domain structure of mammalian Abp1. mAbp1 consists of 433 amino acids and contains several protein-protein interaction domains.

Two tyrosine phosphorylation (YxxP) motifs (at position 337 and 347, respectively) serve as a Src kinase target (Larbolette et al., 1999). As a novel key component of the immunological synapse, Abp1 has been reported to modulate T-cell activation. Abp1 hereby interacts with and is tyrosine phosphorylated by ZAP-70, which is a crucial proximal protein tyrosine kinase for T-cell receptor signaling (Le Bras et al., 2004; Han et al., 2003, 2005). A caspase-3 cleavage motif EHID at position 361 is also situated within the flexible region of Abp1. The SH3 domain, which can bind to proline-rich regions, is located at the C-terminus**.** This SH3 domain mediates the interactions of Abp1 with the GTPase dynamin (Kessels et al., 2001), which controls vesicle formation processes, and with ProSAP/Shank proteins. Importantly, Abp1 associates directly with dynamic cortical actin filaments and ProSAPs/Shanks simultaneously and is incorporated into ProSAP/Shank-positive synapses in response to synaptic stimulation (Qualmann et al., 2004). In line with the dynamin interaction, Abp1 was shown to function in the receptor-mediated endocytosis of transferrin (Kessels et al., 2001; Mise-Omata et al., 2003; Connert et al., 2006).

Cleavage of Abp1 by caspase-3 results in separation of the SH3 domain from the other regions. It is possible that removal of the SH3 domain may alter the properties of its ADF-H and so affect cell signaling to and from the actin cytoskeleton during apoptotic process (Chen et al., 2001). Caspases are implicated in many pathways. Well characterized is their implication in apoptosis and stress response pathways (Nunez et al., 1998), and a potential

involvement of caspase-3 in neurodegenerative disorders such as Parkinson, Alzheimer or Huntington's disease is currently discussed (Jellinger, 2000; Ellerby and Orr, 2006).

Drebrin, an additional member of the actin-binding protein family, shares homology with Abp1 through two actin-binding domains (Larbolette et al., 1999; Kessels et al., 2000). Drebrin inhibits the actin-binding activity of tropomyosin and α-actinin (Ishikawa et al., 1994). Through interactions with actin and actin-regulatory proteins drebrin may regulate spine morphogenesis and may initiate clustering of actin filaments and postsynaptic components (Hayashi and Shirao, 1999; Takahashi et al., 2003).

Abp1 has furthermore similarity with cortactin, an F-actin binding protein that has been reported to bind and activate the Arp2/3 actin nucleation machinery both directly and through WASP proteins, and through these interactions plays a role in the stabilization, branching and polymerization of actin filaments (Du et al., 1998; Weaver et al., 2002). Cortactin binds also via its SH3 domain to Shank1 (Du et al., 1998; Sala et al., 2001) and so promotes spine morphogenesis (Hering and Sheng, 2003).

1.7 The postsynaptic density (PSD)

Structural and scaffolding proteins of PSD are interposed between the actin cytoskeleton and the transmembrane proteins in the postsynaptic plasma membrane including neurotransmitter receptors and cell adhesion molecules. Most PSD proteins are concentrated both at spiny and non-spiny excitatory postsynaptic specializations. Specialized postsynaptic PDZ-containing scaffolding proteins bind to the C-terminal regions of glutamate receptors and thus form the first tier of submembrane proteins beneath the postsynaptic membrane (Rao and Craig, 2000; Hering and Sheng, 2001; see also Fig. 6).

PSD-95, a member of the membrane-associated guanylate kinase (MAGUK) protein family, is one of the prominent components of the PSD scaffolds, which binds to multiple components of the PSD and connects ion channels, enzymes, cell adhesion molecules and structural proteins (Kim et al., 1996; Rao and Craig, 2000). Through several protein interaction domains, also Shanks/ProSAPs act as scaffold for many postsynaptic molecules, including the guanylate kinase-associated protein (GKAP) family of PSD proteins (Boeckers et al., 1999; Naisbitt et al., 1999; Romorini et al., 2004), Homer (Tu et al., 1999), and some actin-binding and regulatory proteins such as cortactin (Du et al., 1998), IRSp53 (Soltau et al., 2002), βPIX (Park et al., 2003) and Abp1 (Qualmann et al.,

2004). Their interfacing between glutamate receptor complexes and actin-associated proteins allows for playing a major role in spine morphogenesis and its regulation by synaptic activity (Sheng and Kim, 2000).

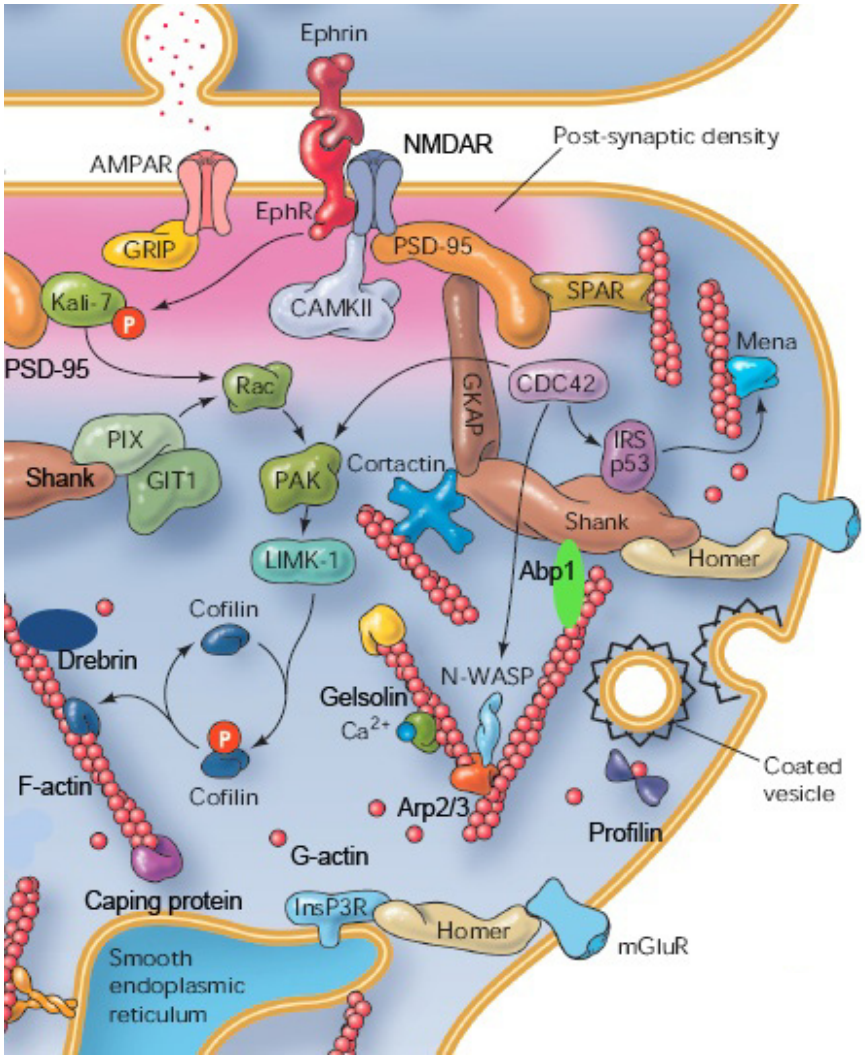

Figure 6. Protein networks within the postsynaptic density (PSD). The postsynaptic density is a specialization of the cytomatrix and the cytoskeleton beneath the postsynaptic plasma membrane facing the active zone. Lateral to the PSD, the postsynaptic plasma membrane contains G protein-coupled metabotropic glutamate receptors (mGluR) and endocytic zones for the recycling of membrane proteins. Neurotransmitter receptors, such as NMDA and AMPA receptors, connect to scaffolding molecules, such as PSD-95, which in turn recruit signaling complexes (e.g., regulators of Rho GTPases, or protein kinases). Actin filaments provide the main structural basis for spine shape. Via a network of protein interactions, actin filaments indirectly link up with the neurotransmittter receptors and other transmembrane proteins that regulate spine shape and development, including Eph receptors. Actin-binding and regulatory molecules such as profilin, drebrin, Abp1, cortactin, cofilin and gelsolin control the extent and rate of actin polymerization (adapted from Calabrese et al., 2006).

Knock-down of Shank1 as well as overexpression of dominant negative constructs of Shank1 reduce spine density in neurons, and overexpression this protein is sufficient to induce formation of functional spines in aspiny cerebellar neurons (Roussignol et al.,

2005). The adaptor protein Homer can bind to mGluR and cooperates with Shank1 in promoting spine enlargements (Sala et al., 2001; 2003).

1.8 Neuropathologies associated with abnormalities in dendritic spines

Dendritic spines are irregularly shaped and have abnormal densities in a number of neurodevelopmental disorders characterized by mental retardation, a deficit in cognitive functioning (Ethell and Pasquale, 2005). Mental retardation, as a disorder in neuronal network connectivity, is associated with abnormalities not only in spines, but also in dendritic branching and thereby in impaired information processing at the cellular and network level (Ramakers, 2002). A study by Purpura (1974) on children with non-specific mental retardation revealed a reduction in dendritic spine number and a predominance of very long and thin spines at the expense of stubby and mushroom-like spines. As the long, thin spine morphology resembled immature spines, the term “spine dysgenesis” was introduced. Fragile X syndrome (FXS), a disorder of excesses synaptic connectivity and protein synthesis, is the most common inherited cause of mental retardation and autism. In FXS, spines are more numerous, longer, tortuous, with irregular dilations and small synaptic contacts, typical of immature spines (Irwin and al., 2000; Negishi and Katoh, 2002).

Mutations or other changes in synaptic actin-binding or signaling proteins, such as αPIX, oligiphrenin-1, PAK, FGD1, which are involved into Rho family GTPase signaling pathways, alter actin dynamics in dendritic spines and cause disorganization of neuronal network formation and eventual neural diseases (Negishi and Katoh, 2002; Newey et al., 2005; Cingolani and Goda, 2008). Sensorimotoric and cognitive deficits were shown by loss of WAVE-1, a member of the WASP/WAVE family proteins. The findings are analogous to the symptoms of patients with 3p-syndrome mental retardation who are haploinsufficient for WRP/MEGAP, a component of the WAVE-1 signaling network (Sonderling et al., 2003).

Abnormal dendritic spines are associated with a number of others neurological and psychiatric conditions, such as schizophrenia, bipolar disorder with psychosis, epilepsy and Alzheimer disease (Fiala et al., 2002; Glantz and Lewis, 2000). The presence of normal shaped spines is a good indicator of the health of the neuron. Spines are an excellent model to study the molecular pathways involved in actin-based cytoskeletal reorganization and motility, and this knowledge can be useful to guide efforts to interfere with spine

abnormalities and improve cognitive function in individuals affected by mental disabilities (Ethell and Pasquale, 2005).

1.9 Aims of the work

Cytomatrices of synaptic contacts, which are localized at the postsynaptic side on dendritic spines and shafts, can organize and link different synaptic functions in time and space and furthermore respond with massive structural reorganizations to different inner and outer cues. The actin cytoskeleton plays a major role in organizing and shaping the postsynaptic compartment. The F-actin-binding protein Abp1 has been reported to bind directly to dynamic F-actin structures and to interact simultaneously via its SH3 domain with members of the ProSAP/Shank family, multidomain scaffolding proteins of the postsynaptic density (PSD) interconnecting glutamate receptors with other synaptic components (Qualmann et al., 2004). ProSAPs may thereby serve as attachment points for the dynamic cortical actin cytoskeleton localizing Abp1 to dendritic spines. Recently, Abp1 have also been shown to influence actin dynamics depended on the Arp2/3 complex-mediated actin nucleation machinery via interactions with and activation of N-WASP (Pinyol et al., 2007). Abp1 therefore represents a prime candidate for mediating and controlling actin cytoskeletal organization and dynamics in neurons, indispensable for the proper establishment as well as plastic reorganization of neuronal networks and synaptic contacts.

Therefore, the aim of this study was to investigate the functions of Abp1 on neuronal cell morphology, including neurite outgrowth and spine formation, in cooperation with its interaction partners. Overexpression of Abp1 and fragments thereof as well as its knock-down in young developing and mature neurons can allow to unravel the molecular mechanism by which Abp1 controls the postsynaptic actin cytoskeleton and thereby modulates spine morphology, and likewise coordinates neuronal network formation by regulating actin filament nucleation and polymerization processes in young hippocampal neurons. Deeper insights into the interaction of Abp1 with ProSAPs should establish the importance of this complex in cytoskeletal rearrangements at the PSD, manifesting in changed spine morphologies, thereby controlling synaptic plasticity processes, a basis for learning and memory formation.

2. Materials and methods

2.1 Materials

2.1.1 Chemical reagents

All chemical reagents of analytical grade used were from the Calbiochem, Invitrogen, Merck, Roche, Roth, Serva and Sigma-Aldrich. Solutions were prepared with water distilled using a Milli-Q System® (Millipore).

2.1.2 Media and antibiotics for bacterial cultures

MEDIUM/REAGENT	COMPOSITION
LB medium	20 g LB broth base powder (Invitrogen) in 1 l H_2O
LB agar	15 g select agar (Invitrogen) in 1 l LB medium.
S.O.C. medium	20 g/l SELECT peptone 140 (Invitrogen); 5 g/l SELECT yeast extract (Invitrogen), 10 mM NaCl, 2.5 mM KCl, 10 mM $MgCl_2$, 10 mM $MgSO_4$, 20 mM glucose.
2-YT medium	31 g 2-YT-Broth (Invitrogen) in 1 l H_2O
Ampicillin	Stock: 50 mg/ml ampicillin sodium salt in water. Final concentration: 100 µg/ml in LB, 2-YT medium or LB agar.
Kanamycin	**25 mg/ml kanamycin disodium salt in water.** Final concentration: 25 µg/ml in LB, 2-YT medium or LB agar.
Tetracyclin	12.5 mg/ml tetracyclin hydrochloride in 50 % (vol/vol) ethanol. Final concentration: 12.5 µg/ml in LB, 2-YT medium or LB agar.

Table 1. Reagents used for growth of bacterial cultures.

2.1.3 Neuronal cell culture instruments, media and reagents

For preparation of primary hippocampal neuronal cultures, these instruments were used (Fine Science Tools, table 2, see the next page to continue):

INSTRUMENT	DESCRIPTION, CATALOG NUMBER
Microspatula	2 mm wide, 12 cm total length
Forceps	DUMONT #5, standard tip, Inox or Dumoxel, 11 cm, No 11251-20 or 11251-30

Forceps	DUMONT #5, biologie tip, Inox or Dumoxel, 11 cm, No 11252-20 or 11252-30 DUMONT #5-45, standard tip, Dumoxel, 11 cm, No 11251-35 DUMONT #7, biologie tip, Dumoxel, 11.5 cm, No 11272-30
Scissors	Wagner, serrated-straight, 12 cm, No 14070-12 Extra Fine Bonn, straight, 8.5 cm, No 14084-08

Table 2. Instruments used for preparation of primary neuronal cultures.

Media and cell culture reagents used were from Gibco and Sigma:

MEDIUM/REAGENT	DESCRIPTION
Trypsin	Stock solution (2.5 %)
DNase I	Stock solution 1 mg/ml in sterile water, working solution 0.1 mg/ml in HBSS with 0.1 ml 1 M Mg_2SO_4 X $7H_2O$
HBSS	Hank's balanced salt solution, Ca^2+, and Mg^2+ free (Invitrogen)
Poly-D-lysine	100 mg/l poly-D-lysine in 100 mM boric acid, pH 8.5, sterile filtered
DMEM	DMEM (Invitrogen), 10% (vol/vol) fetal calf serum, 2 mM L-glutamine, antibioticum/antimycoticum mixture (Gibco): 100 U/ml penicillin, 100 µg/ml streptomycin, 25 µg/ml Chloramfenicol (Fungizone)
Neurobasal	Neurobasal (Invitrogen), 0.5 mM glutamine, 1xB27 (Gibco), antibioticum/antimycoticum mixture (Gibco): 100 U/ml penicillin, 100 µg/ml streptomycin, 25 µg/ml chloramfenicol (Fungizone)

Table 3. Cell culture media and other reagents used.

2.1.4 Bacteria cell strains

E. coli XL1-Blue Bacteria MRF' (Stratagene)

E. coli XL10-Gold® Ultracompetent Cells (Stratagene)

2.1.5 Animals

Rats (Rattus norvegicus) from the strain Wistar, bred in the Leibniz Institute for Neurobiology, were used for the preparation of primary hippocampal cultures.

2.1.6 Antibodies

Primary antibodies:

ANTIBODY	COMPANY/REFERENCE, CATALOG NUMBER	DILUTION (IF)
mouse anti-Flag (M2)	Sigma, F1804	1:500
rabbit anti-Flag	Sigma, F7425	1:500
mouse anti-GFP (mAb 3E6)	Molecular Probes®(Invitrogen), A11120	1:500
rabbit anti-GFP	Abcam, ab290	1:2000
rabbit anti-RFP	BD Biosciences	1:1000
mouse anti-myc (9E10)	Babco, MMS-150P	1:500
rabbit anti-myc (A14)	Santa Cruz, sc-789	1:50
mouse anti-Xpress	Invitrogen, R910-25	1:500-1000
guinea pig anti-syndapin I	Braun et al., 2005	1:150
rabbit anti-Abp1	Fenster et al., 2003	1:50
mouse anti-MAP2	Sigma, M2320, M9942	1:500
rabbit anti-MAP2	Abcam, ab24640	1:500
guinea pig anti ProSAP1	T. Böckers (University Ulm, Germany)	1:1000
rabbit anti NMDA2B	Abcam	1:200
mouse anti-PSD95	Abcam	1:500
mouse anti-synapsin	Synaptic Systems	1:1500
rabbit anti-synapsin	Synaptic Systems	1:1500
guinea pig anti-Piccolo	E. Gundelfinger (Leibniz Institute for Neurobiology, Germany)	1:1500
rabbit anti-Arp3	M.D. Welch (University of California, Berkeley, USA)	1:150

Table 4. Primary antibodies used in immunofluorescence assays (IF)

Secondary antibodies (table 5 on the next page):

ANTIBODY	COMPANY/REFERENCE CATALOG NUMBER	DILLUTION (IF)
Alexa Fluor® 350, 488, 568, 647 goat anti-mouse IgG	Molecular Probes®(Invitrogen)	1:1500
Alexa Fluor® 350, 488, 568, 647 goat anti-rabbit IgG	Molecular Probes®(Invitrogen)	1:1500
Alexa Fluor® 488, 647 goat anti-guinea pig IgG	Molecular Probes®(Invitrogen)	1:1500
FITC goat anti-guinea pig IgG	BD Biomedicals	1:750
Cy5 donkey anti-mouse IgG	Dianova	1:500
Cy5 donkey anti-rabbit IgG	Dianova	1:500

Table 5. Secondary antibodies used in immunofluorescence assays (IF).

2.1.7 Expression constructs

CONSTRUCT	AMINO ACIDS	VECTORS
mAbp1 full length (7)	1-433	pRK5-myc , pEGFP
mAbp1ΔSH3 (6)	1-370	pRK5-myc
mAbp1_ADFH_helical (5)	1-281	pRK5-myc
mAbp1_ADFH (4)	1-163	pRK5-myc
mAbp1_helical (3)	164-281	pRK5-myc
mAbp1_flex_SH3(9)	282-433	pRK5-myc, pEGFP
mAbp1_flex_SH3mut (9*) (P425L, G422R)	282-433	pRK5-myc
mAbp1_SH3(2)	371-433	pRK5-myc
mAbp1_SH3mut (2*) (P425L, G422R)	371-433	pRK5-myc
rat N-WASP CA	464-501	pEGFP
pRNAT- Abp1RNAiSq1 (generated according to recommendations of GenScript Corporation)	Target sequence 172-192	pRNAT_H1.1 (GFP or mRFP, see also chapter 2.2.1.8)
pRNAT- Abp1RNAiSq2 (generated according to recommendations of GenScript Corporation)	Target sequence 181-201	pRNAT_H1.1 (GFP or mRFP, see also chapter 2.2.1.8)

pRNAT- Abp1RNAiSq3 (generated according to recommendations of GenScript Corporation)	Target sequence 67-87	pRNAT_H1.1
mAbp1_RNAi_resistant_Sq1 Residues mutated are underlined	1-433 with silent mutations in target sequence 172-192 CAGCGGGAAG	pCMV-2B
pRNAT- N-WASP_RNAi	Yamaguchi et al., 2005	pRNAT_H1.1
pRNAT- Arp3_RNAi	Steffen et al., 2006	pRNAT_H1.1
pRNAT-scrambled_RNAi	Yamaguchi et al., 2005	pRNAT_H1.1
pSuperProSAP2 _RNAi	From C. Sala (University of Milan, Italy)	pSuper
ProSAP1$^{\Delta Abp1\ interf.}$	240-1252 Δ302-319, 407-414, 946-957	pEGFP

Table 6. Mammalian expression constructs used for overexpression or knock-down of proteins in neuronal cell cultures. pRK5-myc vector and constructs thereof are described by Kessels et al. (2001), pEGFP vector were from Clontech, pRNAT_H1.1 vector were from Genscript, pCMV-2B vector were from Stratagene, pSuper vector and construct thereof are described by Roussignol et al., 2005.

2.2 Methods

2.2.1 Recombinant DNA techniques

2.2.1.1 Generation and transformation of competent bacterial cells

2 ml 2-YT/tetracyclin medium was inoculated with E. coli XL1-Blue or XL10-Gold cells and grown overnight at 37ºC and 300 rpm. The overnight culture was diluted 1:100 with 2YT/tetracyclin medium, was grown again at 37ºC and 300 rpm and harvested during mid-log phase.

For preparation of electrocompetent cells, harvested XL-1 Blue cells were chilled for 10 min in ice-cold water and centrifuged at 2500 g for 10 min. The cell pellet was washed twice with ice-cold sterile water and pelleted at 3000 g for 10 min. Cells were resuspended in 10% (vol/vol) ice-cold sterile glycerol, dispensed into 75 µl aliquots and stored at -80ºC. Electrocompetent cells were transformed through electroporation using a Gene Pulser (BioRad). 0.4-0.6 µg DNA were resuspended in cells thawed on ice, and this mixture was applied for electroshock (C = 25 µF, R = 200 Ω and U = 2.5 kV). After electroporation the

cells were immediately resuspended in S.O.C. medium, incubated for 1 h at 37ºC and 600 rpm and plated on LB agar plates containing the appropriate antibiotics.

For preparation of chemical competent cells, harvested XL-1 Blue cells were also chilled for 10 min in ice-cold water and centrifuged at 2500 g for 10 min. The cell pellet was washed twice with ice-cold sterile water and spun at 3000 g for 10 min. The cell pellet was resuspended in ice-cold sterile transformation and storage solution (20 % (wt/vol) PEG3350, 10 % (vol/vol) DMSO, 100 mM $MgCl_2$ in LB medium, pH 6.5) (Chung et al., 1989). Cells were dispensed into 100 µl aliquots and stored at -80ºC.

To transform chemical competent cells, 0.4 - 0.6 µg DNA were added to cells thawed on ice. After 15 min incubation on ice cells were resuspended in S.O.C. medium, grown for 1 h at 37ºC and 600 rpm and plated on LB agar plates containing the appropriate antibiotics.

For preparation of heat-shock competent cells, harvested XL10-Gold cells were chilled for 15 min in ice-cold water and centrifuged at 3300 g for 10 min. The cell pellet was washed twice in ice-cold sterile $CaCl_2$ solution (60 mM $CaCl_2$, 15 % (vol/vol) glycerol, 10 mM Pipes, pH 7.0) and this cell suspension was incubated for 30 min on ice. Finally, cells were resuspended in 1/100 of the culture volume of ice-cold sterile $CaCl_2$ solution, dispensed into 100 µl aliquots and stored at -80ºC.

To transform heat-shock competent cells, 0.4-0.6 µg DNA were added to cells thawed on ice. Subsequently, the mixture was incubated 5 min on ice, 50 sec at 42ºC and 2 min again on ice. After the heat shock, cells were resuspended in S.O.C. medium, incubated 1 h at 37ºC and 600 rpm and subsequently plated on LB agar plates containing the appropriate antibiotics.

2.2.1.2 Plasmid DNA amplification

Used buffers:

P1: 10 mM EDTA, 50 mM Tris/HCl pH 8.0, 100 µg/ml RNAse)

P2: 0.2 M NaOH, 1% (wt/vol) SDS

P3: 3 M potassium acetate, pH 5.5

Plasmid DNA was prepared at a small analytical scale using the alkaline lysis method for clone screening and at a larger scale to obtain high quantities and purities of the desired constructs using commercial preparation kits.

For alkaline lysis, pellets obtained from 2 - 4 ml of an overnight bacterial culture were resuspended in 0.2 ml of buffer P1. Subsequently, 0.2 ml of buffer P2 was added to this solution to denature proteins, DNA and hydrolyze RNA. The suspensions were neutralized after 5 min incubation at the room temperature with 0.2 ml of chilled buffer P3, which induces the precipitation of the denatured proteins, chromosomal DNA and SDS detergent. The mixture was incubated on ice for 10 min and centrifuged at 14,000 rpm to remove precipitates. After addition of 0.35 ml isopropanol to the DNA-containing supernatants, they were incubated 10 min on ice and again spun at 20000 g for 10 min. Pelleted DNA was washed twice with 70% (vol/vol) ethanol, resuspended in 10 mM Tris/HCl (pH 8.0) and stored at -20ºC.

Large-scale plasmid preparations were performed from 50-100 ml bacterial overnight cultures using Plasmid Midi Kit or EndoFree Kit (Nucleobond, Qiagen) according to the protocol provided by the manufacturer. Plasmids for transfection of mammalian cells were purified exclusively using such commercial kits.

2.2.1.3 Measurement of DNA concentrations

DNA concentrations were measured at 260 nm with a Pharmacia Gene Quant. The following formula was used:

Double-stranded (ds) DNA: OD*x* 50*x* dilution factor = X µg/ml

2.2.1.4 Polymerase chain reaction (PCR)

PCR is a widely used technique to amplify a piece of DNA by *in vitro* enzymatic replication. The heat-stable DNA polymerase assembles a new DNA strand of the nucleotides, using single-stranded DNA of interest as template and DNA primers, required for initiation of DNA synthesis. In thermal cycling steps, at high temperatures, double stranded DNA is separated (denaturation), primers are annealed, and during short subsequent step at appropriate annealing temperatures DNA synthesis is performed by addition of nucleotides corresponding to the sequence of the template DNA to the 3' end of the primers.

To construct ProSAP1$^{\Delta Abp1\ interf.}$, first ProSAP1 pieces were generated by PCR and cloning into pEGFP. Deletion mutants were generated by fusion of these pieces and cloning into pEGFP. PCR reactions were performed at appropriate temperature and time conditions

using 0.5 µM of both forward and reverse primers, 200 µM of deoxynucleoside triphosphate (Roche), 2.5 units of DNA polymerase (Strategene) and 20-50 ng of template DNA. The plasmids generated by PCR were verified by sequencing.

2.2.1.5 Restriction digest of DNA

Restriction endonucleases are enzymes that cleave both plasmid DNA strands after recognizing restriction sites (nucleotide sequences), which are specific for each endonuclease. To clone a cDNA fragment into a vector, both the insert and the vector were subjected to a restriction reaction using the appropriated restriction endonucleases, buffers, reaction temperatures and time conditions (normally 3 h at 37ºC) recommended by the manufacturer (New England Biolabs or Fermentas).
Since double digests are rarely 100% efficient, vectors were dephosphorylated with alkaline phosphatase (Roche) to prevent the religation of the cohesive ends.

2.2.1.6 Separation of DNA fragments on agarose gels

Used buffers:
TAE: 40 mM Tris, 0.2 mM acetic acid, 1 mM EDTA, pH 7.6
6 x loading buffer: 30% (vol/vol) glycerol, 50 mM EDTA, 0.25% (wt/vol) bromphenol blue, 0.25% (wt/vol) xylene cyanol
Cut plasmid DNA was separated horizontally, according to their size, by agarose gel electrophoresis. For gel preparation, 0.5-1.5% (wt/vol) agarose was melted in TAE buffer. 0.1 µg/ml ethidium bromide, a DNA-marker detectable by UV light, was added to the cooled agarose gel solution, and the gel was poured into a gel-chamber. 6x loading buffer was added before loading the DNA samples into the wells of solid agarose gel. As reference size standards SmartLadder (Eurogentec) or 100 bp DNA Ladder (New England Biolabs) were used. Gels were run at 60-70 V in TAE buffer and were documented with the gel documentation system Gel Doc (BioRad).

2.2.1.7 Purification of DNA from agarose gels

After separation of the DNA fragments by electrophoresis, the agarose gel was placed on a Transilluminator (Stratagene) to visualize the localization of the DNA pieces. The required DNA-containing area was cut out with a scalpel, and the DNA was isolated from the

agarose gel using the UltraClean 15 purification kit (MO BIO Laboratories Inc.) following the instructions of the manufacturer.

2.2.1.8 Design and generation of vector-based siRNAi tools

Vector-based siRNA technology involves cloning a small DNA insert of about 70 bp into a commercially available or custom vector. This vector can be transfected into cells, where the DNA insert leads to generation of the short hairpin RNAs. The hairpin RNA is rapidly processed by the cellular machinery into double-stranded siRNA. The siRNAs are then incorporated into an RNA-induced silencing complex (RISC) and unwound into single-stranded siRNAs. Next, the single-stranded siRNAs guide the RISC complex to the target mRNAs for destruction, causing RNA interference. Depending on the amount of siRNA expressed and its inhibitory efficiency, expression of the target gene can be either completely blocked or measurably suppressed.

siRNA design tools from Ambion (siRNA Target Finder), Clontech (RNAi Target Sequence Selector), Dharmacon (Custom siRNA Design Tool) and Invitrogen (Block-It™ RNAi Designer) were used to select targeting sequences for Abp1 knock-down in rat and mouse and human species:

Sq1 AA**C AG**C GG**G** AA**G** GTG ATG TAC (172-192)
Sq2 AAG GTG ATG TAC GCC TTC TGC (181-201)

Sequences were choused using these guidelines:

1. Avoiding first 100 nt downstream of the start codon and last terminal 100 nt of the sequence.
2. Sequence is 21 nt long, with guanyne/cytosine ratio so close as possible to 50 %, preferably start with AA (these too nucleotides must be not included in the sense sequence of siRNA construct)
3. Database search for specificity (if design toll do not include it).

Sq3 (AAG TCC CCG ACC GAC TGG GCT, nt 67-87), used to make the third siRNAi construct of Abp1, is published by Mise-Omata (2003) for knock-down Abp1 in human. Underlined nucleotide is different in mouse and mouse species.

Chemically synthesized oligonucleotides (MWG Genomic Company) for the 3 siRNA constructs were annealed in buffer containing 2x (200 mM NaCl, 100 mM HEPES, pH = 7.4) and phosphorylated using reaction conditions generously provided by A. Braun:

Cycles	**Time and temperature**
<u>Annealing</u> 1X 1X 1X 66X <u>Phophorylation</u> 1X 1X 61X	 4 min at 90°C (condition 1, denaturation) 10 min at 70°C (condition 2, annealing) 25 sec at 70°C (condition 3, cooling down) Cooling down from condition 3 about ever 1°C with 0,3°/s until 4°C 30 min at 37°C (condition 1, incubation) 20 min at 65°C (condition 2, inactivation) Cooling down until 4°C (ever 1°C 10 s and 0,3°/s)

Oligonucleotides were subsequently cloned into pRNAT H1.1(Hygro)GFP (from GenScript) vector using BamHI-HindIII restriction sites giving rise to the following inserts:

Forward (5`- 3´) BamHI (GATCC) – sense – loop (TTGATATCCG) – antisense – TTTTTTA

Reverse (5`- 3´) HindIII (AGCTT) – AAAAAA – sense – loop (CGGATATCAA) – antisense – G

Residues mutated for generation of an RNAi-resistent Abp1 are underlined in Sq1. The construct was kindly provided by R. Pinyol.

GFP-siRNA construts of Abp1 were transformed into RFP-siRNA constructs by exchanging GFP-coding sequence using the NheI – XhoI restriction sites in pRNAT H1.1(Hygro)GFP by a mRFP-coding sequence taken from pc DNA3.1-mRFP-HA-GEX vector, which was kindly provided by Dr. R. Frischknecht.

2.2.1.9 Inserting of a DNA fragment into a vector

To insert a DNA fragment into a vector, T4 DNA ligase (Fermentas) was used. The ligation reactions were performed for 16 h at 16 ºC, the mostly used proportion of

vector/insert was 1/7.5 µg. The reaction product was transformed into electrocompetent/heat-shock competent E. coli XL1-Blue/XL10-Gold cells.

2.2.1.10 Analyzing of cloned or subcloned DNA constructs

Clones isolated after transformation of ligation reactions were analyzed by restriction digest for correct size, insertion and orientation. Cloned PCR products were additionally sequenced for analysis (SEQLAB Sequence Laboratories Goettingen, GmbH).

2.2.2 Cell culture methods

2.2.2.1 Mammalian cell cultures (primary hippocampal neurons)

Hippocampal neuronal cultures were prepared from embryonic day 18–19 rat embryos according to Brewer et al. (1993). Coverslips (Menzel-Gläser) with 12 mm diameter were washed 2 times with sterile water, autoclaved 3 h by 200ºC, and then coated with poly-D-lysine (see materials) in 24-well multidishes (Nunc). After 1 h incubation, coverslips were washed 2 times with sterile water, 1 time with HBSS and stored in incubator until plating.
A pregnant rat was anesthetized with lethal dose of halothane (Sigma), decapitated, and embryos were taken out. Whole embryonic brain hippocampi were cut out under extractor hood from both hemispheres using special instruments (FST, see materials) and microscope (Carl Zeiss); meninges were removed. After this preparation hippocampi were collected into Ø 3 cm Petri dish, washed 3 times with HBSS in a 15 ml Falcon tube (Nunc) and left in 1.8 ml HBSS. 200 µl of 2.5 % trypsin was added to 1.8 ml HBSS containing the hippocampi and this mixture was incubated at 37ºC for 20 min. The digested hippocampi tissue was then washed 5 times and left in 1.6 ml HBSS. 0.4 µl DNAseI solution (see materials) was added, and mixture was first passed 3 times through a sterile 20 G needle (outside diameter 0.9 mm, length 40 mm) and then 3 times through a 26 G needle (outside diameter 0.45 mm, length 25 mm) using a 2 ml syringe. The obtained cell suspension was finally passed through a 125 µm nylon mesh and diluted in 18 ml DMEM medium.
The amount of cells per 500 µl (well) was counted using a Neubauer counting-chamber. Cells were diluted in DMEM, and 50-60.000 cells per well were seeded into 24-well

multidishes. The plated cells were grown at 37ºC, with 5% CO_2 and 95% humidity in DMEM medium, which was replaced after 24 h by Neurobasal medium (see materials).

2.2.2.2 Transfection

Hippocampal primary neuronal cultures were transfected at the 1-st, 4-th, or 10-12-th day after plating (DIV) using Lipofectamine 2000 according to the manufacturer's instructions. Before transfection, growth medium was replaced by 1 ml Neurobasal medium without antibiotic/antimycotic supplements. 1 µl Lipofectamine 2000 (Invitrogen) was diluted in 50 µl Opti-MEM (Gibco) per well. After 5 min incubation at room temperature the lipofectamin solution was mixed with 1-2 µg DNA diluted in 50 µl Opti-MEM per well. This mixture was incubated for 20 min at room temperature and then added to the cells. The transfection medium was removed after 4 h, and the cells were washed with Neurobasal medium without any supplements, and then Neurobasal medium with supplements was added. Cells were then grown for 48-80 hours after transfection and fixed (see 2.2.3.1).

2.2.3 Immunocytochemistry

2.2.3.1 Immunostaining of endogenous proteins

Used buffers:
PBS: 2.7 mM KCl, 1.5 mM KH_2PO_4, 137 mM NaCl, 8 mM Na_2HPO_4, pH 7.4
Block solution: 10% (vol/vol) horse serum, 5% (wt/vol) BSA and 0.2 mg/ml saponin in PBS
Mowiol: 10% (wt/vol) Mowiol (4-88), 25% (wt/vol) glycerol, 100 mM Tris/HCl, pH 8.5

For immunostaining of endogenous and overexpressed proteins, the culture medium was removed, and the coverslips with the hippocampal cultures were directly fixed for 6-8 min with 4% (wt/vol) paraformaldehyde (in PBS) at the room temperature. The paraformaldehyde was removed, and after quenching with 25 mM glycine (in PBS, pH 7.4) for 30 min cells were blocked and permeabilized with block solution containing saponin for 1 h. Samples were then incubated with the primary antibodies for 1.5 h, washed three

times with block solution and incubated with the secondary antibodies for 1 h. Finally, they were subsequently washed with block solution, PBS and water and then embedded in Mowiol.

2.2.3.2 Microscopy and quantitative analyses of spine morphology

Immunofluorescence images were acquired with a Carl Zeiss Axioplan 2 microscope equipped with a CCD camera 2.1.1 from Diagnostic Instruments and processed in MetaVue Software. Morphometric measurements were performed with the aid of NIH Image software (ImageJ). Each experiment was performed on two to four independent coverslips and usually three times with independent neuronal preparations. To ensure maximal reliance and reproducibility, all experiments included the full set of the different controls (both positive and negative) for reference. Neurons for morphometric analyses were sampled quantitatively from each coverslip. In most cases, cells were cotransfected with GFP or mRFP to visualize detailed morphology and to outline the spines. Additional quantitative morphometric analyses as well as high-resolution double-labeling experiments confirmed that also myc–Abp1 immunoreactivity outlines the morphology of the cells in a manner indistinguishable from GFP and mRFP, respectively.

To determine spine size, 300–1000 spines (from 6–19 neurons) were measured for each condition. For spine length, the distance from the base of the neck to the furthest point on the spine head was measured.

Spine group definitions are according to Hering and Sheng (2001). Heads of mushroom spines were measured taking the maximal width of the spine head perpendicular to the axis along the spine neck. For each condition, individual spine dimensions were grouped first and averaged per neuron; means from multiple individual neurons were then averaged to obtain a mean (SD and SEM, respectively) for the population of neurons.

For spine and synaptic puncta density measurements, all clearly evaluable areas of 50–100 µm of primary dendrites from each imaged neuron were used. This excludes a potential bias during area selection. Each individual spine present on the entire dendrite parts was included in the spine density examinations. For the determination of synapse number, each synapse highlighted by presynaptic markers and postsynaptic markers, respectively, was counted, i.e., synapses at both spines and dendrites were included.

Statistical significance was calculated using two-tailed Students t-test on Microsoft Excel Software.

3. Results

3.1 The role of Abp1 in modulating spine morphology

3.1.1 Abp1 promotes spine lengthening

ProSAP/Shank proteins are significant scaffold proteins in the postsynaptic density (PSD), where molecular machinery links synaptic transmission to various signaling cascades and cytoskeletal components. Together with other scaffolds in the PSD, such as PSD-95 and Homer, ProSAP/Shanks can influence synapse development and spine morphogenesis, presumably by recruiting interacting proteins to postsynaptic sites (Kim and Sheng, 2004). They interact also with several regulators of the actin cytoskeleton, including SH3-domain containing proteins cortactin (Du et al., 1998; Naisbitt et al., 1999) and Abp1 (Qualmann et al., 2004). The actin cytoskeleton is a likely target of the molecular mechanisms regulating spine morphology (reviewed in Matus, 2000). Actin-interacting proteins, such as drebrin, cortactin and SPAR, have been shown to alter spine morphology (Hayashi and Shirao, 1999; Hering and Sheng, 2003; Pak et al., 2001). In this line, comes the question: how can Abp1, a protein containing two independent actin-binding modules (Kessels et al., 2000), influence spine shape?

Actin-binding domains of Abp1 (Fig. 7A) were overexpressed individually and in different combinations with other domains (Fig. 7B-G) in hippocampal neurons. To outline spine shape, cells were cotransfected with green (GFP) or red (mRFP) fluorescent proteins. The fluorescence of both marker proteins that were used for control purposes and for double-transfections with Abp1 constructs revealed identical spine shape parameters; the morphology of mature spines was analyzed by quantitative measurements (Fig. 7H, I). The Abp1 protein and fragments thereof were almost equally distributed within the cytosol of transfected neurons (Fig. 8). They filled the cell bodies and also reached peripheral dendrites and spines (magnified images in Fig. 8).

Transfections with full-length Abp1 significantly increased spine length (Fig. 7C) compared to control (Fig. 7B). Quantitative examinations of 500 - 1000 spines per group confirmed this finding and revealed an average length of spines of 1.56 ± 0.09 µm (mean ± SEM) in Abp1-overexpressing cells compared to 1.30 ± 0.07 µm for control cells (Fig. 7H, I). This effect was also observed upon overexpression of an Abp1ΔSH3 deletion mutant. Also deletion of the flexible domain, the target site for Src family kinases (Larbolette et al.,

1999), did not abolish the increased spine length effect. The ADF-H and helical domains of Abp1, which can independently bind the F-actin (Kessels et al., 2000), were sufficient to increase spine length not only in combination but also individually (Fig. 7H, I).

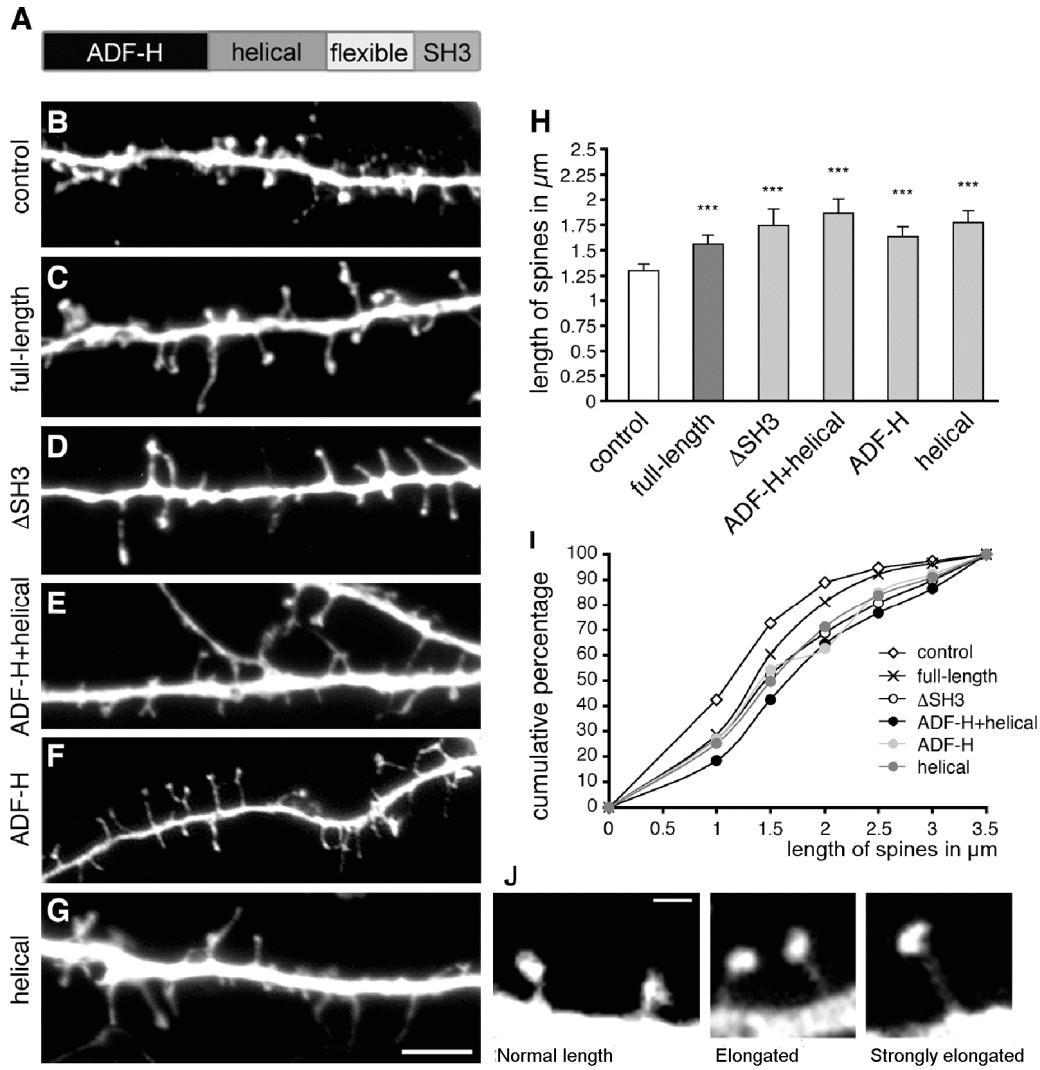

Figure 7. Expression of Abp1 full-length and fragments thereof containing the F-actin binding domains induce increased spine length. *A*, Domain structure of Abp1. *B-G*, Images show the changes in spine morphology of hippocampal neurons at DIV14 double-transfected at 12 DIV with GFP and full-length Abp1 or deletion constructs thereof. In comparison to neurons transfected with GFP as control (*B*), neurons double-transfected with myc-tagged Abp1 full-length (*C*), Abp1ΔSH3 (*D*), ADF- H+helical (*E*), ADF-H (*F*) and helical (*G*) show an increase in spine length. In all cases the GFP channel used to evaluate morphology is shown. Bar 5 µm. *H*, Mean of spine length (µm ± SD) in neurons transfected with the constructs indicated obtained by quantitative analysis confirm that the spine elongation induced by Abp1 and its F-actin binding domains is highly significant (***p < 0.001). *I*, Cumulative distribution of spine length in neurons transfected with the constructs indicated. *J,* Average samples of different spine length: normal (about 1 µm), elongated (about 1.5 µm) and strong elongated (more than 2 µm). Bar, 1 µm.

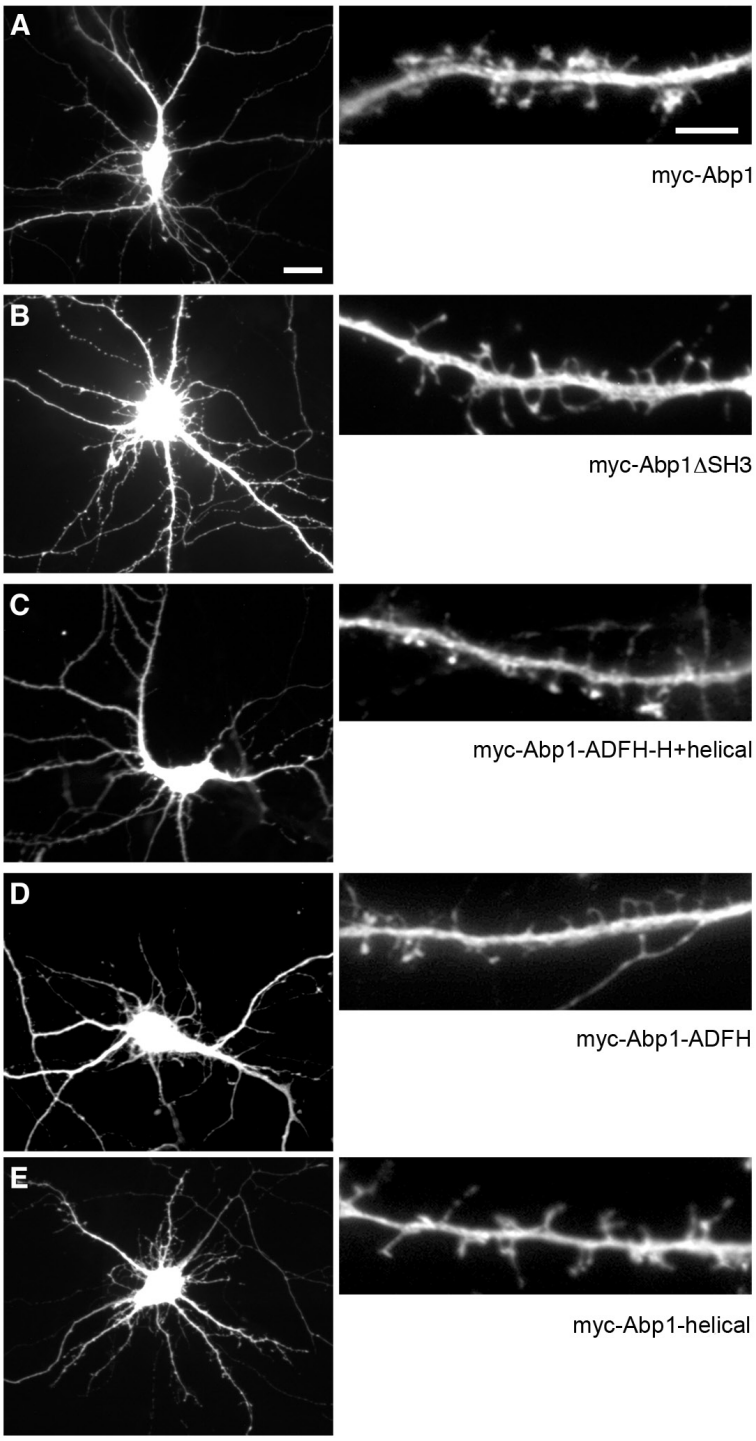

Figure 8. Expression of full-length Abp1 and fragments thereof containing the actin-binding domains in primary hippocampal neurons. Images show the distribution of transfected myc-tagged Abp1 full-length (*A*), ΔSH3 (*B*), ADF-H+helical (*C*), ADF-H (*D*), and helical (*E*) domains in primary hippocampal neurons at DIV14 (2 days after transfection). Right panels represent enlarged examples of the distribution of the proteins along the dendrites. Bars, 20 µm (*A*-*E*) and 5 µm (higher magnification of neurites).

Cumulative analyses (Fig. 7I) showed different effects between overexpression of full-length Abp1 and other Abp1 constructs comprising the actin-binding modules. The full-length curve differed from control in spine size groups between 1 µm and 1.5 µm, but

almost converged with the control curve above spine sizes of 2 µm. Spines of 2.5 µm and longer were very rare in both conditions. In contrast, in neurons overexpressing Abp1 fragments comprising the actin-binding but lacking SH3 domain, about 20% of the spines were 2.5 µm in length and longer (Fig. 7I). Fig.7J shows representative examples of spines of averaged normal (about 1 µm), increased (about 1.5 µm) and strongly increased (more than 2 µm) length.

All four established dendritic spine morphology groups (i.e. filopodia & thin spines, stubby spines, branched spines and mushroom spines, see Fig. 9A-D for examples) were next analyzed. Spine shape is developmentally regulated; generally progressing from filopodia in early development to "stubby", "thin" or "mushroom" shaped spines in mature brain or cultured neurons (Ziv and Smith, 1996; Harris, 1999). In the rat hippocampal neurons used in experimental work (14 DIV), majority (~ 50%) of the dendritic spines on neuronal cells were mushroom shaped (Fig. 3A, 5D), with a thin neck and a single well-defined globular head, where typically synapses are formed. The responsiveness of thin spines to increases and decreases in synaptic activity suggest that they are "learning spines", whereas the stability of mushroom spines predicates that they are "memory spines" (Bourne and Harris 2007), therefore is of particular importance to examine subclasses of spines.

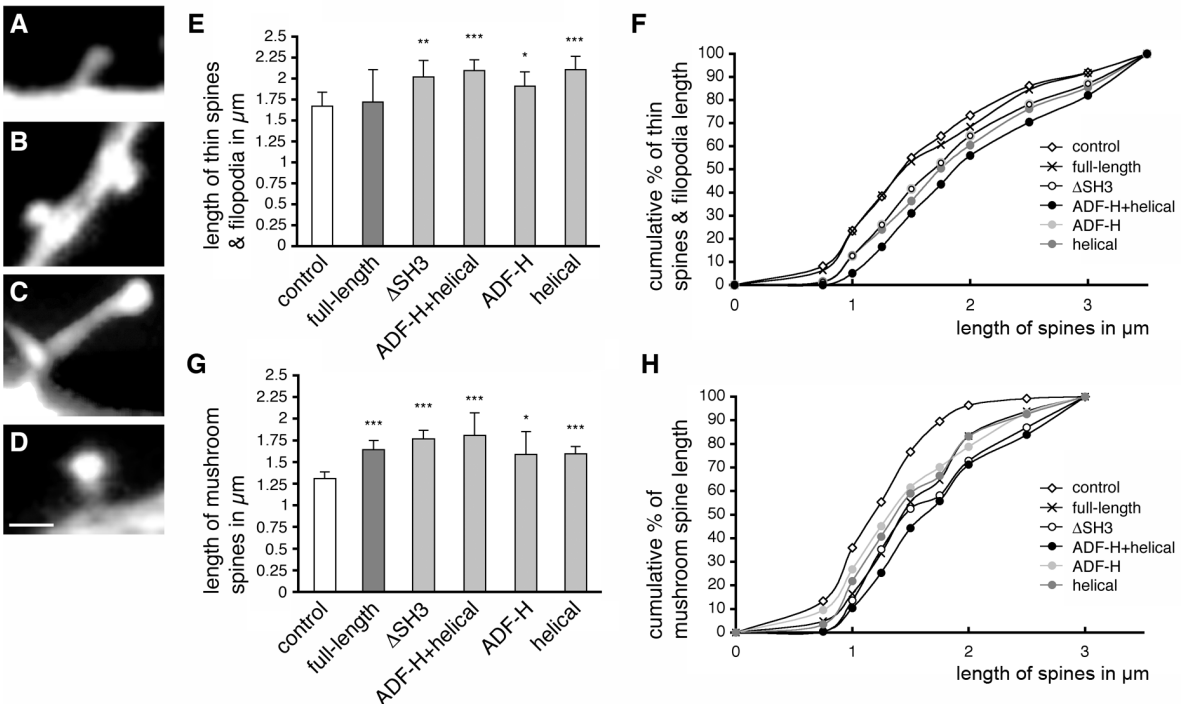

Figure 9. Abp1 overexpression results predominantly in elongation of mushroom-type spines. *A-D*, Typical examples of thin (*A*), stubby (*B*), branched (*C*) and mushroom (*D*) types of spines. *E-H*, whereas the actin-binding domains of Abp1 increase the length of both thin spines & filopodia (*E, F*) and mushroom

spines (*G, H*), overexpression of the full-length protein selectively affects the length of mushroom spines. The means of thin spines & filopodia length (*E*) and mushroom spine length (*G*) (µm ± SD) as well as the cumulative distribution of thin spines & filopodia (*F*) and mushroom spine (*H*) length in neurons transfected with the constructs indicated is depicted (*p < 0.05, **p < 0.01, ***p < 0.001). Bar, 1 µm.

The two major groups of spines, thin spines & filopodia and mushroom spines, showed observable differences in their morphology upon overexpression of Abp1 deletion mutants in comparison to control neurons (Fig. 9E-H). The length of thin spines & filopodia in full-length Abp1-overexpressing cells was unaffected compared to control, but the Abp1 deletion mutants used, comprising the actin-binding domains of Abp1, led to significant length increases (Fig. 9E, F).

In contrast, the length of mushroom spines was highly significantly increased not only upon overexpression of the actin-binding domains but also upon overexpression of full-length Abp1 (Fig. 9G, H). As the cumulative analyses show (Fig. 9H), a decisive part of mushroom spines was about 2 µm long and some even longer. This increase can be explained by a specific lengthening of the spine neck, because head sizes were unchanged (see also Fig. 16). Such elongated spines were almost absent in control cells (Fig. 9H).

To analyze, whether these modified spines developed a postsynaptic apparatus and have presynaptic contacts, immunofluorescence analysis was performed with antibodies against Piccolo (Fig. 10A-C), a prominent protein of the presynaptic active zone, and with antibodies against the postsynaptic scaffold proteins ProSAP1/Shank2 (Fig. 10D-F) and PSD-95 (data not shown). Assay verified that elongated spines that appeared after overexpression of Abp1 contain postsynaptic components and are in contact with presynapses.

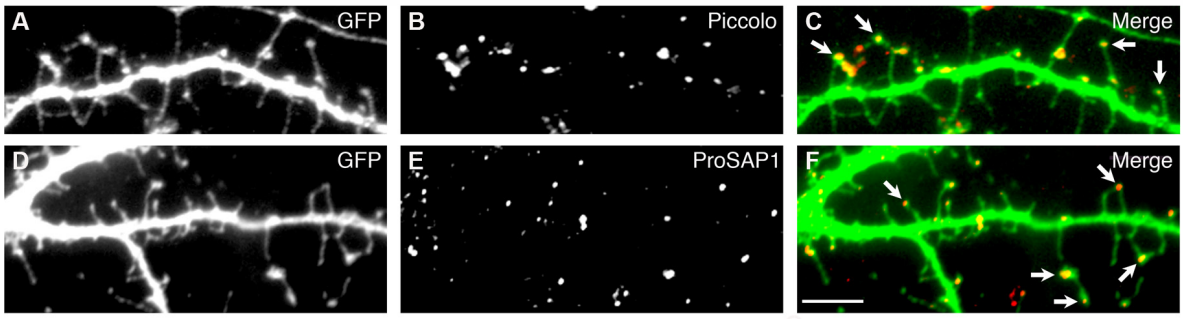

Figure 10. Synaptic integration of spines morphologically altered by Abp1 overexpression. Primary hippocampal neurons were cotransfected with GFP as a volume marker (*A, D;* green in merged images *C* and *F*) and myc-tagged full-length Abp1 and stained at DIV14 for presynaptic (Piccolo; *B*; red in merged image *C*) and postsynaptic (ProSAP1; *E*; red in merged image *F*) marker proteins. Arrows in the merged images *C* and *F* highlight elongated mushroom spines that contain the PSD component ProSAP1 (*C*) and are contacted by presynaptic active zones marked by Piccolo immunoreactivity (*F*), respectively. Bar, 5 µm.

3.1.2 Abp1 facilitates mushroom-type spine formation in two ways: via its ability to directly bind F-actin and via SH3 domain-mediated interactions

An excess of full-length Abp1 led not only to remarkable effects on spine length but also to the slightly increase of spine density in neurons (Fig. 11A). Extensive morphological analyses showed no significant increase in the density of thin spines & filopodia (Fig 11B),

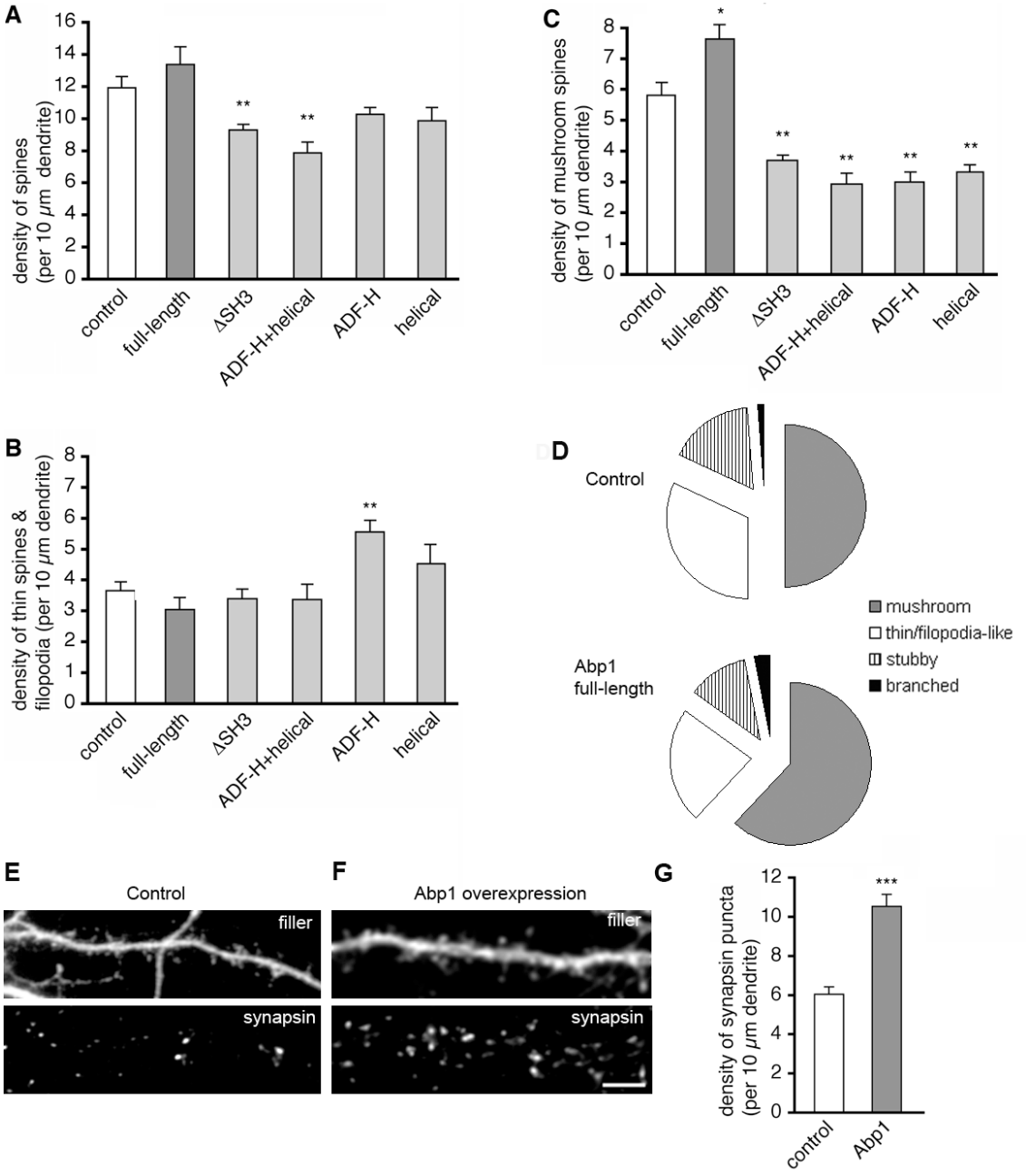

Figure 11. Effects of full-length Abp1 and the actin-interaction domains of Abp1 on the density of mushroom-shaped spines and synapses. Diagrams depict the means ± SEM for the density of spines of all types (*A*) and their individual morphology groups (*B,* thin spines & filopodia; *C*, mushroom spines) for neurons transfected with a cell filling molecule (GFP, mRFP) alone (control) as well as cotransfected with Abp1 and fragments thereof as indicated (*p < 0.05, **p < 0.01). *D,* Relative abundance of the four different spine classes in control and Abp1-overexpressing neurons. *E-F,* Anti-synapsin immunostaining (lower panels) of control (*E*) and Abp1-overexpressing cells (*F*). Bar, 5 µm. *G*, Quantitation of synapse density, as

defined by anti-synapsin immunostaining, in control and Abp1-overexpressing neurons show a highly significant increase in synapse density upon Abp1 overexpression (***$p < 0.001$).

whereas the density of spines with readily distinguishable heads – mushroom-type spines – was clearly increased in Abp1 overexpressing neurons. Compared to control neurons, this density increase was statistically significant ($p < 0.05$; Fig. 11C, D). In contrast, both actin-binding domains expressed individually or in combination had even negative effects (Fig. 11C). This finding that only full-length Abp1 can induce an increased density of mushroom spines suggested a crucial importance of the non-actin-binding C-terminus of Abp1 on mushroom spine density effect. Experiments with a deletion mutant solely lacking the C-terminal SH3 domain showed that not the flexible domain but the SH3 domain is crucial (Fig. 11C).

Further examinations of the Abp1 overexpression effect in spines were orientated towards synapse formation. Is the increase in mushroom spine density proportional to the abundance of synaptic contacts? Quantitation of synapsin-positive puncta in Abp1-overexpressing neurons indeed showed a clear and highly significant increase in synapse number (Fig. 11E-G).

3.1.3 The SH3 domain of Abp1 has a dominant-negative effect on spine density and mushroom spine formation

Is the SH3 domain maybe not only crucial but also sufficient for the increase in spine density overexpression? To answer this question, the entire C-terminal part of the protein - a construct lacking only the both actin-binding domains (flex+SH3) – as well as the SH3 domain alone were overexpressed in neuronal cells (Fig. 12). Immunosignals of both Abp1 deletion mutants were strongest in the cell bodies but additionally a distribution into peripheral dendrites and postsynaptic spines was observed (Fig. 13). The two Abp1 deletion mutants caused a prominent decrease in spine density (Fig. 12B, D) when compared either to control (Fig. 12A) or to overexpression of corresponding function-disabled constructs carrying two point mutations within the SH3 domain (Fig. 12C, E). These mutants cannot undergo classical SH3 domain/PXXP-motif interactions (Kessels et al., 2001). The C-terminal part of Abp1 and of the isolated SH3 domain caused a about equal highly significant decrease in spine density (Fig. 12F, $p < 0.001$).

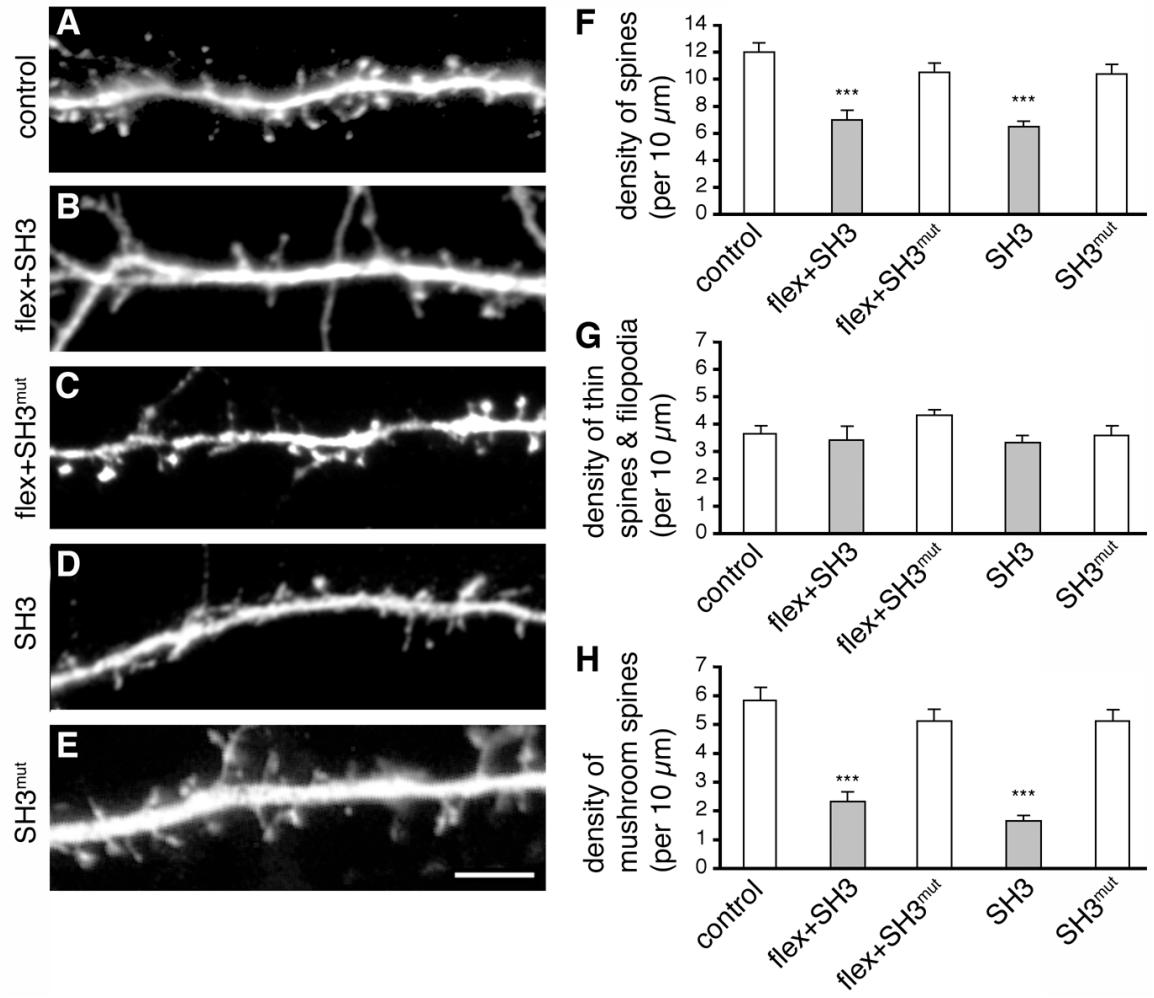

Figure 12. Overexpression of Abp1 fragments encompassing the C-terminal SH3 domain highly significantly decrease the density of mushroom spines. *A-E*, Images show changes in spine density of hippocampal neurons at DIV14 transfected at 12 DIV with C-terminal Abp1 fragments and mutants thereof. For neurons transfected with GFP as control (*A*) and cotransfected with GFP and myc-tagged Abp1 flex+SH3 (*B*), flex+SH3^{mut} (*C*), SH3 (*D*) as well as SH3^{mut} (*E*), GFP staining is shown demonstrating the decrease in dendritic spine density triggered by C-terminal fragments of Abp1 including the wild-type SH3 domain. Bar, 5 µm. *F-H*, Diagrams depict the means ± SEM for the density of spines of all types (*F*) and their individual morphology groups (*G,* thin spines & filopodia; *H*, mushroom spines) for neurons transfected with GFP alone (control) as well as cotransfected with C-terminal Abp1 fragments and mutants thereof as indicated (***$p < 0.001$).

Detailed analyses of the different spine classes revealed that there was no effect on thin spines & filopodia at all (Fig. 12G), but the number of mushroom-shaped spines was strongly reduced. The combination of flexible and SH3 domain as well as the SH3 domain alone induced decay of spine density of about 30% compared to control and to the two different mutants including a non-functional SH3 domain (SH3^{mut} and flex+SH3^{mut}), respectively (Fig. 12H).

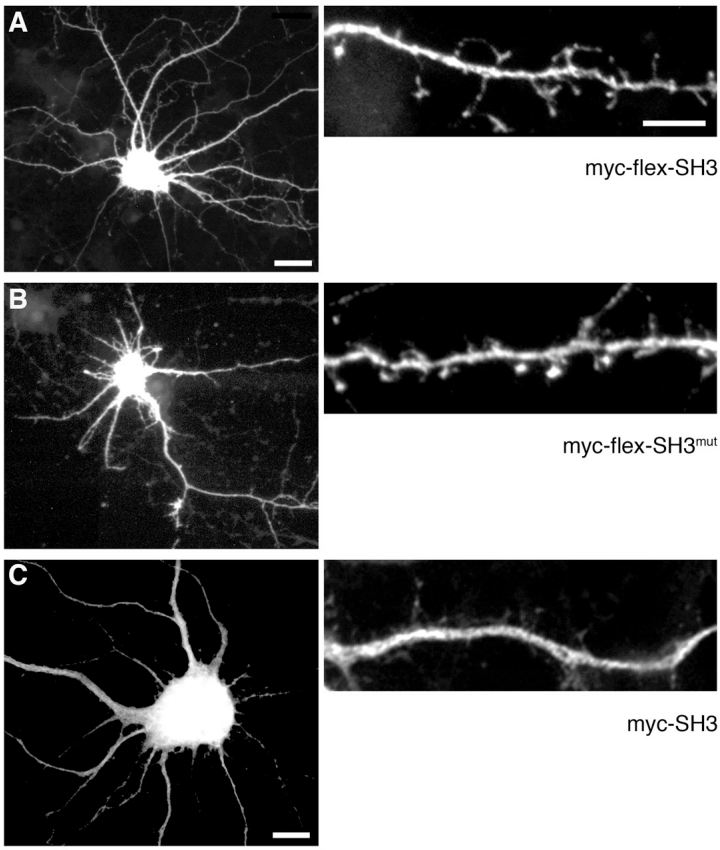

Figure 13. Expression of C-terminal Abp1 fragments and mutants thereof in primary hippocampal neurons. Images show the distribution of transfected myc-tagged Abp1 flex+SH3 (*A*), flex+SH3^{mut} *(B)* and SH3 domain (*C*) in primary hippocampal neurons at DIV14 (2 days after transfection). Right panels represent enlarged examples of the distribution of the proteins along the dendrites. Bars, 20 µm (*A, B*), 10 µm (*C*) and 5 µm (higher magnification of neurites).

In summary, overexpression of full-length Abp1 led to an increased number of mushroom spines and this effect can not be induced by excess of either the actin-binding domains of Abp1 or the C-terminal SH3 domain alone. These findings suggest that the Abp1 SH3 domain is crucial but by itself not sufficient for mushroom spine formation. Instead a combination of SH3 domain interactions and F-actin binding by Abp1 is required.

3.1.4 Abp1 knock-down reduces mushroom spines and synaptic contacts

Is the Abp1 crucial for maturation of mushroom spines? To test this hypothesis three different vector-based RNAi tools against rat Abp1 were constructed, which additionally express GFP as fluorescent marker. Transfected GFP-positive primary hippocampal neurons, as identified by anti-MAP2 staining (Fig. 14A, B), were analyzed for their expression level of endogenous Abp1 by anti-Abp1 immunostaining (Fig. 14C).

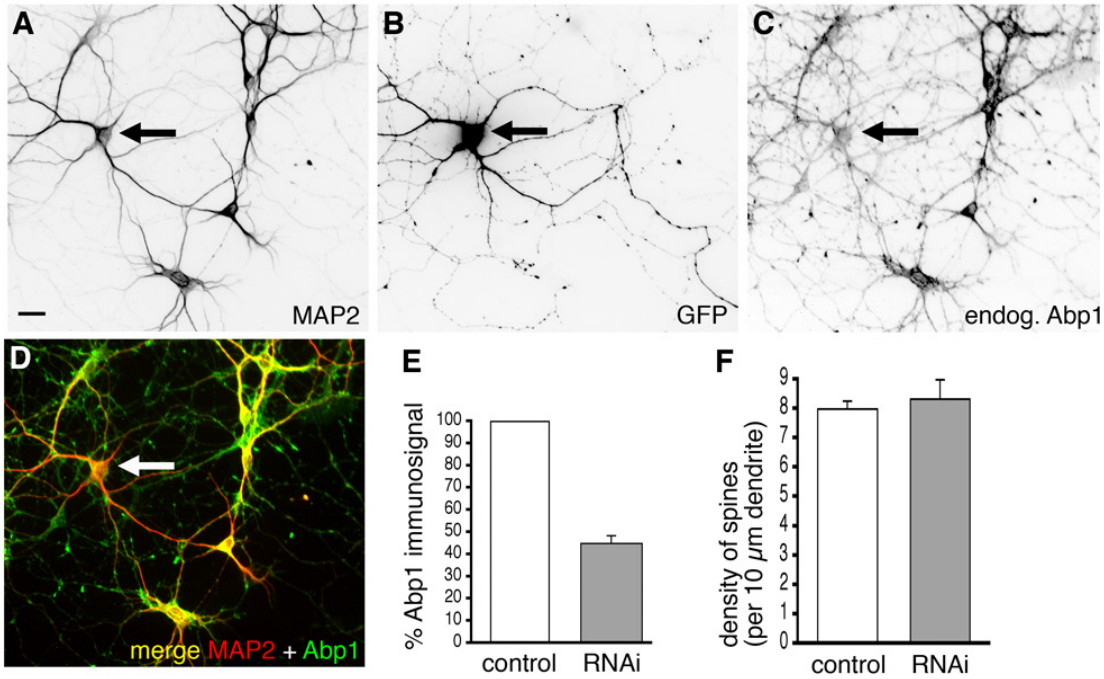

Figure 14. RNAi-based reduction of Abp1 expression levels. *A-D*, Primary hippocampal neurons were transfected at day 12 in culture with a vector encoding for GFP and small interfering RNAs complementary to the Abp1 message under two different promoters. Neuronal cells were identified by anti-MAP2 immunostaining (A; depicted in red (false color) in the merged image D). Neurons transfected with the pRNAT-driven Abp1 RNAi construct are marked by GFP expression (arrow; *B*) and showed a significant reduction in the anti-Abp1 immunoreactivity (*C*; shown in green (false color) in the merged image *D*). *E*, Quantitative analysis of the anti-Abp1 immunoreactivity of 21 neurons transfected with a pRNAT-driven Abp1 RNAi construct (marked by GFP coexpression) demonstrates that Abp1 RNAi results in about 56% reduction of the anti-Abp1 immunofluorescence intensity when compared to untransfected neurons (n = 77). The intensity of fluorescence was measured in the bodies of all MAP-2-positive cells. Data are represented as mean ± SEM. *A-F* represents data for Abp1 RNAi sequence #1 (Abp1 RNAi sequence #2 gave similar results), the density of spines of all types (means ± SEM) (*F*) is unchanged.

Two of the generated RNAi tools showed a significant reduction of the anti-Abp1 signal in transfected neurons (Fig. 14A-D). Quantitative evaluations demonstrated that overexpressed RNAi sequence #1 is reduces the Abp1 signal to less than 44% in comparison to untransfected primary neurons (Fig. 14E). RNAi sequence #2 yielded similar results (not shown).

A quantitative evaluation of the density of all spiny structures in neurons with reduced Abp1 content did not yield any differences compared with the pRNAT control (Fig. 14F). Likewise, the length of spines was unaffected (data not shown).

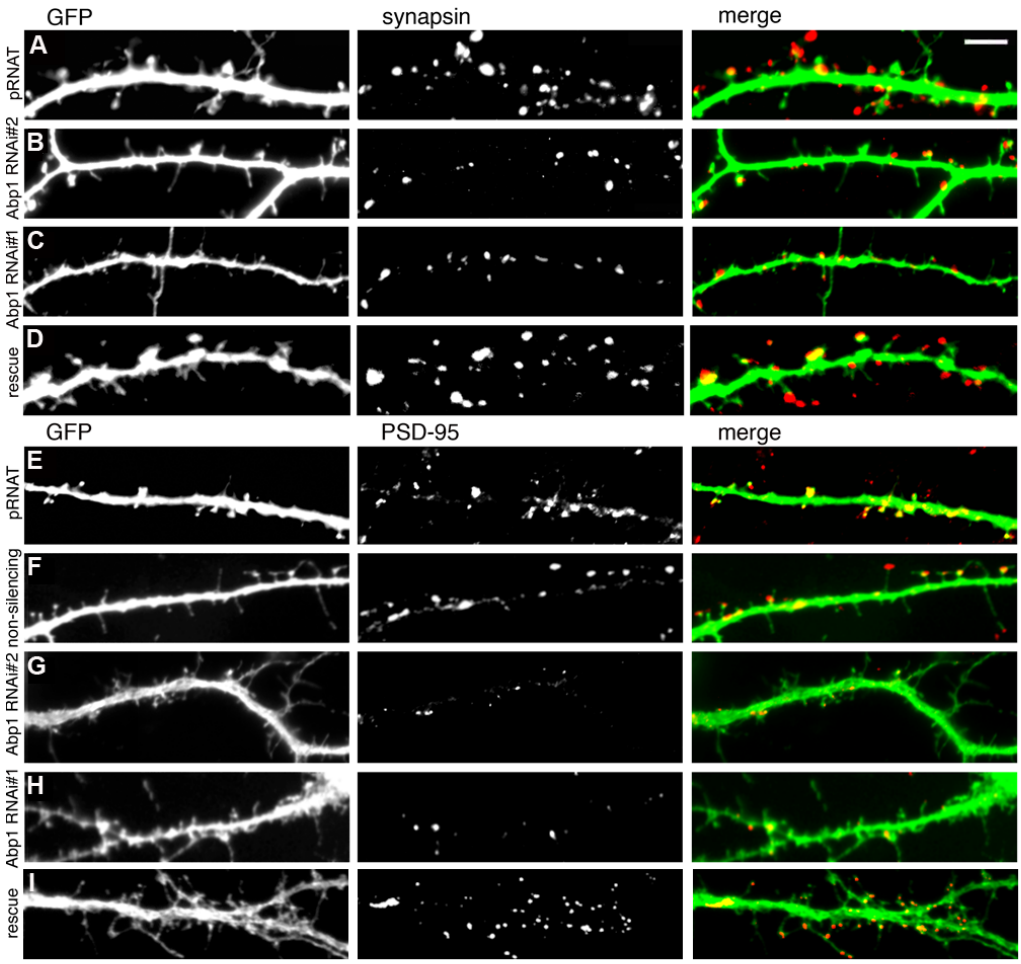
GFP
synapsin
merge
A
pRNAi
B
Abp1 RNAi#2
C
Abp1 RNAi#1
D
rescue
GFP
PSD-95
merge
E
pRNAi
F
non-silencing
G
Abp1 RNAi#2
H
Abp1 RNAi#1
I
rescue

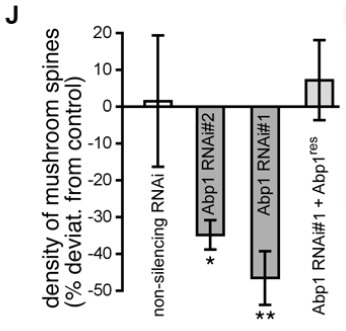
J
density of mushroom spines
(% deviat. from control)
20
10
0
-10
-20
-30
-40
-50
non-silencing RNAi
Abp1 RNAi#2
Abp1 RNAi#1
Abp1 RNAi#1 + Abp1res
*
**

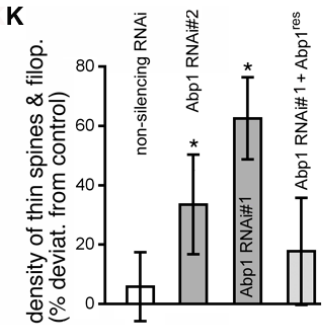
K
density of thin spines & filop.
(% deviat. from control)
80
60
40
20
0
non-silencing RNAi
Abp1 RNAi#2
Abp1 RNAi#1
Abp1 RNAi# 1 + Abp1res
*
*

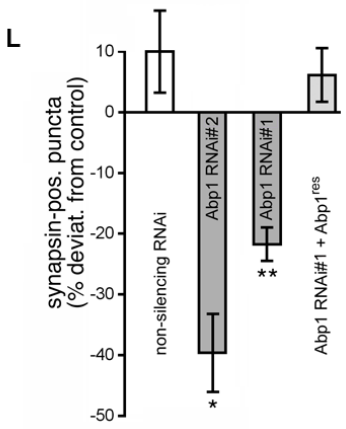
L
synapsin-pos. puncta
(% deviat. from control)
10
0
-10
-20
-30
-40
-50
non-silencing RNAi
Abp1 RNAi#2
Abp1 RNAi#1
Abp1 RNAi#1 + Abp1res
*
**

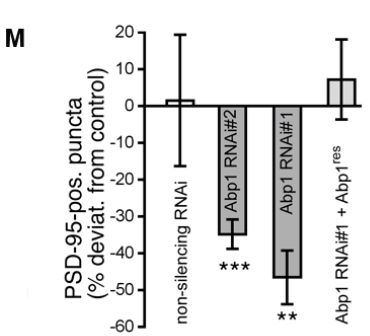
M
PSD-95-pos. puncta
(% deviat. from control)
20
10
0
-10
-20
-30
-40
-50
-60
non-silencing RNAi
Abp1 RNAi#2
Abp1 RNAi#1
Abp1 RNAi#1 + Abp1res
***
**

Figure 15. RNAi-based reduction of Abp1 expression levels reduces the densities of mushroom spines and synapses on hippocampal neurons. *A-I, L, M*, Analyses of synapse density based on immunostaining of the presynaptic marker synapsin (*A-D*) and based on immunostaining of the postsynaptic marker PSD-95 for synapse detection (*E-I*), respectively, reveal reduced numbers (means ± SEM) of PSD-95-positive (*M*) and synapsin-positive (*L*) puncta on dendrites from neurons expressing Abp1 RNAi compared with different sorts of control neurons. Note that restoration of Abp1 levels by cotransfection of an RNAi-resistant Abp1 mutant rescues the reduction of synapses as well as the defects in mushroom spine morphology control. *J-M*, Analyses of the effects of knocking down Abp1 on spine morphology and synapse density. Primary hippocampal neurons were transfected with pRNAT–GFP (control), a non-silencing RNAi construct, pRNAT-driven Abp1 RNAi sequences 1 and 2 and double-transfected with Abp1 RNAi sequence 1, and an RNAi-resistant but otherwise unaltered Abp1 mutant (Abp1 RNAi#1 + Abp1^{res}, rescue), respectively, at 12 DIV and fixed after 48 h. Diagrams show that the densities of spines of individual morphology groups (*J*, mushroom-shaped spines; *K*, thin spines and filopodia in percentage deviation ± SEM from pRNAT-expressing, i.e., GFP-expressing control cells) are significantly different in Abp1-deficient cells. Whereas immature thin spines and filopodia prevail, mushroom spine density is strongly decreased (*$p < 0.05$, **$p < 0.01$, ***$p < 0.001$). Bar, 5 μm.

Detailed analyses of the morphological properties of the spines formed during acute reduction of Abp1 expression levels, however, revealed that Abp1 is a crucial component in the formation of mature, mushroom-type spines. Mushroom spine density showed a reduction of 46.54 ± 7.31 % (mean ± SEM) and 34.85 ± 3.99 % compared with control cells in primary hippocampal neurons transfected with RNAi sequences #1 and #2, respectively (Fig. 15J), whereas thin spine density is correspondingly increased (to 135–162 % of the control value) (Fig. 15K). Importantly, the two different RNAi sequences yielded consistent results. Coexpression of an RNAi-resistant but otherwise unaltered Abp1 mutant (Abp1^{res}, Fig. 15) rescued both of the observed defects. Both the mushroom spine density decrease and the increase of thin spines were abolished, and the densities equaled approximately control levels (Fig. 15J, K). Together, this firmly proves the specificity of the RNAi approach.

The effect of Abp1 knockdown mirrors the reduction in mushroom spine density observed during overexpression of either the isolated SH3 domain (Fig. 12H) or the actin-binding modules of Abp1 (Fig. 11C), which both seem to act in a dominant-negative manner. Furthermore, it can be concluded that Abp1 knock-down has an effect opposite to the gain-of-function manipulation, the overexpression of wild-type full-length Abp1 (Fig. 11C). The decrease in mushroom spine abundance during Abp1 RNAi corresponded with a pronounced reduction in the number of synaptic structures. Both the number of contacting presynaptic structures (identified as synapsin-positive puncta) (Fig. 15A-D) and the number of postsynapses (identified as PSD-95-positive puncta) (Fig. 15E-I) were diminished by 40% in neurons with reduced Abp1 expression (Fig. 15B, C, G, H) compared with neurons expressing pRNAT–GFP (control) (Fig. 15A, E) and a non-silencing RNAi construct (Fig. 15F), respectively. Again, the two different RNAi

sequences led to consistent effects. The specificity of this Abp1 RNAi effect is also demonstrated by experiments, in which we restored Abp1 expression levels by cotransfection of an RNAi-resistant Abp1 mutant. Cotransfection of this Abp1 mutant with Abp1 RNAi sequence #1 completely abolished the highly significant reduction of synapsin-positive and PSD-95-positive structures observed in RNAi-transfected neurons (Fig. 15D, I). The quantitative values obtained in such rescue experiments were not significantly different from the two control incubations, pRNAT and non-silencing RNAi, respectively (Fig. 15L, M).

The negative Abp1 loss-of-function effect on synapse density is consistent with Abp1 overexpression showing the opposite effect, i.e., a highly significant increase in synapse density (Fig. 9G).

3.1.5 Abp1 and ProSAP/Shanks cooperate in mushroom spine morphology control

The cytoskeletal component Abp1 associates in the PSD via its SH3 domain directly with members of the ProSAP/Shank protein family (Qualmann et al., 2004), which are major scaffolding components. This indicates that Abp1 may cooperate with ProSAP/Shank proteins in regulating spine morphology. As described previously, overexpression of full-length Abp1 or actin binding parts thereof causes highly significant increases in the length of mushroom spines (Fig. 9). Interestingly, this effect is quenched by co-overexpression of the Abp1 binding partners, ProSAP1 (Shank2) and ProSAP2 (Shank3), respectively (Fig. 16B-G). Thus, lengthening of mushroom spines upon Abp1 overexpression, promoted by the actin-binding modules, is outweighed by an increase in ProSAP expression levels demonstrating the importance of a tight balance between Abp1 and its postsynaptic interaction partners in spine development.

It has been reported, that Shank1 induces an enlargement of spine heads upon overexpression in primary hippocampal neurons (Sala et al., 2001). This work shows that also ProSAP1/Shank2 and ProSAP2/Shank3 affect spine head size. Quantitative measurements revealed that the average width of spine heads is increased by about 20% upon overexpression of ProSAP1 and ProSAP2, respectively (Fig. 16C, D and H).

Wild-type full-length Abp1 had no effect on head size of mushroom-shaped spines after single overexpression (Fig. 16B and H), coexpression of Abp1 with both ProSAP1 (Fig. 16E) and ProSAP2 (Fig. 16F) caused a further and highly significant increase in the head width of mushroom spines (Fig. 16H) thereby ProSAP2-mediated spine width increase was

even doubled (Fig. 16H). These results show cooperative effects of Abp1 with ProSAPs in spine morphology control. The finding that Abp1 and ProSAPs only in combination but not individually promote the formation of irregular, multi-headed spines further strengthens this conclusion. Co-overexpression of Abp1 with ProSAP1/Shank2 or ProSAP2/Shank3 induces a highly significant, about 400% increase of branched structures,

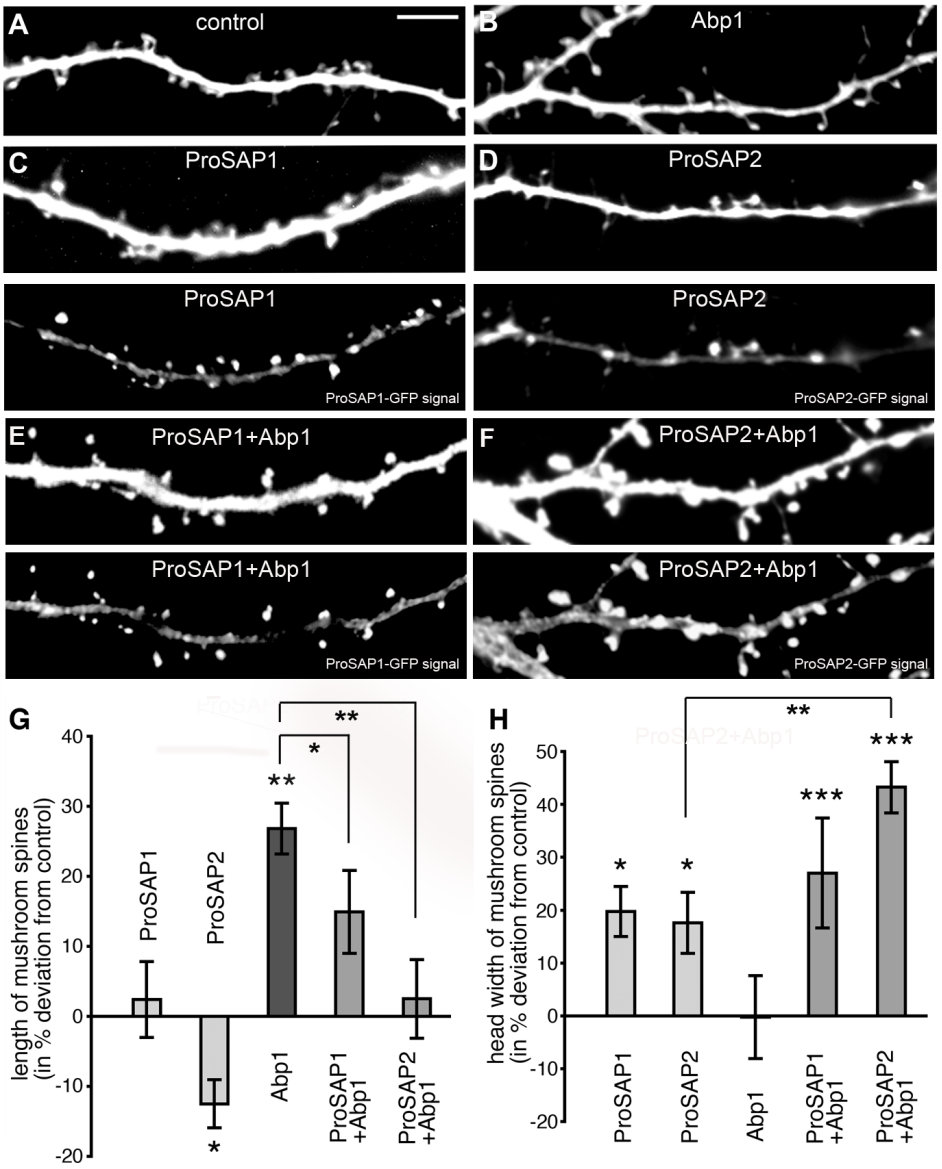

Figure 16. The physical interaction partners Abp1 and ProSAP/Shanks cooperate in controlling mushroom-type spine morphology. *A-F*, Images show enlarged heads of mushroom-shaped spines of primary hippocampal neurons at DIV 14 upon overexpression of ProSAP1 (*C*) and ProSAP2 (*D*) in comparison to spine heads of mRFP-expressing cells (control, *A*) and Abp1-expressing cells (*B*). Coexpression of ProSAP1 + Abp1 (*E*) and ProSAP2 + Abp1 (*F*), respectively, led to a further promotion of ProSAP-induced head extension and to a decrease in Abp1-induced spine neck elongation. Images represent the fluorescence signals of cell filling molecules cotransfected to highlight the morphology. Lower panels in *C-F* show the fluorescence signals of GFP-ProSAP1 and 2. *G-H*, Diagrams depict the means ± SEM for the length of mushroom spines (*G)* and the head width of mushroom spines (*H*) in % deviation from mRFP-transfected control cells for neurons expressing ProSAP1, ProSAP2, Abp1 or combinations thereof as indicated (*p < 0.05, **p < 0.01, ***p < 0.001). Bar, 5 µm.

which often appeared as huge multi-headed spine aggregates (Fig. 17A-D) and were very rare in control conditions (Fig. 17E). Furthermore, the few branched structures found in controls were mostly thin branched spines, which usually do not even have heads, whereas in cells co-overexpressing ProSAPs and Abp1, the structures counted as branched spines were much larger and multi-headed.

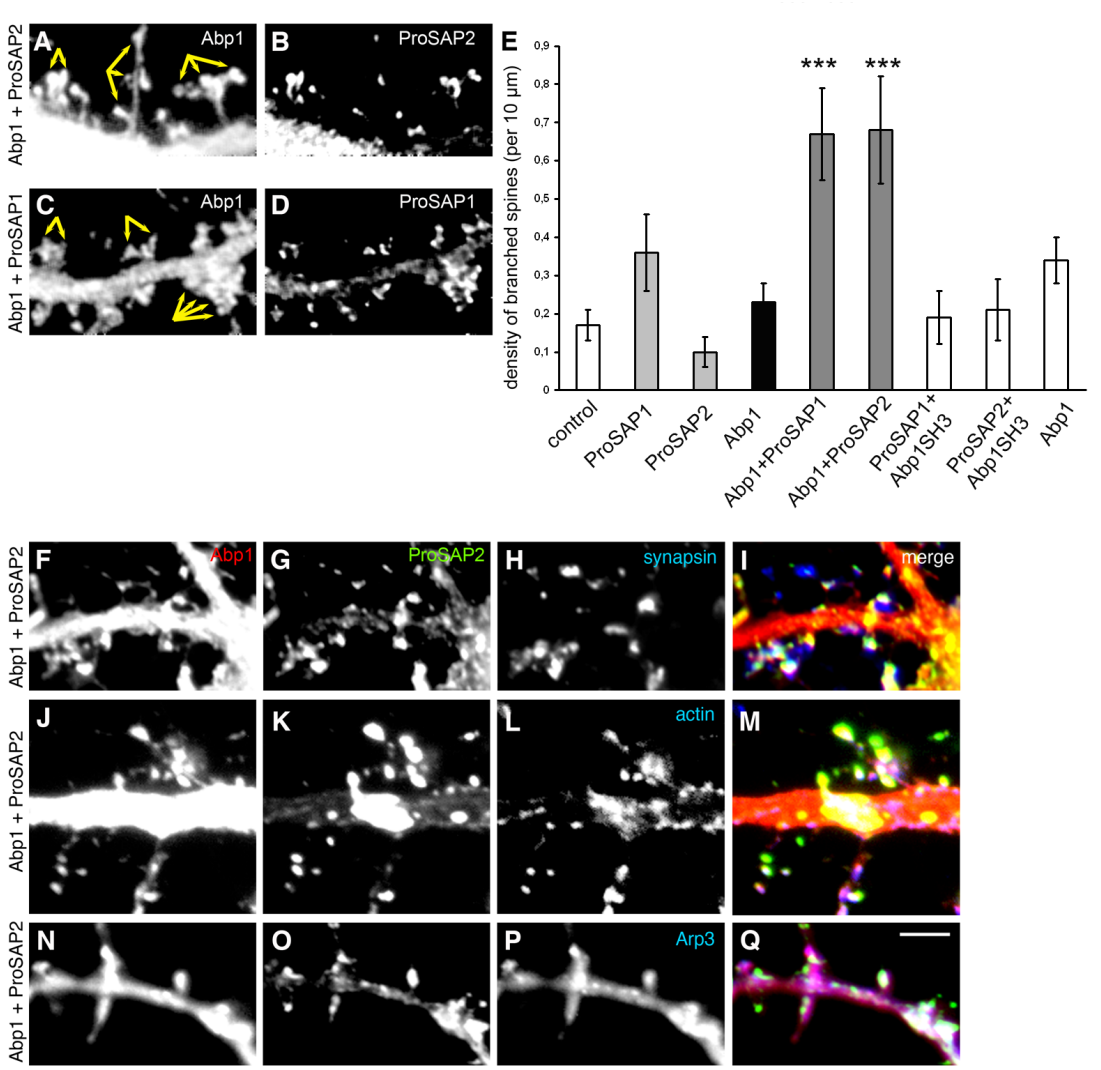

Figure 17. Abp1 and ProSAP coexpression leads to highly branched and complex spines with multiple enlarged spine heads. *A-D*, Coexpression of Abp1 (*A, C*) with ProSAP2 (*B*) and ProSAP1 (*D*), respectively, results in highly branched spines with cauliflower- or broccoli-like appearance in primary hippocampal neurons at DIV14 (examples marked by arrows). *E*, Quantitative analysis of the density of branched spines – depicted are the means ± SEM - reveals that cooverexpression of Abp1 with ProSAP1 as well as with ProSAP2 but not expression of the individual proteins leads to a highly significant increase in irregular, branched, multi-headed spines in comparison to control cells transfected with the cell-filling molecule mRFP. In contrast, coexpression of the isolated SH3 domain of Abp1 with ProSAPs was not sufficient for the induction of these highly branched and complex spines with multiple enlarged heads (***$p < 0.001$). *F-Q*, Enlarged spines induced by coexpression of Abp1 (*F, J, N*; red in merged images) and ProSAP2 (*G, K, O*; green in merged images *I, M, Q*) are aligned with presynaptic structures marked by synapsin immunoreactivity (*H*; blue in merged image *I*), are marked by high content of F-actin stained with phalloidin (*L*; blue in merged image M) and also contain immunoreactivity for the actin nucleation machinery Arp2/3 complex (anti-Arp3, *P*; blue in merged image *Q*). Colocalization of Abp1 and ProSAP2 with synapsin, F-actin and Arp3, respectively, appears white in the merged images. Bar, 5 µm.

Interestingly, cotransfection of the Abp1 SH3 domain instead of the full-length protein failed to elicit this Abp1/ProSAP-mediated effect suggesting that the actin binding properties of Abp1 functionally contribute to the induction of multiple spine heads (Fig.17E). The irregular spines caused by Abp1 and ProSAP overexpression were positive for Abp1, for ProSAPs, for further postsynaptic markers, such as the NMDA receptor subunit 2B (not shown), also for presynaptic markers, such as synapsin (Fig. 17F-I), for F-actin (Fig. 17J-M) and for the actin nucleation machinery Arp2/3 complex (Fig. 17N-Q).

3.1.6 ProSAP/Shank-induced enlargements of spine heads in mushroom spines are critically dependent on SH3 domain-mediated complex formation with Abp1

Abp1 cooverexpression can potentate the ProSAP-induced enlargements of spine heads and is involved in the formation of irregular multi-headed spine structures (Fig. 16, 17).

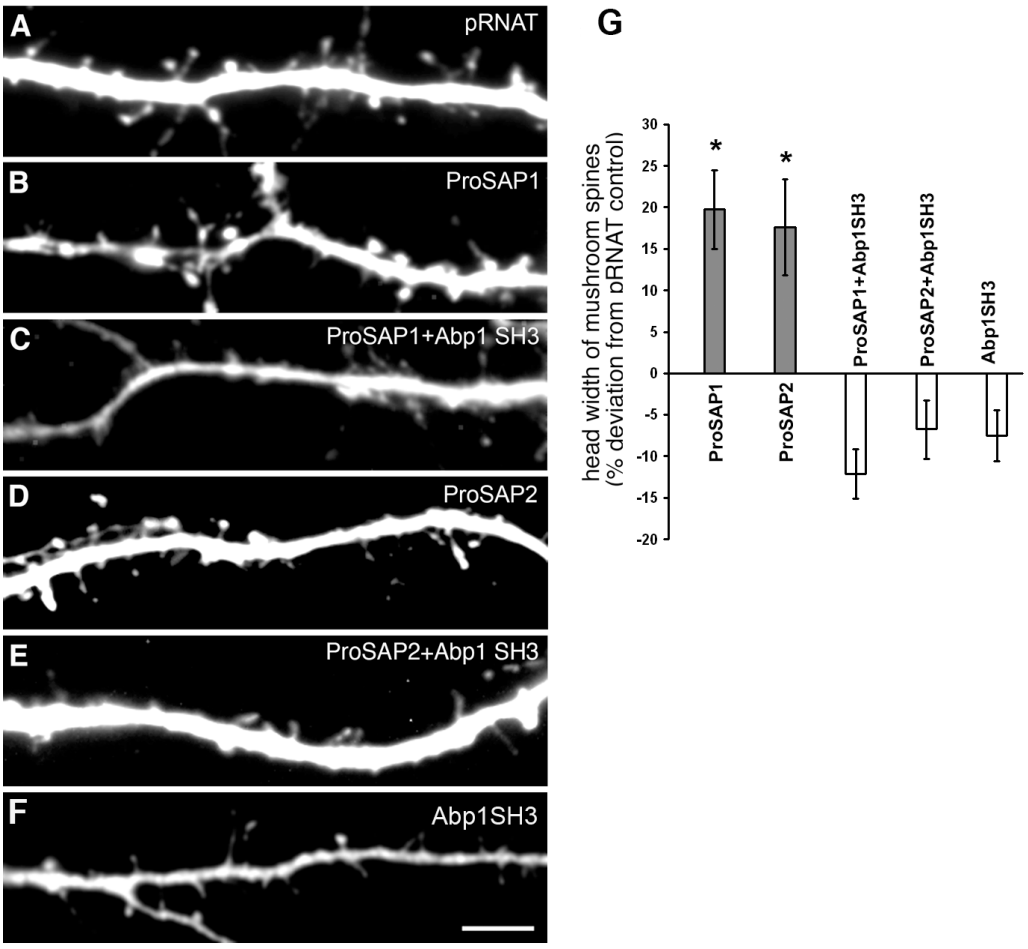

Figure 18. Abp1/ProSAP complex formation is crucial for ProSAP-induced enlargements of spine heads. *A-F*, Images of spine morphology of primary hippocampal neurons at DIV 14 expressing a cell filling molecule alone (*A*, pRNAT-driven GFP expression) and of cells transfected with ProSAP1 (*B*), ProSAP1 + Abp1 SH3 (*C*), ProSAP2 (*D*), ProSAP2 + Abp1 SH3 (*E*) and Abp1 SH3 (*F*) respectively. Images show the fluorescence channel for the cell-filling molecule to highlight cell morphology irrespective of cotransfected components. *G*, Quantitative analysis of head widths of mushroom spines reveals that the increase in head

width of mushroom spines – depicted are the means ± SEM in % deviation from control (cells transfected with GFP-expressing pRNAT vector) - for neurons expressing ProSAP1 and ProSAP2 is abolished upon cotransfection of the isolated Abp1 SH3 domain (*p < 0.05). Bar, 5 µm.

It was therefore tempting to hypothesize that interfering with the ProSAP-Abp1 interaction would cause any effects on the ProSAP/Shank-induced head enlargement process. The isolated ProSAP-binding interface, the SH3 domain of Abp1, was therefore used as a dominant-negative tool (Fig. 18). Visual inspection (Fig. 12A-E) and the quantitative analyses showed that the increase in head width of mushroom spines of neurons expressing ProSAP1 (Fig. 18B, G) and ProSAP2 (Fig. 18D, G) is completely abolished upon cotransfection of the isolated Abp1 SH3 domain (Fig. 18C, E, G).

3.1.7 ProSAP-mediated spine enlargements depend on the Arp2/3 complex, its activator N-WASP and Abp1

The huge irregular spine structures caused by cooverexpression of ProSAPs and Abp1 contain filamentous actin and the actin nucleator Arp2/3 complex (Fig. 17J-Q). This suggested that ProSAPs promotes spine head enlargements by facilitation of local formation of actin filaments. Indeed, coexpression of the Arp2/3 complex inhibitor N-WASP CA (Strasser et al., 2004; Pinyol et al., 2007) and of the Arp3 RNAi plasmid (Pinyol et al., 2007), which causes a specific lack of the Arp2/3 complex (Steffen et al., 2006), abolished ProSAP-mediated enlargements of mushroom-type spine heads (Fig. 19A, B, C, H). These results suggested that the ProSAP-induced spine morphology changes require new actin filaments, whose polymerization is activated by the actin nucleator Arp2/3 complex, which Abp1 is able to steer it via N-WASP activation (Pinyol et al., 2007). Thus, the effects of knocking down N-WASP were tested next. Indeed, ProSAP-mediated spine head enlargement was also suppressed by RNAi-mediated N-WASP deficiency (Fig. 19D, H).

Is Abp1 crucial for ProSAP-mediated spine size changes? Expression of Abp1 RNAi plasmids together with ProSAP2 (Fig. 19E) revealed that ProSAPs effects on mushroom spine head size were almost completely suppressed by reduction of Abp1 expression level (Fig. 19H).

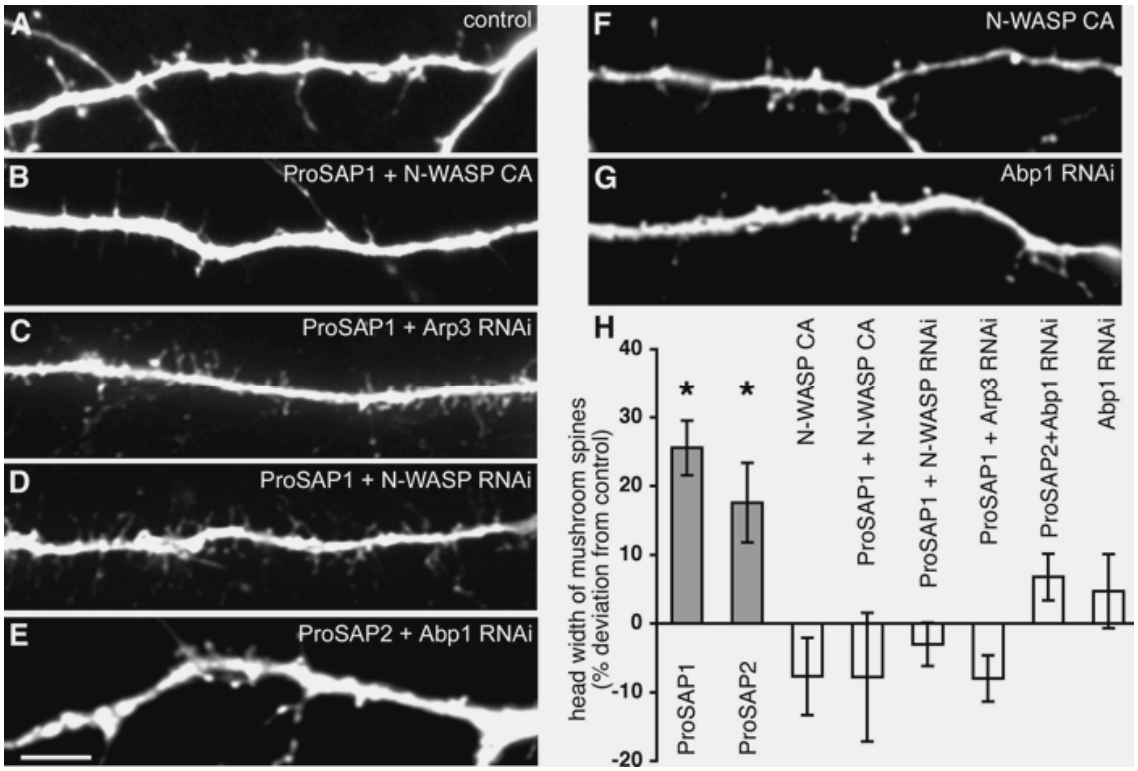

Figure 19. Arp2/3 complex activation, the Arp2/3 complex activator N-WASP and the N-WASP-controlling and ProSAP-binding protein Abp1 are crucial for ProSAP-induced enlargements of spine heads. *A*-*G*, Images of spine morphology of primary hippocampal neurons at DIV 14 expressing a cell filling molecule alone (*A*) and of cells cotransfected with ProSAP1 + N-WASP CA (*B*), ProSAP1 + Arp3 RNAi (*C*), ProSAP1 + N-WASP RNAi (*D*) and ProSAP2 + Abp1 RNAi (*E*), as well as with N-WASP CA (*F*) and Abp1 RNAi alone (*G*), respectively. Cell morphologies are shown represent the fluorescence signals for the cell-filling molecules employed. For examples of enlarged spines observed upon expression of ProSAP1 and ProSAP2, respectively, please see figure 8B and 8D. *H*, Quantitative analysis of head widths of mushroom spines (means ± SEM in % deviation from control) show that ProSAP1- and 2-induced head enlargements are dependent on Arp2/3 complex activity and sufficient supplies of Arp3, N-WASP and Abp1 (*$p < 0.05$). Bar, 5 μm.

Experiments in this work thus demonstrate that Abp1 is crucial for ProSAP/Shank functions and suggest that Abp1–ProSAP complex formation via the Abp1 SH3 domain is an underlying molecular mechanism.

3.1.8 A ProSAP1 mutant lacking all Abp1 binding sites cannot evoke spine head changes

We have demonstrated that Abp1 is crucial for spine head and synapse formation. Both its SH3 domain and functions of the N-terminal F-actin binding modules seem important, because the SH3 domain alone has a dominant-negative effect. Also, we were able to demonstrate that Abp1 is crucial for the effects mediated by its interaction partners ProSAPs and that ProSAP-mediated effects seem to specifically depend on Abp1–ProSAP complex formation. From these data, it can be hypothesized that a ProSAP mutant, which is

incapable of binding Abp1, should be unable to elicit ProSAP-mediated spine head extension. To address this hypothesis, a ProSAP1 mutant was constructed, in which two prolines of the deduced Abp1 SH3 domain-binding proline-rich motif (PP950/1AA, Qualmann et al., 2004) in the ProSAP1 C-terminus were exchanged for alanine (Fig. 20A).

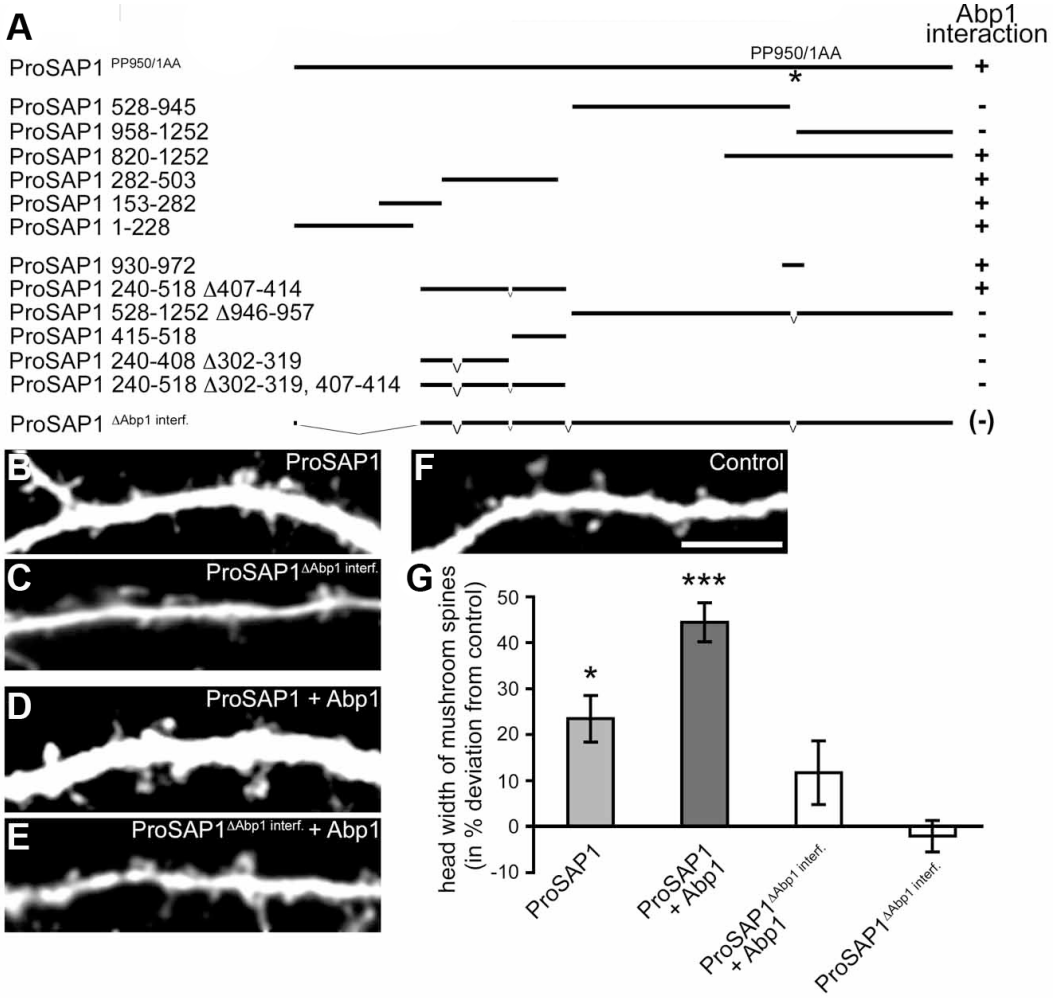

Figure 20. A ProSAP1 mutant lacking all the Abp1 binding sites fails to elicit spine head enlargement when overexpressed alone or in combination with Abp1. *A*, Schematic depiction of ProSAP1 constructs used for the analyses of the ProSAP1 mutant with all Abp1 SH3 domain interfaces deleted (ProSAP1$^{\Delta Abp1\ interf.}$) and of their Abp1 SH3 domain binding capability (+, Abp1 binding; -, no Abp1 binding; (-) concluded not to bind, as the pieces used to assemble this construct all fail to bind when tested individually). *B-F*, Images of spine morphology, as highlighted by coexpressed cell-filling molecules, of primary hippocampal neurons at DIV 14 expressing ProSAP1 (*B*), the ProSAP1$^{Abp1\ interf.}$ mutant (*C*), ProSAP1 + Abp1 (*D*) and the ProSAP1$^{\Delta Abp1\ interf.}$ mutant + Abp1 (*E*) in comparison to control cells overexpressing only cell filling molecules (mRFP) (*F*). *G*, Quantitative analysis of head widths of mushroom spines revealed that the ProSAP1$^{\Delta Abp1\ interf.}$ mutant fails to increase spine heads both alone or in combination with Abp1. (*p < 0.05, ***p < 0.001). Bar, 5 µm.

This mutant, however, was still associated with the Abp1 SH3 domain suggesting that there may be more thus far unknown Abp1 binding sites within ProSAP1.

In silico analyses of the sequences of ProSAP1 and 2 in conjunction with hints on Abp1 SH3 domain-binding preferences from peptide screening (Yamabhai and Kay, 1997) led to the prediction of at least 5 Abp1 binding sites in ProSAP1. In collaboration with R. Ahuja, in addition to the deduced binding site from aa 946 to aa 957 (Qualmann et al., 2004), several binding sites in N-terminal part of ProSAP1 were confirmed by testing several pieces and deletion mutants of ProSAP1 in co-precipitation experiments with the Abp1 SH3 domain (Fig. 20). Similarly, ProSAP2 has a variety of independent Abp1 SH3 domain binding sites (data not shown).

To create a ProSAP1 mutant deficient for Abp1 binding, the very N-terminus (aa 1-228) was deleted en bloc as it seemed encompass several binding sites, which precluded their individual deletion. Further co-precipitation experiments demonstrated that between amino acids 228 and 528 it was sufficient to delete the three following sites, aa 302-319, 407-414 and 518-527 to ensure lack of binding. With this knowledge it was finally possible to create a ProSAP1 mutant deficient for Abp1 binding (ProSAP1$^{\Delta Abp1\ interf.}$). This mutant lacks the far N-terminus, the three central Abp1 binding sites as well as the established site at aa 946-957.

In contrast to wild-type ProSAP1 (Fig. 20B, C, G), overexpressed ProSAP1 $^{\Delta Abp1\ interf.}$ was unable to induce spine head enlargement in primary hippocampal neurons. The cooperative effect of ProSAPs with Abp1 on spine head extension observed for the wild-type protein (Fig. 20D) was also not seen with the ProSAP1 $^{\Delta abp1\ interf.}$ mutant. Spine heads observed in both groups of cells overexpressing ProSAP1 $^{\Delta Abp1\ interf.}$ alone or in combination with Abp1 had the same size as control cells (Fig. 20C, E-G). This clearly shows that ProSAP1 is unable to enlarge spine heads without the ability to associate with the cytoskeletal component Abp1.

3.1.9 Abp1-induced spine head and synapse formation is dependent on ProSAP2

As previous experiments demonstrate, Abp1 has a strong influence on spine morphology control as well as on formation of spine heads and synapses. It is also clear that Abp1 promotes ProSAP-dependent spine head growth via SH3 domain/poly-proline motif-mediated Abp1/ProSAP complex formation and thereby is a crucial component for ProSAP-mediated spine growth. To evaluate whether vice versa Abp1-mediated effects on spine head and synapse formation depend on ProSAPs, RNAi-mediated knock down of ProSAP2 was performed, which was recently established by Roussignol et al. (2005).

Although only one of the two Abp1 binding partners of the ProSAP/Shank-family – ProSAP2 – was knocked down, dramatic negative effects on the Abp1-induced increase in mushroom spine density (Fig. 21A-D) and synapse formation (Fig. 21E-K) were observed.

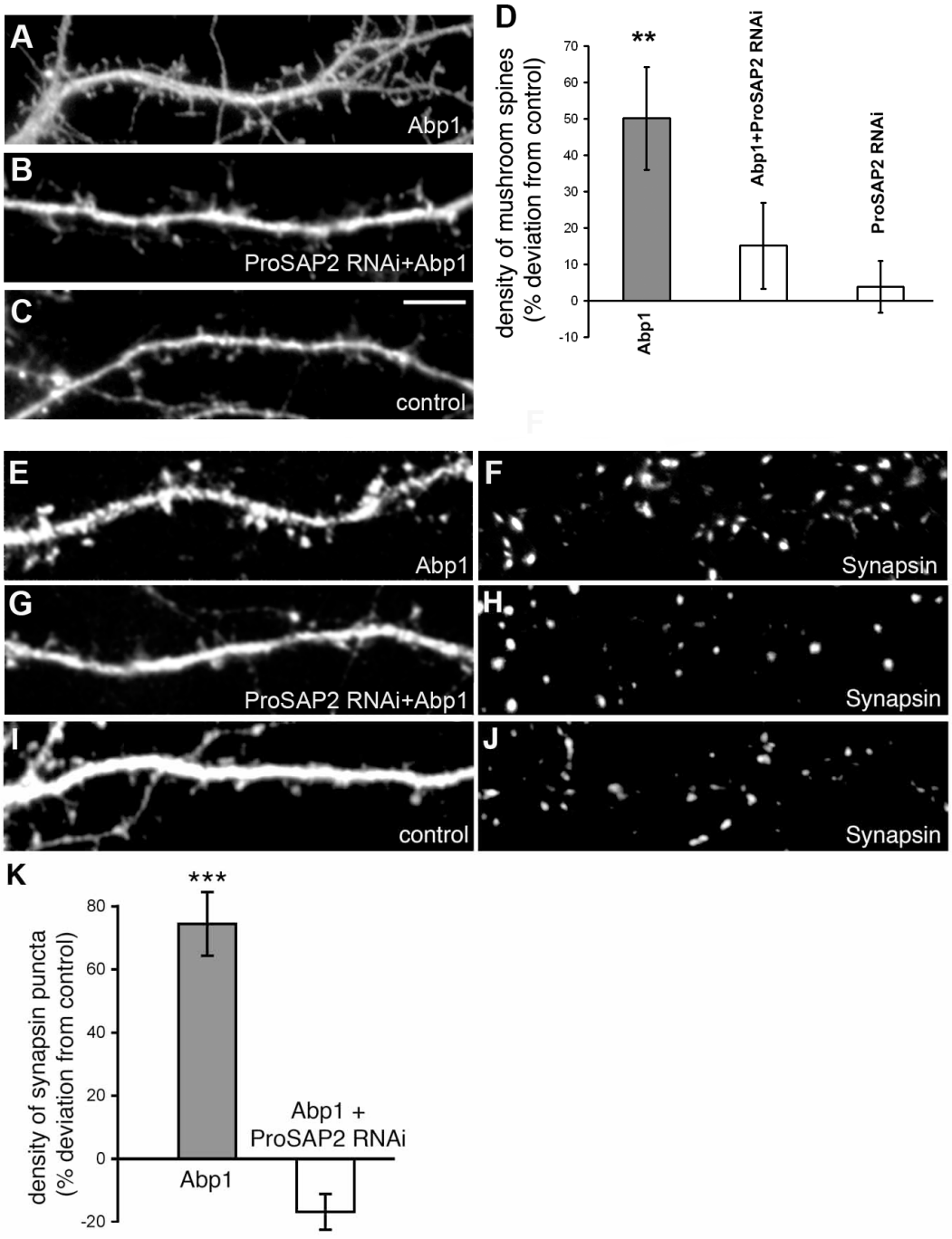

Figure 21. The Abp1-mediated increase in mushroom spine and synapse density is dependent on ProSAP2. *A-C*, Images of spine morphology of primary hippocampal neurons at DIV 14 expressing Abp1 (*A*), ProSAP2 RNAi + Abp1 (*B*) in comparison to control cells (*C*). *D*, Quantitative analysis of mushroom spine density (means ± SEM in % deviation from control) shows that ProSAP2 RNAi effectively suppresses the Abp1-mediated increase in mushroom spine density. *E-J*, Images of dendrites of Abp1 (*E, F*), Abp1 + ProSAP2 RNAi (*G, H*) and RFP-expressing cells (*I, J*; control) immunostained for the synaptic marker

synapsin show an increase of synapses on Abp1-overexpressing cells (*F*). *A-C, E, G* and *I* show the fluorescence channel for the cell-filling molecule to highlight cell morphology. *K*, Quantitative analysis of synapse density as determined by counting synapsin puncta per 10 µm dendrite showed that the Abp1-mediated increase in synapses is completely suppressed by coexpression of ProSAP2 RNAi constructs (means ± SEM in % deviation from control). **p < 0.01, ***p < 0.001. Bar, 5 µm.

Whereas Abp1 overexpression led to a pronounced increase in mushroom spine density and synapse number, (Fig. 21A, D, E, F, K; compare also with Fig. 9), combination of Abp1 with ProSAP2 RNAi failed to cause Abp1-mediated effects and only led to values of control level (Fig. 21B, D, G, H, K). Density of synapses marked by anti-synapsin staining even dropped below control values (Fig. 21G-K). Thus, Abp1 executes its functions in synapse and spine head formation in close functional cooperation with ProSAPs.

3.2 The role of Abp1 in neurite development

3.2.1 Reduced Abp1 expression level leads to an increased axon length of neurons in early stages of development

Actin plays major role in neuronal development because the structure, polarity and functionality of cells depend on actin filament organization and dynamics. Abp1, a characterized cytoskeletal component, is present at distinct high levels in both the axonal and the dendritic compartment in first stages of neuronal development (Kessels et al., 2000; Fenster et al., 2003; Qualmann et al., 2004).

These facts suggest that knock-down of Abp1 in neurons can induce significant morphological changes. To proof this, two different RNA interference (RNAi) sequences, used previously for experiments in mature neurons (Fig. 14), were expressed in young neurons. As in mature neurons, both sequences again yielded very similarly results - an almost 60% decrease in the fluorescence intensity of Abp1 immunosignal (Fig. 22). Developing neurons with low Abp1 expression level had in average 150.7 ± 7.4% (Abp1 RNAi sequence #1) and 152.5 ± 8.5% (Abp1 RNAi sequence #2) longer axons in comparison to control cells (empty pRNAT-transfected neurons where control axon length was defined as 100%, Fig. 23A-D). The phenotype was specifically induced by Abp1 deficiency because cotransfection of the cells with an Abp1 construct carrying several silent mutations, which render the mRNA resistant to RNAi, restored the wild-type situation (Fig. 23D).

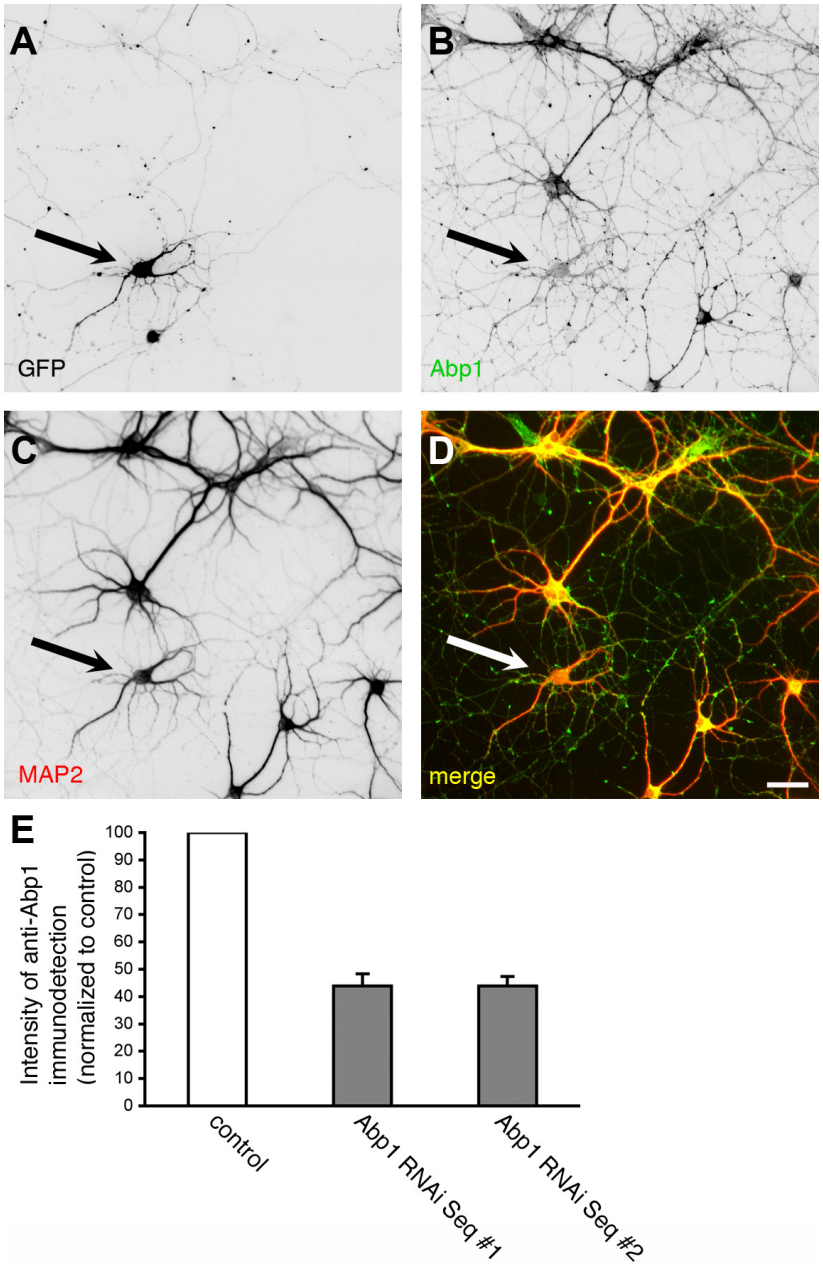

Figure 22. RNAi-based reduction of Abp1 expression levels. *A–D*, Primary hippocampal neurons were transfected at day 5 in culture with a vector encoding for GFP and small interfering RNAs complementary to the Abp1 message under two different promoters. Neuronal cells were identified by anti-MAP2 immunostaining (*C*). Neurons transfected with pRNAT-driven Abp1 RNAi sequence #1 are marked by GFP expression (arrow; *A*) and showed a significant reduction in the anti-Abp1 immunoreactivity (*B*). Labeling of images reflects the color of the fluorescence signal in the merged image (D; colocalization appears yellow). (*E*) Quantitative analysis of the anti-Abp1 immunoreactivity of 50 neurons transfected with pRNAT-driven Abp1 RNAi construct (marked by GFP coexpression) demonstrates that both Abp1 RNAi sequences tested result in an almost 60% reduction of the anti-Abp1 immunofluorescence intensity when compared to the pRNAT control. Data are represented as mean ± SEM. Bar, 20 µm.

In contrast to axon lengthening, the morphological parameters of dendrites were unchanged by Abp1 knock down. This observed specific effect was identical to Arp2/3 complex inhibition through overexpression N-WASP CA (Figure 23C, see also Strasser et

al. 2004): axon length from neurons with Arp2/3 complex inhibition increased to 138.8 ± 5.2% of control (Fig. 23D).

To verify that the N-WASP CA-induced effects represent an inhibition of the Arp 2/3 complex, the levels of Arp3 were reduced by an RNAi targeting sequence established by Steffen et al. 2006. Arp3 RNAi indeed caused a significant elongation of axons. Quantifications showed an average axon length of 143.0 ± 9.7% of control (Fig. 23D).

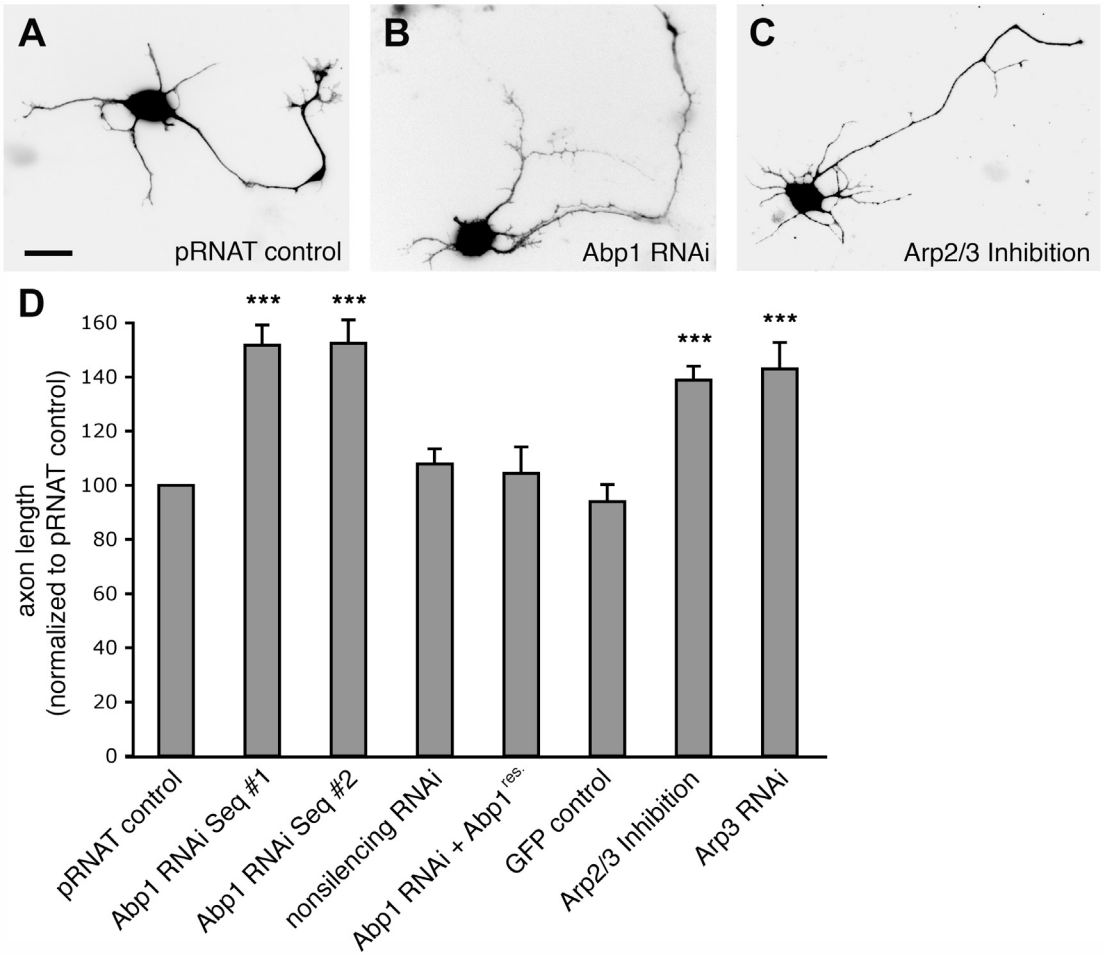

Figure 23. Abp1 knock down selectively results in increased axon length. *A–D,* Primary hippocampal neurons transfected with pRNAT-GFP (control; A), with a pRNAT-driven Abp1 RNAi construct (sequence #1; *B*), and with GFP-N-WASP CA (Arp2/3 complex inhibition; *C*), respectively, at day 2 in culture. The cells were fixed and processed for immunofluorescence microscopy at day 3. Quantitative evaluations (*D*) show that neurons (as evidenced by MAP2 staining) expressing the pRNAT-driven Abp1 RNAi sequences #1 and #2 both show highly significantly (***$p < 0.001$) elongated axons when compared to controls (transfection with pRNAT, pEGFP and non-silencing RNAi) and to cells in rescue experiments, in which Abp1 RNAi and an RNAi-insensitive Abp1 construct were cotransfected. Effects almost identical to those caused by Abp1 RNAi were observed when Arp2/3 complex functions were impaired by overexpression of GFP-N-WASP CA (*C, D*) and Arp3 RNAi (*D*), respectively. Morphological data were normalized to pRNAT-control and are represented as mean (in percent) ± SEM. Bar, 10 µm.

3.2.2 Abp1 activates N-WASP in cooperation with Cdc42 *in vitro* and *in vivo*

Abp1 directly binds N-WASP via its SH3 domain, as experimental work of R. Pinyol has shown (Pinyol et al., 2007). Since knock-down of Abp1 and of Arp3 induced similar changes in neurons, the question arose, whether Abp1 may directly influence the kinetics of actin filament nucleation and polymerization stimulated by N-WASP and the Arp2/3 complex. *In vitro* reconstitutions of actin polymerization with purified actin, N-WASP and Arp2/3 complex performed by R. Pinyol (Pinyol et al., 2007) indeed showed that the addition of the Abp1 SH3 domain was sufficient to significantly stimulate actin nucleation as determined by monitoring the kinetics of actin polymerization by the fluorescence increase of pyrene.

The effect of the Abp1 SH3 domain was dose-dependent. In line with the Abp1 SH3 domain being the N-WASP-binding domain of Abp1, the Abp1 SH3 domain had no effect in the absence of N-WASP.

Taken together, these reconstitution experiments are strong evidence for the involvement of Abp1 in the regulation of actin dynamics by stimulating the N-WASP/Arp2/3 complex-mediated actin polymerization and indicate that Abp1 is an activator of N-WASP.

Another well-described activator of N-WASP is Cdc42. The GTP form of Cdc42 associates with the N-WASP GTPase-binding domain and thereby releases the autoinhibition of N-WASP (Miki et al., 1998; Rohatgi et al., 1999). Abp1 binds to the central PRD next to the GTPase binding domain and also activates N-WASP. Therefore seemed be possible that Abp1 and Cdc42 cooperate in N-WASP autoinhibition release. In order to address this, experiments were designed, in which Arp-mediated actin filament formation was examined induced by a five-fold excess of GTPγS-loaded Cdc42 over N-WASP (full saturation) with and without Abp1 SH3 domain added. Presence of the Abp1 SH3 domain and Cdc42 caused a much higher increase of N-WASP/Arp2/3 complex-mediated actin polymerization as addition of Abp1 or Cdc42 separately.

Thus, Abp1 does not compete with Cdc42 for binding to the Arp2/3 complex-activator N-WASP but both activators cooperate and in combination lead to a very strong activation of N-WASP in *in vitro* reconstitutions of actin filament formation.

In order to address the *in vitro* relevance and the physiological role of Abp1-mediated N-WASP activation, neuronal cells were examined, as N-WASP and Abp1 are both highly expressed in the nervous system. Abp1 is enriched in growth cones of young hippocampal neurons, as well as N-WASP and Arp2/3 complex (Fenster et al., 2003; Strasser et al.,

2004; Ho et al., 2001). Therefore was tested whether the outgrowth and/or the morphology of neurites would be affected by Abp1-regulated N-WASP-mediated actin polymerization. Primary rat hippocampal neurons were transfected with GFP as a control and with GFP-N-WASP. Neurons were identified and their dendritic arborization was visualized by immunostaining for microtubuli-associated protein 2 (MAP2, Fig. 24A-D). Neurons transfected with GFP-N-WASP showed a prominent increase in the number of neurites and a highly branched dendritic arbor compared to control cells transfected with GFP alone. These findings were statistically highly significant (16.9 ± 0.6 neurites per N-WASP-transfected cell versus 12.2 ± 0.5 in GFP control; $p < 0.001$; 16.7 ± 1.0 branch points of dendritic arbor per cell versus 10.2 ± 0.5 for GFP-control; $p < 0.001$; Fig. 24K).

This strong N-WASP-induced phenotype gave the opportunity to ask whether it would depend on Abp1. Cotransfection of neurons with N-WASP and an Abp1 RNAi vector abolished the N-WASP overexpression effects: the number of neurites (12.5 ± 0.6) as well as arborization level of dendrites per neuron (9.3 ± 0.8) was significantly reduced to the level of control neurons (Fig. 24A-B, E-F, K). Expression of Abp1 RNAi alone as well as expression of the empty RNAi vector had no significant influence on neurite number and dendritic branching (Figure 24A-B, G-H, K). These results demonstrate that the Abp1 RNAi induced suppression of the N-WASP overexpression phenotype was specific.

Cooverexpression of the dominant-negative form of Cdc42, Cdc42 N17 (Figure 24I), also eliminated N-WASP-triggered neurite initiation (12.3 ± 0.5) and dendritic arborization (10.0 ± 0.7, Fig. 24K). It has to be noted, however, that overexpression of Cdc42 N17 alone already massively affected morphogenesis.

Summarized these data clearly show that Abp1 and Cdc42 do not only influence the activity of the Arp2/3 complex activator N-WASP in vitro but that both proteins are essential for N-WASP-induced reorganizations of the actin cytoskeleton in developing neurons.

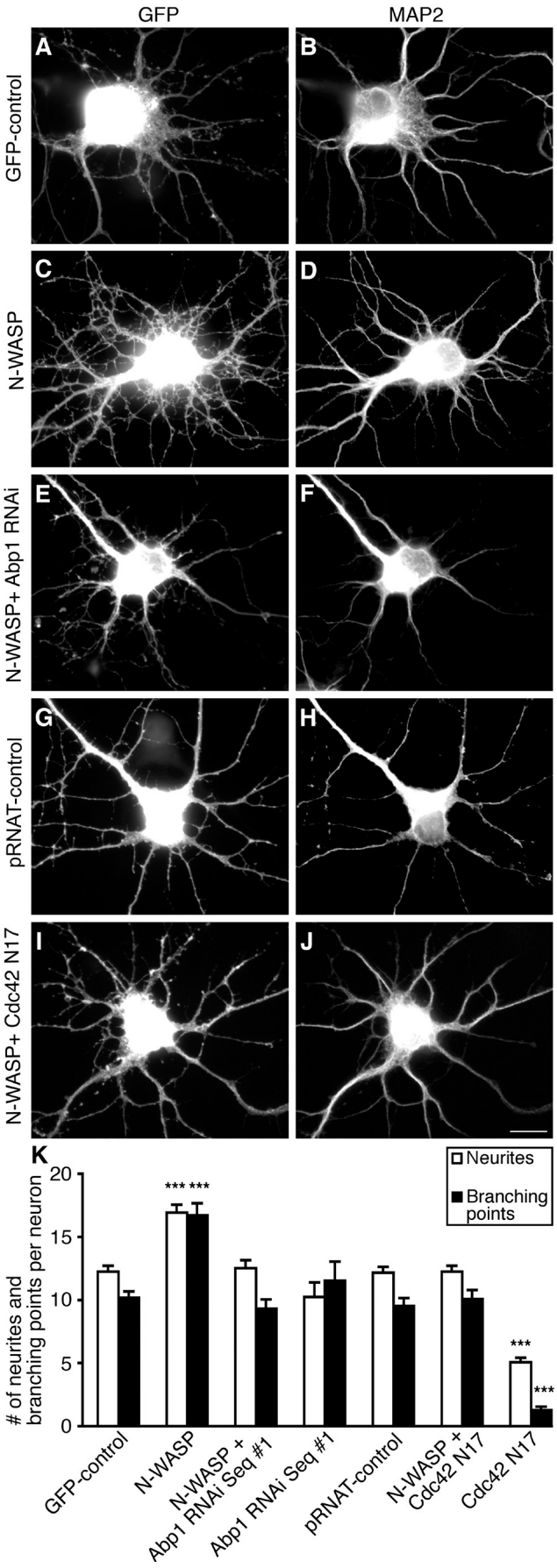

Figure 24. Abp1 and Cdc42 are crucial for the N-WASP-induced increase in neurites and branching points. Primary hippocampal neurons were transfected with pEGFP (GFP-control; *A, B*), with N-WASP (*C,*

D), with N-WASP plus a pRNAT/mRFP-driven Abp1 RNAi construct (*E, F*), with pRNAT-GFP (pRNAT-control; *G, H*), with N-WASP in combination with myc-Cdc42 N17 (*I, J*), as well as with the pRNAT/mRFP-driven Abp1 RNAi construct and myc-Cdc42 N17 alone (no images shown; see *K* for quantitative data), respectively, at day 5 in vitro and fixed 38 h later. The number and branching of MAP2-immunopositive neurites (*B, D, F, H, J*) are markedly increased upon N-WASP overexpression, as also evident from quantitative analyses (*K*). This N-WASP effect was completely suppressed by Cdc42 N17 coexpression and reduction of Abp1 levels, respectively (*K*). Data are represented as mean ± SEM (***$p < 0.001$). Bar, 10 μm.

3.2.3 Reduced functional inhibition of N-WASP induces an axonal development phenotype similar to that demonstrated by Abp1 or Arp2/3 complex deficiency

As reported previously, reduced availability of the Arp2/3 complex or Abp1 abolishes axon development (Fig. 23), and Abp1 is an activator of N-WASP (Pinyol et al., 2007). It was therefore interesting to investigate the function of Abp1/N-WASP complexes in axonal development. For this purpose, N-WASP mutants were constructed, which lacked the binding interfaces for Abp1 (GFP-N-WASP ΔPRD) and Cdc42 (GFP-N-WASP PWA). The hypothesis was that such mutants should mimic the effects of Abp1 knock down and of Arp2/3 complex inhibition, respectively, on axon length in developing neurons because both N-WASP mutants, which may not be fully functional in vivo as they lack domains important for activation, may compete with endogenous N-WASP for N-WASP binding and activating proteins, such as Abp1 and Cdc42, and thereby disturb N-WASP function. Indeed, both mutants induced significantly ($p < 0.001$) elongated axons when compared to control cells (Fig. 25A-C, E).

In contrast to overexpression of the mutants, overexpression of wild-type N-WASP did not show any significant increase in axon length. This clearly excludes the possibility that the effects on axon length observed just reflect N-WASP overexpression-related effects. Strong and distinct evidence that overexpression of N-WASP mutants deficient for Abp1 and Cdc42 binding disrupts the functions of endogenous N-WASP was obtained by comparison to the effects of reducing N-WASP levels by RNAi. N-WASP RNAi (using a construct produced according to Yamaguchi et al., 2005) also caused enhanced axon growth as well (Fig. 25D, E).

Taken together, Abp1 is a novel N-WASP binding and activation molecule, and cooperative action of Abp1 and Cdc42 seems to be necessary for controlling N-WASP/Arp2/3 complex-mediated actin polymerization, which is essential for proper axonal development and thereby for proper formation of neuronal networks.

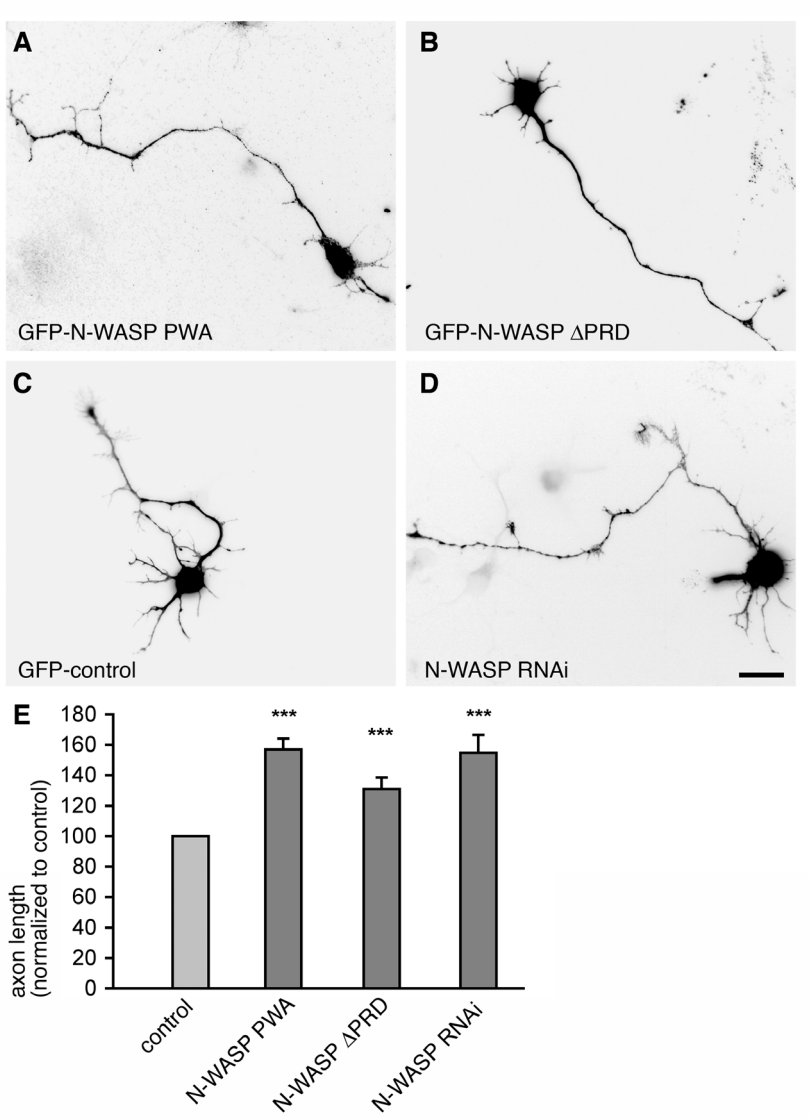

Figure 25. N-WASP mutants deficient for Abp1 or Cdc42 binding and N-WASP RNAi cause increased axon lengths. Primary hippocampal neurons overexpressing GFP-N-WASP PWA (*A*) and GFP-N-WASP ΔPRD (*B*) show significantly (***$p < 0.001$) elongated axons when compared to control neurons expressing GFP alone (*C*). Similarly, N-WASP RNAi (*D*) leads to elongated axons in comparison to control. *E*, quantitative evaluations of axon length. Data were normalized to control and are represented as mean (in percent) ± SEM. Bar, 10 μm.

4. Discussion

4.1 Abp1 controls dendritic spine morphogenesis in cooperation with ProSAPs and N-WASP

The cortical actin cytoskeleton, which underlies the entire plasma membrane, strongly determines cellular morphology and plasma membrane topology. Thereby, actin dynamics is crucial for induction and proper development of spines as well as for their maturation and changes in morphology (Matus, 2000; Schubert et al., 2006; Tada and Sheng, 2006).
During neuronal development long thin filopodia protrude from dendrites and subsequently are replaced by shorter spines with well-defined heads in more mature neurons. Although the exact steps in spinogenesis are not clear, it appears that spines can either form from dendritic protrusions or extend directly from the dendritic shaft (Hering and Sheng, 2001, 2003; Ethell and Pasquale, 2005). The emergence of filopodia and spines is presumably the result of the protrusive force of actin polymerization. A linear bundle of actin reported in the spine, most dense in the neck, may represent the primordial axis of the original filopodial extension (Smart and Halpain, 2000). However, every change in the postsynaptic cytoskeleton, which is regulated by multiple actin binding proteins (Cooper and Schafer, 2000), has to be tightly controlled by synaptic activity sensed by further components of the PSD (Hering and Sheng, 2001).
This study reveals that the F-actin-binding protein Abp1 does not only interconnect the actin cytoskeleton with ProSAP/Shank proteins, major PSD scaffolding proteins linking different receptors and signaling components (Gundelfinger et al., 2006), but additionally serves as a cytoskeletal effector-protein regulating Arp2/3 complex activity and thereby controls early neuronal development and spine morphogenesis.
In vitro, Abp1 uses two distinct N-terminal domains for F-actin binding (Kessels et al., 2000). Our analyses show that both domains individually as well as in combination localize to postsynaptic spines and have the capability to modulate spine shape by increasing the length regardless of spine type. These data for the first time show that F-actin binding by Abp1 modulates the actin cytoskeleton in living cells. Because Abp1 associates with five actin monomers within filaments (Kessels et al., 2000), the observed spine elongations are very likely attributable to filament side binding and stabilization, i.e., promotion of the polymerized state of actin.

Actin binding of Abp1 alone, however, is unable to explain the crucial role of Abp1 in maturation of spines, which are characterized by a distinct head containing the PSD. Instead, promotion of head formation and extension clearly requires the Abp1 SH3 domain in conjunction with F-actin binding. In line with a coordinated role of these two functional parts of Abp1, an excess of the actin-binding domains has a strong negative impact on mushroom spine density. Such Abp1 deletion mutants will occupy places for endogenous Abp1 and other proteins with closely related functions, such as cortactin. As a consequence, Abp1 SH3 domain functions become uncoupled from actin binding.

The same phenotype, a strong decrease in mushroom-type spines, is caused by the SH3 domain containing part of Abp1 lacking the actin-binding domains. This also argues for a coordinated role of both actin-binding and SH3 domain interactions. Consistently, also acute reduction of Abp1 levels by RNAi caused a reduction of mushroom spine and synapse density. Because Abp1 knockdown did not decrease total spine density but resulted in a selective decrease in mushroom-type spines with a concomitant increase in thin spines and filopodia, it can be concluded that Abp1 is critically involved in the maturation of spines and the development of spine heads. The reduction of spine head width upon Abp1 knock-down results in the loss of spines in the mushroom category and a corresponding increase in the category of thin spines, i.e. spines without discernable heads.

Similar to the loss-of-function phenotype observed upon Abp1 knock-down, reduction of the actin-binding protein cortactin, which shares a similar domain structure with Abp1, also decreased the density of spines and synaptic structures (Hering and Sheng, 2003). In addition to spine elongation, mutants lacking the C-terminal region of cortactin resulted in thinner spines, i.e. shrinkage/loss of spine heads that is similar to results observed in this study with mutants of Abp1 lacking C-terminal part of protein. It has been also mentioned by Hering and Sheng (2003) that the spine-elongating activity of cortactin may be related to the promotion of actin branching via binding to the Arp2/3 complex. The longitudinal growth-promoting activity of cortactin was localized to the N-terminal half of the protein that binds to the Arp2/3 complex and F-actin. Overexpression of drebrin A, an actin binding protein sharing homology with Abp1 through two actin-binding domains but lacking an SH3 domain, has been reported to elongate the spine length in mature neurons (Hayashi and Shirao, 1999) and to form very long dendritic filopodia in developing neurons (Mizui et al., 2005).

What exactly may be the crucial role of Abp1 in spine head formation? It is already reported that Abp1 directly binds ProSAP1/Shank2 and ProSAP2/Shank3 via its SH3

domain and can simultaneously associate with dynamic, newly formed actin filaments (Qualmann et al., 2004).

Interestingly, a recent study revealed that ProSAP/Shanks do not just serve as platforms for organizing postsynaptic cytoskeletal functions but that also the maintenance of ProSAP/Shanks at the PSD – at least to some extend – is affected by disrupting actin filaments by incubation with latrunculin A (Kuriu et al., 2006). The fact that the Abp1 SH3 domain alone has a strong negative impact on mushroom spine density but in the full-length context, i.e. in combination with Abp1's F-actin-binding ability, specifically promotes the formation of mushroom-type spines, suggests that one function of Abp1 in establishing spine heads is to interconnect ProSAP/Shank proteins with dynamic F-actin (Fig. 26).

In line with this, Rostaing et al. (2006) demonstrated by quantitative immunoelectron microscopy and tomography that the localization domains of ProSAP/Shanks and F-actin overlap at the cytoplasmic surface of the PSD. Interestingly, reducing ProSAP2/Shank3 expression levels in hippocampal neurons led to a decrease in the density of spines with discernable necks and heads (Roussignol et al., 2005), i.e. to a phenotype similar to Abp1 knock-down.

In contrast to the situation in aspiny neurons (Roussignol et al., 2005), spine density in primary hippocampal neurons was not significantly increased upon ProSAP/Shank overexpression (my unpublished observations). Also cooverexpression of Abp1 and ProSAPs failed to induce more spines (unpublished observations). The observation that cooverexpression of Abp1 and ProSAP1 or ProSAP2 resulted in a highly significant increase in the density of highly branched and complex spines with multiple enlarged heads but single expression of any of these proteins individually had no effects demonstrates the cooperative action of Abp1 and ProSAPs in spine head formation and morphology control.

Results in this study show that ProSAP/Shank-induced enlargement of spine heads, which was previously only described for Shank1 (Sala et al., 2001), is a general function of ProSAP/Shank proteins. The cooperativity of Abp1 and ProSAP1/Shank2 and ProSAP2/Shank3 in this process is highlighted by the fact that the Abp1-mediated increases of mushroom spine and synapse density are dependent on ProSAP2 and on complex formation with ProSAPs and that vice versa the spine head enlargements induced by ProSAP1/Shank2 and ProSAP2/Shank3 are dependent on Abp1. This latter relationship manifests in strong promoting effects of Abp1 coexpression and in a suppression of

ProSAP effects upon Abp1 RNAi. In line with the importance of Abp1/ProSAP complexes in spine head and synapse formation, overexpression of a ProSAP1 mutant lacking all the Abp1-binding sites failed to synergize with Abp1 in head extension. Also overexpression of such a mutant did not lead to increased heads widths when overexpressed alone.

In line with the molecular domains that mediate the Abp1/ProSAP interaction (Qualmann et al., 2004, this study), an excess of the isolated Abp1 domain responsible for the interaction, the SH3 domain, was sufficient to suppress ProSAP-mediated spine head enlargements. This can be explained by the isolated SH3 domain associating with ProSAPs (Qualmann et al., 2004, this study) but lacking the F-actin binding capability of Abp1 (Kessels et al., 2001). It thus prevents the formation of functional Abp1-ProSAP complexes.

Observations of this work suggest that the Abp1 SH3 domain is of special importance for formation and enlargement of spine heads and thus for formation of synapses. We have recently demonstrated that Abp1 does not only interconnect SH3 domain interaction partners including ProSAPs with a dynamic, newly polymerizing actin network but also has a crucial role in actin dynamics. Abp1 steers Arp2/3 complex-dependent actin nucleation by regulating Arp2/3 complex activators, such as N-WASP (neural Wiskott-Aldrich Syndrome protein) via SH3 domain interactions, and thereby controls early neuronal morphology (Pinyol et al., 2007).

In spines, the capability of Abp1 to coordinate SH3 domain-mediated functions with dynamic actin filaments has the potential to serve as a powerful feed-forward mechanism (Fig. 26). Abp1 is not only able to link dynamic actin fibers to ProSAP/Shank proteins and to stabilize actin filaments (Fig. 26A, B), but it is also able to link the SH3 domain interaction partners of the WASP superfamily of Arp2/3 complex activators with F-actin and to activate N-WASP. This leads to Abp1-controlled Arp2/3 complex-mediated nucleation of actin filaments in the microenvironment of the actin- and ProSAP/Shank-rich PSD. Formation of new actin filaments then provides even more Abp1 attachment sides, because Abp1 prefers freshly polymerized actin filaments (Kessels et al., 2000). More F-actin-attached Abp1 then in turn means more SH3 domain interactions with Abp1 binding partners involved in PSD organization and actin polymerization and creates an elaborate actin network in spines, which has the power to expand the spine head (Fig. 26).

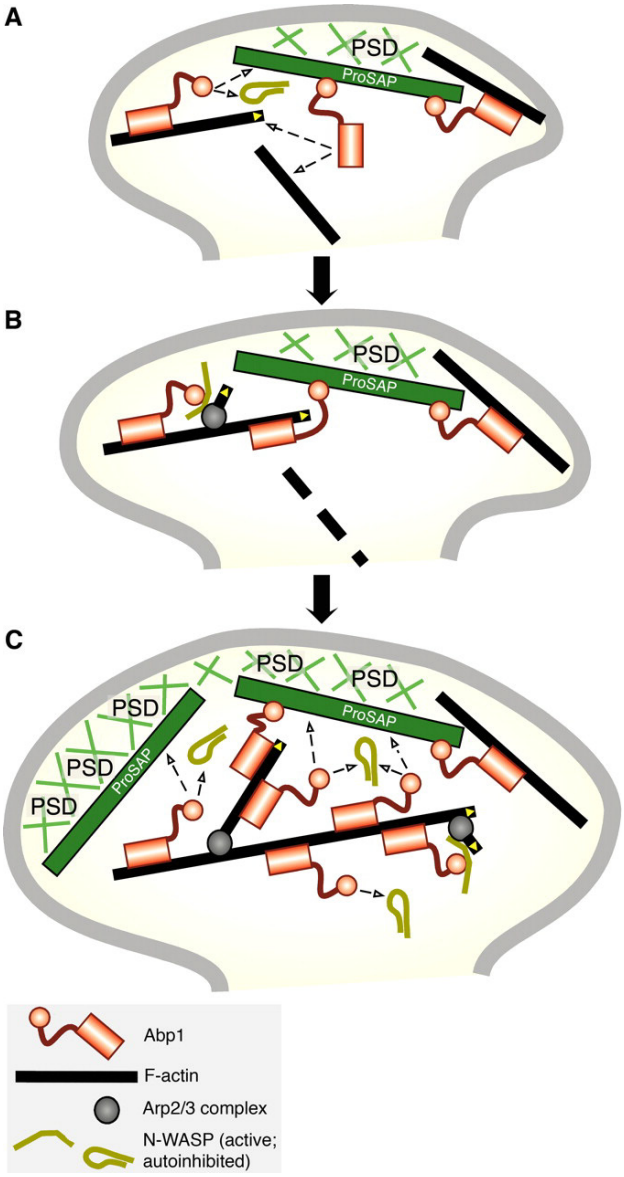

Figure 26. Model of the Abp1 functions in spine morphology control and synapse formation. *A*, ProSAP molecules incorporated at sites of forming synapses allow for recruitment of Abp1 molecules in addition to those molecules interacting with dynamic F-actin at the cell cortex. Abp1 can interconnect ProSAPs with dynamic actin filaments contributing to the stability and growth of a ProSAP-attached actin cytoskeleton. Newly polymerizing actin filaments stabilized in the vicinity of ProSAPs efficiently recruit more Abp1 molecules, which may stabilize these actin filaments by side binding (*A*), whereas unbound filaments may show a higher sensitivity for depolymerization (*B*). Since ProSAPs seem to be the minimum factor in Abp1/ProSAP complex formation, as an excess of ProSAPs efficiently uses the pool of endogenous Abp1 for at least some spine head enlargement while just providing more Abp1 without increasing the availability of ProSAPs has no effect, this F-actin-mediated recruitment of Abp1 to forming and/or extending postsynapses rapidly provides more binding sites for SH3 domain interaction partner than can be complexed with the limiting component in Abp1/ProSAP complex formation, ProSAP. This leads to a promotion of SH3 domain interactions with further binding partners at postsynaptic sites. *B*, Among these binding partners is N-WASP, a normally autoinhibited activator of the Arp2/3 complex actin nucleation machinery, which upon Abp1 SH3 domain binding is brought into an open conformation able to activate the Arp2/3 complex. The result is strong de novo polymerization of actin filaments in the ProSAP- and Abp1-enriched spine head. *C*, Enhanced actin filament formation and further recruitment of Abp1 and ProSAPs increases the spine head. In cells lacking sufficient Abp1, growth of spine heads is inhibited because of the lack of the Abp1-dependent transition from initial stages (A) to dynamic, extended postsynaptic structures (C). Under such condition, mature synaptic structures are thus not efficiently and thin, immature spine structures without synaptic contact prevail.

In line with such a scenario, some Abp1 may be present in forming synapses but an accumulation of Abp1 in postsynapses was only observed at time points of neuronal development after the incorporation of the first pool of ProSAP/Shank molecules into forming postsynapses (Qualmann et al., 2004). Also, this model would explain why subsequent extension of existing postsynaptic spines during ProSAP1 or ProSAP2 overexpression is dependent on Abp1. In line with a role of Abp1 in transmitting signals from the PSD to Arp2/3 complex-mediated actin dynamics, my analyses show that ProSAP/Shank-mediated spine enlargements are not only dependent on Abp1 but also require a functional Arp2/3 complex.

The Arp2/3 complex plays a central role in a wide range of basic processes throughout the eukaryotes by promoting nucleation and branching of actin filaments (Goley and Welch, 2006; Pollard, 2007). Recently, the Arp2/3 complex was shown also to play a key role in regulating the morphology of dendritic spines (Wegner et al., 2008; Kim et al., 2006). The fact that arresting the Arp2/3 complex in an inactive state by overexpression of the N-WASP C-terminus and that knocking down either the Arp2/3 complex component Arp3 or the Abp1-binding Arp2/3 complex activator N-WASP disrupted ProSAP-induced head expansion strongly indicates that the Arp2/3 complex is an important effector for ProSAP-mediated morphology control in postsynaptic spines. In line with this, overexpressed cofilin homology and acidic (CA) domain of N-WASP, acting as a dominant-negative inhibitor that blocks the N-WASP−Arp2/3 interaction, inhibited spine formation (Irie and Yamaguchi, 2002), and Wegner et al. (2008) showed that knock down of endogenous N-WASP resulted in a significant decrease in the density of spines and synapses and that the C-terminal region of the protein, which binds and activates the Arp2/3 complex, is critical for this function of N-WASP.

Knock down of Arp3, an important protein in the Arp2/3 complex, caused a similar defect in the formation of spines and synapses, pointing to the significance of the activation of the Arp2/3 complex in this process (Wegner et al., 2008).

In summary, this study thus reveals that Abp1 with its dual role of interconnecting actin filaments and ProSAP/Shanks on one side and of mediating Arp2/3 complex-dependent actin dynamics on the other side is a crucial factor in the establishment of mature spines and the formation of synapses because it functionally coordinates both processes.

4.2. Abp1 regulates N-WASP and the Arp2/3 complex in controlling neuronal morphology

During development, neuronal growth cones - the specialized structures at the tips of extending axons and dendrites - follow specific pathways and navigate a series of intermediate choice points to find their correct targets. Stereotyped steering decisions are regulated by signaling mechanisms, which integrate and transmit signals from the surface receptors into changes in the growth cone actin cytoskeleton (Dickson, 2002; O'Donnell et al., 2009). The features of the actin cytoskeleton are regulated by a diverse array of actin-binding proteins, which are thereby modulators of cellular dynamics and key components of signaling processes. This study reports that the mammalian actin-binding protein Abp1 plays an indispensable role in Arp2/3 complex-mediated actin polymerization controlled by the Arp2/3 complex activator N-WASP. The moderately related counterpart of Abp1 in S. cerevisiae, Abp1p, has been demonstrated to bind directly to the Arp2/3 complex (Goode et al., 2001). The ability of mammalian Abp1 to interface functionally with the Arp2/3 complex is not direct but relies on SH3 domain-mediated interactions with the Arp2/3 complex activator N-WASP (Pinyol et al., 2007).

In neurons, the N-WASP-induced increase of neurites and of dendritic branch points was very effectively suppressed by both Abp1 RNAi and dominant-negative Cdc42 and is thus dependent on both Abp1 and Cdc42. Dendritic branches originate during a highly dynamic process, which consists of the addition and retraction of new extensions (Wu and Cline, 1998), where the GTPases Rac and Cdc42 regulate branch addition; Rho and Rho kinase inhibit branch elongation (Wong et al. 2000; Li et al., 2002). The fact that Abp1 RNAi alone had no effect on dendritogenesis is important to note because this demonstrates that specifically the effects of the excess of Abp1/N-WASP complexes are blocked by reducing Abp1 and excludes that putative indirect effects, which are unrelated to N-WASP, account for the suppression of the N-WASP overexpression phenotype. Experiments of Rocca et al. (2008) suggest that inhibition of the Arp2/3 complex by PICK1, a PDZ- and BAR-domain-containing protein that binds to a number of membrane proteins, including AMPA receptor subunits GluR2/3, is required for correct neuronal morphology, and that aberrant and highly branched dendrites occurring after PICK1 knock down are due to over activity of the Arp2/3 complex.

A special feature of Abp1 as N-WASP activator is that in addition to its N-WASP interacting domain it has two N-terminal F-actin binding modules. Abp1/N-WASP/Arp2/3 complexes can thus associate with F-actin via both the side binding activity of the Arp2/3

complex (Mullins et al., 1997) and via Abp1's ability to bind actin fibers (Kessels et al., 2000). This may be an important mechanism for the generation of new sites of nucleation on actin fibers and thereby promote branched actin superstructures. Since *in vivo*, Abp1 specifically associates in a signal-responsive manner with highly dynamic F-actin newly generated by Arp2/3 complex activity (Kessels et al., 2000), assembly of Abp1/N-WASP/Arp2/3 complexes at such sites will thus act as a feed-forward mechanism promoting branched structures. Such an effective generation of highly branched and complex F-actin networks is especially important for the formation of the dynamic actin structures at the leading edge of lamellipodia, of short-lived actin structures occurring at sites of endocytosis and of the actin networks in neuronal growth cones that are important for their organization and neuronal pathfinding. Consistently, all these structures are marked by both Arp2/3 complex and Abp1 accumulation (Kessels et al., 2000, 2001; Strasser et al., 2004; Welch et al., 1997; Merrifield et al., 2004; Pinyol et al., 2007).

The colocalization of Abp1, N-WASP and Arp2/3 complex in growth cones (Pinyol et al., 2007) suggested that all three components mediate actin dynamics in neurite outgrowth and differentiation. The identical phenotypes of Abp1 and Arp3 knock down as well as Arp2/3 complex inhibition on axon outgrowth strongly support this view.

The finding that suppression of Abp1 and Arp2/3 complex-mediated actin nucleation promotes axon outgrowth hereby seems somewhat counter-intuitive considering the well-established role of the Arp2/3 complex in actin nucleation and its pivotal role in creating the branched actin structures extending lamellipodia during cell migration (Welch and Mullins 2002; Millard et al., 2004). Quantitative data in this study for Arp2/3 inhibition are, however, very well in line with the measurements of Strasser et al. (2004) and are corroborated by the effects we observed upon Arp3 RNAi. Previous findings have furthermore shown that F-actin destabilization enhances axon formation and elongation in hippocampal neurons (Bradke and Dotti, 1999; da Silva et al., 2005).

Two conclusions can be drawn from these findings. First, at least in neurons, there must be considerable functional redundancy of the Arp2/3 complex with other actin nucleators that help to ensure that neurites are formed, elongated and branched properly to give rise to polarized cells that can form functional neuronal networks. Cobl (Cordon-bleu), a novel recently identified actin nucleator (Ahuja et al., 2007), has dramatic influences on neuronal morphology. Overexpression of Cobl led to drastic increases in the number of neurites protruding from the cell body and of the branching of both axon and of dendrites. Correspondingly, Cobl depletion resulted in decreased dendritic arborization (Ahuja et al.,

2007). Interestingly, the formation of neurites and their arborization critically involving Cobl has been revealed not to rely on Arp2/3 complex-mediated cytoskeletal functions.

Second, in axonal growth cones Arp2/3 complex functions interfere to some extend with the mere extension of the growth cone. The work of Strasser et al. (2004) suggested that Arp2/3 complex-mediated organization of branched filaments and three-dimensional networks residing in the center of growth cones may be important for growth cone translocation and guidance because these actin networks also functionally interface with the microtubule cytoskeleton. Some studies have shown that there is a direct correlation between the levels of tyrosinated microtubules and the rate of axon elongation (Bamburg, 2003; Rochlin et al., 1996). The work from Strasser et al. (2004) also demonstrates that inhibition of Arp2/3 complex activity in neurons alters the relative levels of tyrosinated microtubules and results in pathfinding defects suggesting that Arp2/3 complex-dependent actin structures normally function to regulate growth cone microtubules. Inhibition of Arp2/3 complex removes this regulation, which enhances microtubule dynamics and in turn enhances axon elongation. Longer axons usually have very stable microtubules, but the long Arp2/3 complex-inhibited axons had overly dynamic microtubules. Their instability may impair the coordination of actin and microtubule networks that is needed for growth cone turning: “The microtubules seem to be out of control, like on a highway, if you go too fast, you might see the exit, which is the turning cue, but you might not respond in time” (Le Brasseur, 2004).

In this context, it is conceivable that inhibiting the formation of stable microtubule network by knocking down Abp1, N-WASP and Arp3, respectively, or by inhibiting the Arp2/3 complex may further promote the rapid extension of the mostly unbranched and parallel actin fibers in the periphery of axonal growth cones that are formed independently of Arp2/3 complex functions and drive growth cone extension (Fig. 27).

Importantly, data of this study do not only show that Abp1 and the Arp2/3 complex function in the same cellular process but that also the molecular link between Abp1 and Arp2/3 we discovered, N-WASP, does. Expressing an N-WASP mutant that lacks the Abp1-binding PRD caused a phenotype similar to that of Arp2/3 complex inhibition, Arp3 RNAi or Abp1 RNAi. The same is true for reducing the availability of N-WASP as a whole by RNAi. Together, these data strongly suggest that Abp1, N-WASP and the Arp2/3 complex work together in one complex and that Abp1 is a crucial component in N-WASP/Arp2/3 complex-mediated cytoskeletal functions.

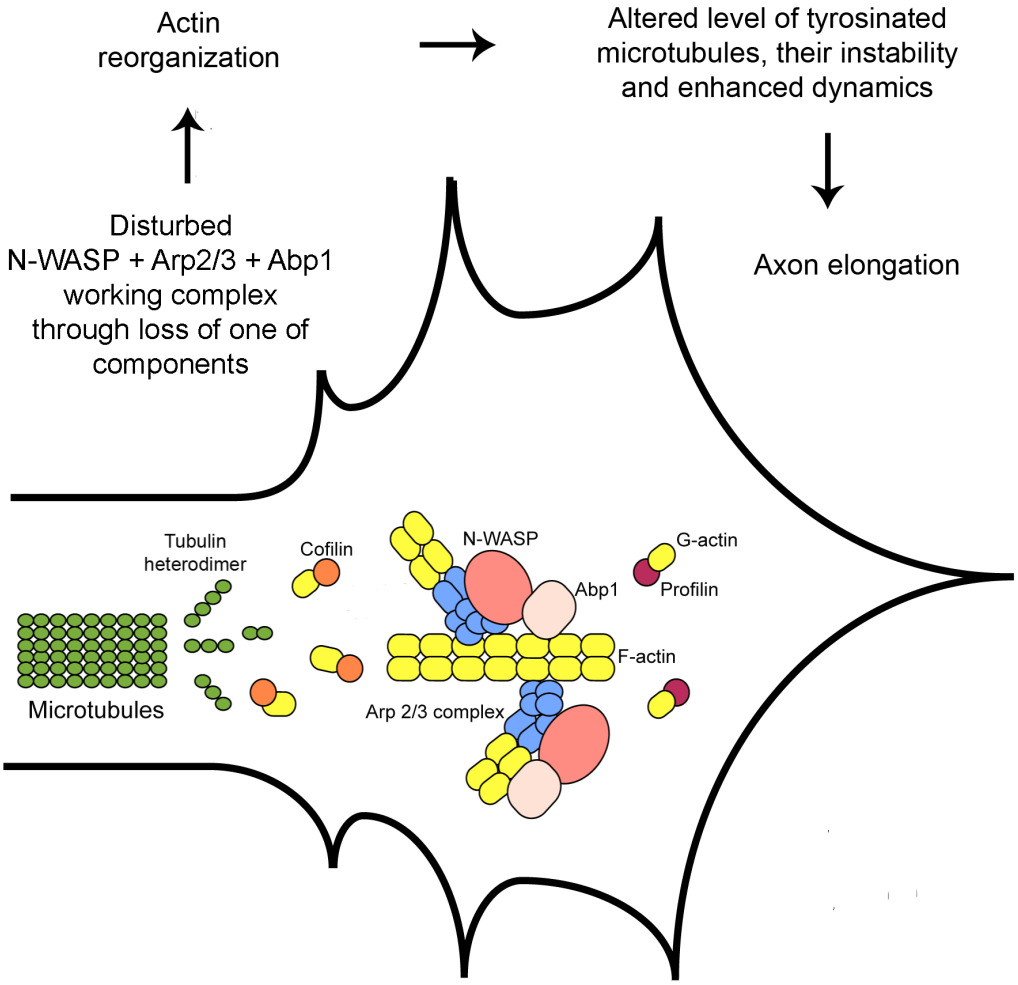

Figure 27. Model for the function of Abp1 in cooperation with N-WASP and Arp2/3 complex in axonal development. Abp1, N-WASP and Arp2/3 working complex negatively regulates axon elongation and branching by influencing microtubule stability at growth cones (modified from Kakimoto et al., 2006 and Dickson, 2001).

The N-WASP RNAi data are well in line with results recently reported by Kakimoto et al. (2006). This study compared the effects of N-WASP and Toca-1 (transducer of Cdc42-dependent actin assembly) RNAi in hippocampal neurons and revealed that in contrast to interfering with N-WASP, knock down of the N-WASP binding and activating protein Toca-1 failed to cause any effects on axon elongation. Toca-1 binds both N-WASP and Cdc42 and mediates actin nucleation by either directly activating N-WASP and/or inhibiting WIP, which is a negative regulator of N-WASP (Ho et al., 2004). It can thus be concluded that Toca-1, although it binds N-WASP and releases its autoinhibition *in vitro*, regulates neuronal morphology aspects different from N-WASP. The study by Kakimoto et al. (2006) thereby highlights that it is of extreme importance to substantiate *in vitro* data for N-WASP autoinhibition release by N-WASP-binding proteins with studies *in vivo* and

with examinations that address the functional cooperativity of N-WASP and a given N-WASP binding protein in physiological processes. Data in this work clearly show that Abp1 is an important component in N-WASP/Arp2/3 complex-mediated actin dynamics in neuronal morphology control and network formation.

Some reports suggest that growth cone guidance and axon elongation depend on activation of Src kinases (Maness et al., 1996; Wen and Zheng, 2006). AFAP120, a neuronal-specific actin cross-linking protein, which binds to and is regulated by Src, has recently been reported to control axon elongation in a phosphorylation-dependent manner (Harder et al., 2008). Cortactin, another target of Src, has also been shown to play a role in controlling neurite branching and growth. Complex formation between δ-catenin and cortactin has been proposed to promote the extension of unbranched primary processes, whereby tyrosine phosphorylation disrupted this complex and resulted in enhanced branching in PC-12 cells (Martinez et al. 2003). Furthermore, cortactin bundles actin in its dephosphorylated state, but upon phosphorylation by Src it exhibits reduced actin-cross-linking abilities (Huang et al., 1997). Cortactin and mammalian Abp1 share a functionally similar domain structure, both proteins are Src substrates, both are likely to participate in dynamic actin rearrangements underlying cell growth and membrane trafficking (see Introduction), thereby a role of Abp1 in Src-dependent axonal growth is a point of future investigations.

In addition to control of neuronal morphology, N-WASP-mediated Arp2/3 complex-dependent actin polymerization controlled by Abp1 might play a role during endocytic vesicle formation, a process supported by transient, local actin nucleation (Qualmann et al., 2000; Qualmann and Kessels, 2002). Both Abp1 (Kessels et al., 2001; Mise-Omata et al., 2003; Connert et al., 2006) and N-WASP (Kessels and Qualmann, 2002; Innocenti et al., 2005; Benesch et al., 2005) have been shown to be important components for endocytic internalization. Since the dominant-negative effect of N-WASP on receptor-mediated endocytosis is exclusively dependent on the PRD (Kessels and Qualmann, 2002), i.e. the binding interface of Abp1, Abp1 might also integrate N-WASP functions into endocytosis. Further studies are required to reveal the mechanistic functions of Abp1/N-WASP complexes in this process. Interestingly, proper regulation of Arp2/3 complex has also been shown to be important for NMDA receptor-mediated endocytosis of AMPA receptors (Rocca et al., 2008).

In mature neurons, a functional crosstalk between the cytoskeletal and membrane trafficking machineries might be of particular importance in nerve terminals to ensure the high speed, efficiency and accuracy of vesicle formation and recycling – important for both synaptic transmission and plasticity (Gundelfinger et al., 2003). In line with this hypothesis, we observed N-WASP and Abp1 as well as the Arp2/3 complex at sites of the neuronal network in mature neurons that are likely to represent synapses. Abp1 localizes to both the pre- and the postsynaptic compartment and binds specifically to cytomatrix components involved in the organization and orchestration of subsynaptic structure and functions at both sites of the synaptic cleft (Fenster et al., 2003; Qualmann et al., 2004). Together with its F-actin binding capabilities and its ability to induce Arp2/3 complex-mediated actin polymerization, Abp1 therefore integrates essential features for a key organizing element for the establishment and reorganization of neuronal networks and synaptic contacts.

References

Ahuja, R., Pinyol, R., Reichenbach, N., Custer, L., Klingensmith, J., Kessels, M. M., Qualmann, B. (2007). Cordon-bleu is an actin nucleation factor and controls neuronal morphology. Cell, 131 (2), 337-350.

Bamburg, J. R. (2003). Introduction to cytoskeletal dynamics and pathfinding of neuronal growth cones. J. Histochem. Cytochem., 51 (4), 407-409.

Banzai, Y., Miki, H., Yamaguchi, H., Takenawa, T. (2000). Essential role of neural Wiskott-Aldrich syndrome protein in neurite extension in PC12 cells and rat hippocampal primary culture cells. J. Biol. Chem., 275 (16), 11987-11992.

Benesch, S., Polo, S., Lai, F. P., Anderson, K. I., Stradal, T. E., Wehland, J., Rottner, K. (2005). N-WASP deficiency impairs EGF internalization and actin assembly at clathrin-coated pits. J. Cell Sci., 118, 3103-3115.

Boeckers, T. M., Bockmann, J., Kreutz, M. R., Gundelfinger, E. D. (2002). ProSAP/Shank proteins - a family of higher order organizing molecules of the postsynaptic density with an emerging role in human neurological disease. J. Neurochem., 81, 903-910.

Boeckers, T. M., Kreutz, M. R., Winter, C., Zuschratter, W., Smalla, K. H., Sanmarti-Vila, L., Wex, H., Langnaese, K., Bockmann, J., Garner, C. C., Gundelfinger, E. D. (1999). Proline-rich synapse-associated protein-1/cortactin binding protein 1 (ProSAP1/CortBP1) is a PDZ-domain protein highly enriched in the postsynaptic density. J. Neurosci., 19 (15), 6506-6518.

Bourne, J., and Harris, K. M. (2007). Do thin spines learn to be mushroom spines that remember? Curr. Opin. Neurobiol., 17 (3), 381-386.

Bradke, F., and Dotti, C. G. (1999). The role of local actin instability in axon formation. Science, 283, 1931-1934.

Braun, A., Pinyol, R., Dahlhaus, R., Koch, D., Fonarev, P., Grant, B. D., Kessels, M. M., Qualmann, B. (2005). EHD proteins associate with syndapin I and II and such interactions play a crucial role in endosomal recycling. Mol. Biol. Cell, 16 (8), 3642-3658.

Brewer, G. J., Torricelli, J. R., Evege, E. K., Price, P. J. (1993). Optimized survival of hippocampal neurons in B27-supplemented Neurobasal, a new serum-free medium combination. J. Neurosci. Res., 35 (5), 567-576.

Calabrese, B., Wilson, M. S., and Halpain, S. (2006). Development and regulation of dendritic spine synapses. Physiology, 21, 38-47.

Carlisle, H. J., and Kennedy, M. B. (2005). Spine architecture and synaptic plasticity. Trends Neurosci., 28, 182-187.

Chen, Y. R., Kori, R., John, B., Tan, T. H. (2001). Caspase-mediated cleavage of actin-binding and SH3-domain-containing proteins cortactin, HS1, and HIP-55 during apoptosis. Biochem. Biophys. Res. Commun., 288 (4), 981-989.

Chung, C. T., Niemela, S. L., Miller, R. H. (1989). One-step preparation of competent Escherichia coli: transformation and storage of bacterial cells in the same solution. PNAS, 86, 2172-2175.

Cingolani, L. A., and Goda, Y. (2008). Actin in Action: The interplay of actin cytoskeleton and synaptic efficacy. Nat. Rev. Neurosci., 9, 344-356.

Cline, H. T. (2001). Dendritic arbor development and synaptogenesis. Curr. Opin. Neurobiol., 1, 118-26.

Connert, S., Wienand, S., Thiel, C., Krikunova, M., Glyvuk, N., Tsytsyura, Y., Hilfiker-Kleiner, D., Bartsch, J. W., Klingauf, J., Wienands, J. (2006). SH3P7/mAbp1 deficiency leads to tissue and behavioral abnormalities and impaired vesicle transport. EMBO J., 25, 1611-1622.

Cooper, J. A., and Schafer, D. A. (2000). Control of actin assembly and disassembly at filament ends. Curr. Opin. Cell Biol., 1, 97-103.

da Silva, J. S., and Dotti, C. G. (2002). Breaking the neuronal sphere: regulation of the actin cytoskeleton in neuritogenesis. Nat. Rev. Neurosci., 9, 694-704.

da Silva, J. S., Hasegawa, T., Miyagi, T., Dotti, C. G., Abad-Rodriguez, J. (2005). Asymmetric membrane ganglioside sialidase activity specifies axonal fate. Nat. Neurosci., 8, 606-615.

Dailey, M.E., and Smith, S.J. (1996). The dynamics of dendritic structure in developing hippocampal slices. J. Neurosci., 16 (9), 2983-2994.

Dickson, B. J. (2001). Rho GTPases in growth cone guidance. Curr. Opin. Neurobiol., 11 (1), 103-110.

Dickson, B. J. (2002). Molecular mechanisms of axon guidance. Science, 298 (5600), 1959-1964.

Du, Y., Weed, S. A., Xiong, W. C., Marshall, T. D., Parsons, J. T. (1998). Identification of a novel cortactin SH3 domain-binding protein and its localization to growth cones of cultured neurons. Mol. Cell Biol., 18, 5838-5851.

Ellerby, L. M., and Orr, H. T. (2006). Neurodegenerative disease: cut to the chase. Nature, 442, 641-642.

Ethell, I. M., and Pasquale, E. B. (2005). Molecular mechanisms of dendritic spine development and remodeling. Prog. in Neurobiol., 75, 161-205.

Fenster, S. D., Kessels, M. M., Qualmann, B., Chung, W. J., Nash, J., Gundelfinger, E. D., Garner, C. C. (2003). Interactions between Piccolo and the actin/dynamin-binding protein Abp1 link vesicle endocytosis to presynaptic active zones. J. Biol. Chem., 278 (22), 20268-20277.

Fiala, J. C., Spacek, J., Harris, K. M., (2002). Dendritic spine pathology: cause or consequence of neurological disorders? Brain Res. Rev., 39, 29-54.

Fiala, J.C., Feinberg, M., Popov, V., Harris, K.M. (1998). Synaptogenesis via dendritic filopodia in developing hippocampal area CA1. J. Neurosci., 18 (21), 8900-8911.

Glantz, L. A., and Lewis, D. A. (2000). Decreased dendritic spine density on prefrontal cortical pyramidal neurons in schizophrenia. Arch. Gen. Psychiat., 57, 65-73.

Goley, E. D., and Welch, M. D. (2006). The ARP2/3 complex: an actin nucleator comes of age. Nat. Rev. Mol. Cell Biol., 7, 713-726.

Goode, B. L., Rodal, A. A., Barnes, G., Drubin, D. G. (2001). Activation of the Arp2/3 complex by the actin filament binding protein Abp1p. J. Cell Biol., 153, 627-634.

Govek, E. E., Newey, S. E., Van Aelst, L. (2005). The role of the Rho GTPases in neuronal development. Genes Dev., 19 (1), 1-49.

Gundelfinger, E. D., Boeckers, T. M., Baron, M., Bowie, J. U. (2006). A role for zinc in post-synaptic density asSAMbly and plasticity? Trends Biochem. Sci., 31, 366-373.

Gundelfinger, E. D., Kessels, M. M., Qualmann, B. (2003). Temporal and spatial coordination of exocytosis and endocytosis. Nat. Rev. Mol. Cell Biol., 4 (2), 127-139.

Halpain, S. (2000). Actin and the agile spine: how and why do dendritic spines dance? Trends Neurosci., 23, 141-146.

Han, J., Kori, R., Shui, J. W., Chen, Y. R., Yao, Z., Tan, T. H. (2003). The SH3 domain-containing adaptor HIP-55 mediates c-Jun N-terminal kinase activation in T cell receptor signaling. J. Biol. Chem., 278, 52195-52202.

Han, J., Shui. J. W., Zhang, X., Zheng, B., Han, S., Tan, T.H. (2005). HIP-55 is important for T-cell proliferation, cytokine production, and immune responses. Mol. Cell Biol., 25 (16), 6869-6878.

Harder, J., Xu, X., Letourneau, P., Lanier, L. M. (2008). The actin cross-linking protein AFAP120 regulates axon elongation in a tyrosine phosphorylation-dependent manner. Neurosci: Lett., 444 (2), 132-136.

Harris, K. M. (1999). Structure, development, and plasticity of dendritic spines. Curr. Opin. Neurobiol., 9, 343-348.

Harris, K.M., Jensen, F.E., Tsao, B. (1992). Three-dimensional structure of dendritic spines and synapses in rat hippocampus (CA1) at postnatal day 15 and adult ages: implications for the maturation of synaptic physiology and long-term potentiation. J. Neurosci., 12, 2685-2705.

Hayashi, K., and Shirao, T. (1999). Change in the shape of dendritic spines caused by overexpression of drebrin in cultured cortical neurons. J. Neurosci., 19, 3918-3925.

Hering, H., and Sheng, M. (2001). Dendritic spines: structure dynamics and regulation. Nat. Rev. Neurosci., 2, 880-888.

Hering, H., and Sheng, M. (2003). Activity-dependent redistribution and essential role of cortactin in dendritic spine morphogenesis. J. Neurosci., 23, 11759-11769.

Higgs, H.N., and Pollard, T.D. (2001). Regulation of actin filament network formation through Arp2/3 complex: activation by a diverse array of proteins. Annu. Rev. Biochem., 70, 649-676.

Ho, H. Y., Rohatgi, R., Lebensohn, A. M., Le Ma, L. J., Gygi, S. P., Kirschner, M. W. (2004). Toca-1 mediates Cdc42-dependent actin nucleation by activating the N-WASP-WIP complex. Cell, 118 (2), 203-216.

Ho, H. Y., Rohatgi, R., Ma, L., Kirschner, M. W. (2001). CR16 forms a complex with N-WASP in brain and is a novel member of a conserved proline-rich actin-binding protein family. Proc. Natl. Acad. Sci. USA, 98, 11306-11311.

Huang C., Ni Y., Wang T., Gao Y., Haudenschild C. C., Zhan X. (1997). Down-regulation of the filamentous actin cross-linking activity of cortactin by Src-mediated tyrosine phosphorylation. J. Biol. Chem., 272, 13911-13915.

Innocenti, M., Gerboth, S., Rottner, K., Lai, F. P., Hertzog, M., Stradal, T. E., Frittoli, E., Didry, D., Polo, S., Disanza, A. (2005). Abi1 regulates the activity of N-WASP and WAVE in distinct actin-based processes. Nat. Cell Biol., 7, 969-976.

Irie, F., and Yamaguchi, Y. (2002). EphB receptors regulate dendritic spine development via intersectin, Cdc42 and N-WASP. Nat. Neurosci., 5, 1117-1118.

Irwin, S. A., Galvez, R., Greenough, W. T. (2000). Dendritic spine structural anomalies in fragile-X mental retardation syndrome. Cereb. Cortex, 10, 1038-1044.

Ishikawa, R., Hayashi, K., Shirao, T., Xue, Y., Takagi, T., Sasaki, Y., Kohama, K. (1994). Drebrin, a development-associated brain protein from rat embryo, causes the dissociation of tropomyosin from actin filaments. J. Biol. Chem., 269, 29928-29933.

Jellinger, K. A. (2000). Cell death mechanisms in Parkinson's disease. J. Neural Transm., 107 (1), 1-29.

Kakimoto, T., Katoh, H., Negishi, M. (2006). Regulation of neuronal morphology by Toca-1, an F-BAR/EFC protein that induces plasma membrane invagination. J. Biol. Chem., 281, 29042-29053.

Kessels, M. M., Engqvist-Goldstein AE. Y., Drubin, D. G., Qualmann, B. (2001) Mammalian Abp1, a signal-responsive F-actin-binding protein, links the actin cytoskeleton to endocytosis via the GTPase dynamin. J. Cell Biol., 153, 351-366.

Kessels, M. M., Engqvist-Goldstein, AE. Y., Drubin, D. G. (2000). Association of mouse actin-binding protein 1 (mAbp1/SH3P7), an src kinase target, with dynamic regions of the cortical actin cytoskeleton in response to Rac1 activation. Mol. Biol. Cell 11, 393-412.

Kim, E., and Sheng, M. (2004). PDZ domain proteins of synapses. Nat. Rev. Neurosci., 5, 771-781.

Kim, E., Cho, K. O., Rothschild, A., Sheng, M. (1996). Heteromultimerization and NMDA receptor-clustering activity of Chapsyn-110, a member of the PSD-95 family of proteins. Neuron, 17 (1), 103-113.

Kim, Y., Sung, J. Y., Ceglia, I., Lee, K. W., Ahn, J. H., Halford, J. M., Kim, A. M., Kwak, S. P., Park, J. B., Ho Ryu, S., Schenck, A., Bardoni, B., Scott, J. D., Nairn, A. C., Greengard, P. (2006). Phosphorylation of WAVE-1 regulates actin polymerization and dendritic spine morphology. Nature, 442, 814-817.

Korkotian, E. and Segal, M. (2000). Structure-function relations in dendritic spines: is size important? Hippocampus, 5, 587-595.

Kuriu, T., Inoue, A., Bito, H., Sobue, K., Okabe, S. (2006). Differential control of postsynaptic density scaffolds via actin-dependent and -independent mechanisms. J. Neurosci., 26 (29), 7693-7706.

Larbolette, O., Wollscheid, B., Schweikert, J., Nielsen, P. J., Wienands, J. (1999). SH3P7 is a cytoskeleton adapter protein and is coupled to signal transduction from lymphocyte antigen receptors. Mol. Cell Biol., 19, 1539-1546.

Le Bras, S., Foucault, I., Foussat, A., Brignone, C., Acuto, O., Deckert, M. (2004). Recruitment of the actin-binding protein HIP-55 to the immunological synapse regulates T cell receptor signaling and endocytosis. J. Biol. Chem., 279, 15550-15560.

LeBrasseur, N. (2004). Arp2/3 for axon turning. J. Cell Biol., 166 (3), 307.

Li, X., Saint-Cyr-Proulx, E., Aktories, K., Lamarche-Vane, N. (2002). Rac1 and Cdc42 but not RhoA or Rho kinase activities are required for neurite outgrowth induced by the Netrin-1 receptor DCC (deleted in colorectal cancer) in N1E-115 neuroblastoma cells. J. Biol. Chem., 277 (17), 15207-15214.

Luo, L. (2000). Rho GTPases in neuronal morphogenesis. Nat. Rev. Neurosci., 1, 173-180.

Luo, L. (2002). Actin cytoskeleton regulation in neuronal morphogenesis and structural plasticity. Annu. Rev. Cell Dev. Biol., 18, 601-635.

Machesky, L. M., and Insall R. H. (1999). Signalling to actin dynamics. J. Cell Biol., 146 (2), 267-272.

Machesky, L.M., Mullins, R. D., Higgs, H. N., Kaiser, D. A., Blanchoin, L., May, R. C., Hall, M. E., Pollard T. D. (1999). Scar, a WASp-related protein, activates nucleation of actin filaments by the Arp2/3 complex. Proc. Natl. Acad. Sci. USA, 96, 3739-3744.

Maness, P. F., Beggs, H. E., Klinz, S. G., Morse, W. R. (1996). Selective neural cell adhesion molecule signaling by Src family tyrosine kinases and tyrosine phosphatases. Perspect. Dev. Neurobiol., 4, 169-181.

Marrs, G.S., Green, S.H., Dailey, M.E. (2001). Rapid formation and remodeling of postsynaptic densities in developing dendrites. Nat. Neurosci., 4, 1006-1013.

Martinez, M. C., Ochiishi, T., Majewski, M., Kosik, K. S. (2003). Dual regulation of neuronal morphogenesis by a delta-catenin-cortactin complex and Rho. J. Cell Biol., 162, 99-111.

Matsuzaki, M., Ellis-Davies, G. C., Nemoto, T., Miyashita, Y., Iino, M., Kasai, H. (2001). Dendritic spine geometry is critical for AMPA receptor expression in hippocampal CA1 pyramidal neurons. Nat. Neurosci., 4, 1086-1092.

Matus, A. (2000). Actin-based plasticity in dendritic spines. Science, 290, 754-758.

Matus, A., Ackermann, M., Pehling, G., Byers, H. R., Fujiwara, K. (1982). High actin concentrations in brain dendritic spines and postsynaptic densities. Proc. Natl. Acad. Sci. U.S.A., 79, 7590-7594.

McAllister, A. K. (2000). Cellular and molecular mechanisms of dendrite growth. Cereb. Cortex, 10, 963-973.

Merrifield, C. J., Qualmann, B., Kessels, M. M., Almers W. (2004). Neural Wiskott Aldrich Syndrome Protein (N-WASP) and the Arp2/3 complex are recruited to sites of clathrin-mediated endocytosis in cultured fibroblasts. Eur. J. Cell Biol., 83, 13-18.

Miki, H., Sasaki, T., Takai, Y., Takenawa, T. (1998). Induction of filopodium formation by a WASP-related actin-depolymerizing protein N-WASP. Nature, 391 (6662), 93-96.

Miki, H., Takenawa, T. (2003). Regulation of actin dynamics by WASP family proteins. J. Biochem., 134 (3), 309-313.

Millard, T. H., Sharp, S. J., Machesky, L. M. (2004). Signalling to actin assembly via the WASP (Wiskott-Aldrich syndrome protein)-family proteins and the Arp2/3 complex. Biochem. J., 380 (1), 1-17.

Mise-Omata, S., Montagne, B., Deckert, M., Wienands, J., Acuto, O. (2003). Mammalian actin binding protein 1 is essential for endocytosis but not lamellipodia formation: functional analysis by RNA interference. Biochem. Biophys. Res. Commun., 301 (3), 704-710.

Mizui, T., Takahashi, H., Sekino, Y., Shirao, T. (2005). Overexpression of drebrin A in immature neurons induces the accumulation of F-actin and PSD-95 into dendritic filopodia, and the formation of large abnormal protrusions. Mol. Cell Neurosci., 30 (4), 630-638.

Mullins, R. D., Heuser, J. A., Pollard, T. D. (1998). The interaction of Arp2/3 complex with actin: nucleation, high affinity pointed end capping, and formation of branching networks of filaments. Proc. Natl. Acad. Sci. U.S.A., 95, 6181-6186.

Naisbitt, S., Kim, E., Tu, J. C., Xiao, B., Sala, C., Valtschanoff, J., Weinberg, R. J., Worley, P. F., Sheng, M. (1999). Shank, a novel family of postsynaptic density proteins that binds to the NMDA receptor/PSD-95/GKAP complex and cortactin. Neuron, 23, 569-582.

Nakayama, A. Y., Harms, M. B., Luo, L. (2000). Small GTPases Rac and Rho in the maintenance of dendritic spines and branches in hippocampal pyramidal neurons. J. Neurosci., 20, 5329-5338.

Negishi, M., and Katoh, H. (2002). Rho family GTPases as key regulators for neuronal network formation. J. Biochem.,132 (2), 157-166.

Newey, S. E., Velamoor, V., Govek, E. E., Van Aelst, L. (2005). Rho GTPases, dendritic structure and mental retardation. J. Neurobiol., 64 (1), 58-74.

Nunez, G., Benedict, M. A., Hu, Y., Inohara, N. (1998). Caspases: the proteases of the apoptotic pathway. Oncogene, 17, 3237-3245.

O'Donnell, M., Chance, R. K., Bashaw G. J. (2009). Axon growth and guidance: receptor regulation and signal transduction. Annu. Rev. Neurosci., 32, 383-412.

Oikawa, T., Yamaguchi H., Itoh T., Kato M., Ijuin T., Yamazaki D., Suetsugu S., Takenawa T. (2004). PtdIns(3,4,5)P3 binding is necessary for WAVE2-induced formation of lamellipodia. Nat. Cell Biol., 6, 420-426.

Pak, D. T., Yang, S., Rudolph-Correia, S., Kim, E., Sheng, M. (2001). Regulation of dendritic spine morphology by SPAR, a PSD-95-associated RapGAP. Neuron, 31 (2), 289-303.

Park, E., Na, M., Choi, J., Kim, S., Lee, J. R., Yoon, J., Park, D., Sheng, M., Kim, E. (2003). The Shank family of postsynaptic density proteins interacts with and promotes synaptic accumulation of the beta PIX guanine nucleotide exchange factor for Rac1 and Cdc42. J. Biol. Chem., 278 (21), 19220-1929.

Pilpel, Y., and Segal, M. (2005). Rapid WAVE dynamics in dendritic spines of cultured hippocampal neurons is mediated by actin polymerization. J. Neurochem., 95 (5), 1401-1410.

Pinyol, R., Haeckel, A., Ritter, A., Qualmann, B., Kessels, M. M. (2007). Regulation of N-WASP and the Arp2/3 complex by Abp1 controls neuronal morphology. PLoS ONE, 2 (5), e400.

Pollard, T. D. (2003). The cytoskeleton, cellular motility and the reductionist agenda. Nature, 422, 741-745.

Pollard, T. D. (2007). Regulation of actin filament assembly by arp2/3 complex and formins. Annu. Rev. Biophys. Biomol. Struct., 36, 451-477.

Purpura, D. P. (1974). Dendritic spine "dysgenesis" and mental retardation. Science, 20, 186 (4169), 1126-1128.

Qualmann, B., Boeckers, T. M., Jeromin, M., Gundelfinger, E. D., Kessels, M. M. (2004). Linkage of the actin cytoskeleton to the postsynaptic density via direct interactions of Abp1 with the ProSAP/Shank family. J. Neurosci., 24, 2481-2495.

Qualmann, B., and Kessels, M. M. (2002). Endocytosis and the cytoskeleton. Int. Rev. Cytol., 220, 93-144.

Ramakers, G.J. (2002). Rho proteins, mental retardation and the cellular basis of cognition. Trends Neurosci., 25, 191-199.

Rao, A., and Craig, A. M. (2000). Signaling between the actin cytoskeleton and the postsynaptic density of dendritic spines. Hippocampus, 10, 527-541.

Redmond, L., and Ghosh, A. (2001). The role of Notch and Rho GTPase signaling in the control of dendritic development. Curr. Opin. Neurobiol., 11, 111-117.

Rocca, D. L., Martin, S., Jenkins, E. L., Hanley, J. G. (2008). Inhibition of Arp2/3-mediated actin polymerization by PICK1 regulates neuronal morphology and AMPA receptor endocytosis. Nat. Cell Biol., 10, 259-271.

Rochlin, M. W., Wickline, K. M., Bridgman, P. C. (1996). Microtubule stability decreases axon elongation but not axoplasm production. J. Neurosci., 16 (10), 3236-3246.

Rohatgi R., Ho H. Y., Kirschner M.W. (2000). Mechanism of N-WASP activation by Cdc42 and phosphatidylinositol 4,5-bisphosphate. J. Cell Biol., 150, 1299-1309.

Rohatgi, R., Ma, L., Miki, H., Lopez, M., Kirchhausen, T., Takenawa, T., Kirschner, M. W. (1999). The interaction between N-WASP and the Arp2/3 complex links Cdc42-dependent signals to actin assembly. Cell, 97, 221-231.

Romorini, S., Piccoli, G., Jiang, M., Grossano, P., Tonna, N., Passafaro, M., Zhang, M., Sala, C. (2004). A functional role of postsynaptic density-95-guanylate kinase-associated protein complex in regulating Shank assembly and stability to synapses. J. Neurosci., 24, 9391-9404.

Rostaing, P., Real, E., Siksou, L., Lechaire, J. P., Boudier, T., Boeckers, T. M., Gertler, F., Gundelfinger, E. D., Triller, A., Marty, S. (2006). Analysis of synaptic ultrastructure without fixative using high-pressure freezing and tomography. Eur. J. Neurosci., 24 (12), 3463-3474.

Roussignol, G., Ango, F., Romorini, S., Tu, J. C., Sala, C., Worley, P. F., Bockaert, J., Fagni, L. (2005). Shank expression is sufficient to induce functional dendritic spine synapses in aspiny neurons. J, Neurosci., 25 (14), 3560-3570.

Sabatini, B. L, Maravall, M., Svoboda, K. (2001). $Ca(^{2+})$ signaling in dendritic spines. Curr. Opin. Neurobiol., 3, 349-356.

Sala, C., Cambianica, I., Rossi, F. (2008). Molecular mechanisms of dendritic spine development and maintenance. Acta Neurobiol. Exp. (Wars), 68(2), 289-304.

Sala, C., Futai, K., Yamamoto, K., Worley, P. F., Hayashi, Y., Sheng, M. (2003). Inhibition of dendritic spine morphogenesis and synaptic transmission by activity-inducible protein Homer1a. J. Neurosci., 23, 6327-6337.

Sala, C., Piech, V., Wilson, N. R., Passafaro, M., Liu, G., Sheng, M. (2001). Regulation of dendritic spine morphology and synaptic function by Shank and Homer. Neuron, 31, 115-130.

Schubert, V., da Silva, J. S., Dotti, C. G. (2006). Localized recruitment and activation of RhoA underlies dendritic spine morphology in a glutamate receptor-dependent manner. J. Cell Biol., 172, 453-467.

Scott, E. K., and Luo, L. (2001). How do dendrites take their shape? Nat. Neurosci., 4, 359-365.

Sheng, M., and Kim, E. (2000). The Shank family of scaffold proteins. J. Cell Sci., 113 (11), 1851-1856.

Smart, F. M., and Halpain, S. (2000). Regulation of dendritic spine stability. Hippocampus, 10, 542-554.

Soderling, S. H., Binns, K. L., Wayman, G. A., Davee S. M., Ong S. H., Pawson, T., Scott, J. D. (2002). The WRP component of the WAVE1 complex attenuates Rac-mediated signalling. Nat. Cell Biol., 4 (12), 970-975.

Soderling, S. H., Guire, E. S., Kaech, S., White, J., Zhang, F., Schutz, K., Langeberg, L. K., Banker, G., Raber, J., Scott, J. D. (2007). A WAVE-1 and WRP signaling complex regulates spine density, synaptic plasticity, and memory. J. Neurosci., 27 (2), 355-365.

Soderling, S. H., Langeberg, L. K., Soderling, J. A., Davee, S. M., Simerly, R., Raber, J., Scott, J. D. (2003). Loss of WAVE-1 causes sensorimotor retardation and reduced learning and memory in mice. Proc. Natl. Acad. Sci. U. S. A., 100 (4), 1723-1728.

Soltau, M., Richter, D., Kreienkamp, H. J. (2002). The insulin receptor substrate IRSp53 links postsynaptic Shank1 to the small G-protein cdc42. Mol. Cell. Neurosci., 21, 575-583.

Steffen, A., Faix, J., Resch, G.P., Linkner, J., Wehland, J., Small, J. V., Rottner, K., Stradal, T. E. (2006). Filopodia formation in the absence of functional WAVE- and Arp2/3-complexes. Mol. Biol. Cell, 17, 2581-2591.

Strasser, G. A., Rahim, N. A, VanderWaal, K. E., Gertler, F. B., Lanier, L. M. (2004). Arp2/3 is a negative regulator of growth cone translocation. Neuron, 43, 81-94.

Suetsugu, S., Hattori, M., Miki, H., Tezuka, T., Yamamoto, T., Mikoshiba, K., Takenawa, T. (2002). Sustained activation of N-WASP through phosphorylation is essential for neurite extension. Dev. Cell, 3 (5), 645-658.

Tada, T., and Sheng, M. (2006). Molecular mechanisms of dendritic spine morpho-genesis. Curr. Opin. Neurobiol., 16, 95-101.

Takahashi, H., Sekino, Y., Tanaka, S., Mizui, T., Kishi, S., Shirao, T. (2003). Drebrin-dependent actin clustering in dendritic filopodia governs synaptic targeting of postsynaptic density-95 and dendritic spine morphogenesis. J. Neurosci., 23, 6586-6595.

Tarrant, S. B., and Routtenberg, A. (1979). Postsynaptic membrane and spine apparatus: proximity in dendritic spines. Neurosci. Lett., 11, 289-294.

Tashiro, A., Minden, A., Yuste, R. (2000). Regulation of dendritic spine morphology by the Rho family of small GTPases: antagonistic roles of Rac and Rho. Cereb. Cortex, 10, 927-938.

Trachtenberg, J.T., Chen, B.E., Knott, G.W., Feng, G., Sanes, J.R., Welker, E., Svoboda, K. (2002). Long-term in vivo imaging of experience-dependent synaptic plasticity in adult cortex. Nature, 420, 788-794.

Tu, J. C., Xiao, B., Naisbitt, S., Yuan, J. P., Petralia, R. S., Brakeman, P., Doan, A., Aakalu, V. K., Lanahan, A. A., Sheng, M., Worley, P. F. (1999). Coupling of mGluR/Homer and PSD-95 complexes by the Shank family of postsynaptic density proteins. Neuron, 23, 583-592.

van Rossum, D., Hanisch, U. K. (1999). Cytoskeletal dynamics in dendritic spines: direct modulation by glutamate receptors? Trends Neurosci., 22, 290-295.

Weaver, A. M., Heuser, J. E., Karginov, A. V., Lee, W. L., Parsons, J. T., Cooper, J. A. (2002). Interaction of cortactin and N-WASP with Arp2/3 complex. Curr. Biol., 12, 1270-1278.

Wegner, A. M., Nebhan, C. A., Hu, L., Majumdar, D., Meier, K. M., Weaver, A. M., Webb, D. J. (2008). N-Wasp and the Arp2/3 complex are critical regulators of actin in the development of dendritic spines and synapses. J. Biol. Chem., 283 (23), 15912-15920.

Welch, M. D., and Mullins, R. D. (2002). Cellular control of actin nucleation. Annu. Rev. Cell Dev. Biol., 18, 247-288.

Welch, M.D., DePace, A. H., Verma, S., Iwamatsu, A., Mitchison, T.J. (1997). The human Arp2/3 complex is composed of evolutionarily conserved subunits and is localized to cellular regions of dynamic actin filament assembly. J. Cell Biol., 138, 375-384.

Wen, Z., and Zheng, J. Q. (2006). Directional guidance of nerve growth cones. Curr. Opin. Neurobiol., 16, 52-58.

Wong, W. T., Faulkner-Jones, B. E., Sanes, J. R., Wong, R. O. (2000). Rapid dendritic remodeling in the developing retina: dependence on neurotransmission and reciprocal regulation by Rac and Rho. J. Neurosci., 20 (13), 5024-5036.

Wu, G. Y., Cline, H. T. (1998). Stabilization of dendritic arbor structure in vivo by CaMKII. Science, 279, 222-226.

Yamabhai, M., and Kay, B. K. (1997). Examining the specificity of Src homology 3 domain-ligand interactions with alkaline phosphatase fusion proteins. Anal Biochem., 247 (1), 143-151.

Yamaguchi, H., Lorenz, M., Kempiak, S., Sarmiento, C., Coniglio, S., Condeelis, J. (2005). Molecular mechanisms of invadopodium formation: the role of the N-WASP-Arp2/3 complex pathway and cofilin. J. Cell Biol., 168, 441-452.

Yamazaki, D., Suetsugu, S., Miki, H., Kataoka, Y., Nishikawa, S., Fujiwara, T., Yoshida, N., Takenawa, T. (2003). WAVE2 is required for directed cell migration and cardiovascular development. Nature, 424, 452-456.

Yuste, R., and Bonhoeffer, T. (2001). Morphological changes in dendritic spines associated with long-term synaptic plasticity. Annu. Rev. Neurosci., 24, 1071–1089.

Ziv, N.E., Smith, S.J. (1996). Evidence for a role of dendritic filopodia in synaptogenesis and spine formation. Neuron, 17, 91-102.

Abbreviations

% (vol/vol)	volume percent
% (wt/vol)	weight/volume percent or mass/volume percent
aa	amino acid
Abp1	actin binding protein 1
ADF	actin-depolymerisation factor
ADF-H	actin-depolymerisation factor - homology
AMPA	alpha-amino-3-hydroxy-5-methyl-4-isoxazolepropionic acid
Arp2/3	actin related protein 2/3
BAR	bin-amphiphysin-rvs
bp	base-pair
Ca^{2+}	calcium
$CaCl_2$	calcium chloride
Cdc42	cell division cycle 42
cm	centimeter
Cobl	Cordon-bleu
C-terminus	carboxyl-terminus
DIV	day in vitro
DMEM	Dulbecco's Modified Eagle Medium
DNA	deoxyribonucleic acid
DNAse	deoxyribonuklease
E. coli	Escherichia coli
Ena	drosophila enabled
F-actin	filamentous actin
FGD1	faciogenital dysplasia 1
FXS	fragile X syndrome
g	gram
G-actin	globular (monomeric) actin
GFP	green fluorescent protein
GKAP	glucokinase-associated phosphatase
GluR	glutamate receptor

GTPase	guanosintriphosphatase
h	hour
HBSS	Hank’s balanced salt solution
HIP-55	hematopoietic progenitor kinase 1 (HPK1)-interacting protein of 55 kDa
IRSp53	insulin receptor tyrosine kinase substrate p53
kV	kilovolt
l	liter
LB	lysogeny broth
MAGUK	membrane associated guanylate kinase
mg	milligram
Mg^{2+}	magnesium
$MgCl_2$	magnesium chloride
mGluR	metabotropic glutamate receptor
min	minute
ml	milliliter
mm	millimeter
mM	millimole
mRFP	monomeric red fluorescent protein
ng	nanogram
nm	nanometer
NMDA	N-methyl-D-aspartic acid
nt	nucleotide
N-terminus	amino-terminus
N-WASP	neuronal (neural) Wiskott-Aldrich syndrome protein
ºC	degree Celsius
Opti-MEM	optimized Eagle's Minimum Essential Media
PAK	p21-activated kinase
PBS	phosphate buffered saline
PICK1	protein interacting with alpha-protein kinase C
PIP_2	Phosphatidylinositol-4,5-bisphosphate
PIP_3	Phosphatidylinositol-3,4,5-triphosphate
PIX	Pak-interactive exchange factor

PRD	proline-rich domain
ProSAP	proline-rich synapse associated protein
PSD	postsynaptic density
PSD-95	postsynaptic density protein 95
Rac	Ras(rat sarcoma)-related C3 botulinum toxin substrate 1
RNA	ribonucleic acid
RNAi	ribonucleic acid interference
rpm	revolutions per minute
SOC	super optimal broth (sob) - derivate
Scar	suppressor of cyclic adenosine monophosphate (cAMP) receptor
SD	standard deviation
sec	second
SEM	standard error mean
SH3	Src homology 3
TAE	Tris- Acetate- EDTA
TCR	T-cell receptor
Toca-1	transducer of Cdc42 activation 1
U	unit
V	volt
VASP	vasodilator-stimulated phosphoprotein
VCA	verprolin-cofilin-acidic region
WASP	Wiskott-Aldrich syndrome protein
WAVE	WASP-family verprolin-homologous protein
WIP	WASP-interacting protein
WRP/MEGAP	WAVE-associated Rac GTPase-activating protein / mental disorder-associated Rac GTPase-activating protein
YT	yeast extract tryptone
ZAP-70	zeta-chain-associated protein kinase 70
µF	microfarad
µg	microgram

µl	microliter
µM	micromole
Ω	ohm

Curriculum Vitae

Name:	Akvile
Family name:	Haeckel
Birth name:	Inciute
Date of birth:	1977. 10. 13
Place of birth:	Vilnius, Lithuania
Nationality:	Lithuanian

Since 2009-02 Scientific coworker. Molecular Imaging Group, Institute for Radiology, Charité University Medicine Berlin, Berlin, Germany.

Education:

2004 - 2009 Doctoral thesis. Otto-von-Guericke University, Leibniz Institute for Neurobiology, Magdeburg, Germany; Friedrich Schiller University Jena, Institute for Biochemistry, Jena, Germany.

2002 - 2004 Scientific coworker. Leibniz Institute for Neurobiology, Magdeburg, Germany.

2000 - 2002 Master of Sciences degree in biology. Vilnius University, Faculty of Natural Sciences, Vilnius, Lithuania.

1996 - 2000 Bachelor of Sciences degree in nursing. Vilnius University, Faculty of Medicine, Vilnius, Lithuania.

1985 - 1996 University-entrance diploma. Middle school Salininkai, Vilnius, Lithuania.

2010-04-12 Lutherstadt Wittenberg

Scientific Publications

Haeckel, A., Ahuja, R., Gundelfinger, E. D., Qualmann, B., Kessels, M. M. (2008). The actin-binding protein Abp1 controls dendritic spine morphology and is important for spine head and synapse formation. J. Neurosci., 28(40), 10031-44.

Pinyol, R., **Haeckel, A.**, Ritter, A., Qualmann, B., Kessels, M. M. (2007). Regulation of N-WASP and the Arp2/3 complex by Abp1 controls neuronal morphology. PLoS ONE, 2 (5), e400.

Dharmalingam, E., **Haeckel A.**, Pinyol, R., Schwintzer, L., Koch, D., Kessels, M., Qualmann, B. (2009). F-BAR proteins of the syndapin family shape the plasma membrane and are crucial for neuromorphogenesis. J. Neurosci., 29(42), 13315-27.